1969

A study of the anodic oxidation of acetylene on platinum-gold alloys

Christopher Kuo-chieh Wu

Department: Chemical and Biochemical Engineering

A STUDY OF THE ANODIC OXIDATION OF ACETYLENE ON PLATINUM-GOLD ALLOYS

by

CHRISTOPHER KUO-CHIEH WU , 1936

A DISSERTATION

Presented to the Faculty of the Graduate School of the

UNIVERSITY OF MISSOURI - ROLLA

In Partial Fulfillment of the Requirements for the Degree

DOCTOR OF PHILOSOPHY

in

CHEMICAL ENGINEERING

1969

James D. Johnson
Advisor

Glen Haddock

W. R. Stewart

E. H. L. Jacobs

W. J. James

A STUDY OF THE ANODIC OXIDATION OF ACETYLENE ON PLATINUM-GOLD ALLOYS

by

Christopher Kuo-Chieh Wu

An Abstract of a Dissertation

Presented to the Faculty of the Graduate School

University of Missouri - Rolla

In Partial Fulfillment of the Requirements for the Degree

Doctor of Philosophy

in

Chemical Engineering

1969

ABSTRACT

The anodic oxidation of acetylene on Pt-Au alloys of four compositions (80-20, 60-40, 40-60, and 20-80 Pt-Au) was studied at 80°C in solutions of constant pH and unit normality. Currents were measured as a function of potential and partial pressure of acetylene. The effects of temperature on current in 1 N H_2SO_4 and 1 N NaOH and the coulombic efficiencies for CO_2 production were determined.

The experimental results indicated that the alloys can be classified into three groups, Pt-rich, Au-rich, and intermediate compositions.

A transition region (change of the mechanism) was found for the Au-rich alloys. The oxidation can be interpreted in terms of two mechanisms. For the Pt-rich and Au-rich alloys below the transition region, the proposed reaction sequence consists of the following steps:

$$C_2H_2(sol) \longrightarrow C_2H_2(ads) \qquad [1]$$

$$H_2O\ (sol) \longrightarrow OH^{\cdot}(ads) + H^{+} + e \qquad [2a]$$

$$OH^{-}\ (sol) \longrightarrow OH^{\cdot}(ads) + e \qquad [2b]$$

$$C_2H_2(ads) + OH^{\cdot}(ads) \longrightarrow \text{products} \qquad [3]$$

The rate determining step depends on the composition of the alloy. For the Pt-rich alloys, Step 3 is rate determining. For the Au-rich alloys, it is changed to Step 2.

Above the transition region (for the Au-rich alloys), the proposed mechanism consists of the following steps:

$$C_2H_2(sol) \longrightarrow C_2H_2(ads) \quad [1]$$

$$C_2H_2(ads) + H_2O(sol) \longrightarrow C_2H_2OH^{\bullet}(ads) + H^+ + e \quad [4a]$$

$$C_2H_2(ads) + H_2O(sol) \longrightarrow C_2H_2OH^{\bullet}(ads) + H^+ + e \quad [4b]$$

$$C_2H_2OH^{\bullet}(ads) \longrightarrow \text{products} \quad [5]$$

Step 4 is the rate determining step. The change in mechanism on the Au-rich alloys is attributed to a decrease in the acetylene coverage.

The total current on the heterogeneous phases can be represented as the sum of the currents on the phases.

ACKNOWLEDGEMENTS

The author wishes to express his gratitude to Dr. J. W. Johnson, Professor of Chemical Engineering and Research Associate in Materials, and Dr. W. J. James, Director of the Graduate Center for Materials Research, University of Missouri-Rolla, for their guidance, support, and encouragement during the course of this investigation. He also wishes to thank Dr. K. G. Mayhan, Associate Professor of Chemical Engineering, University of Missouri-Rolla, and Dr. G. D. Achenbach, Research Scientist of Continental Oil Company, for their assistance and consultation concerning certain chemical analyses performed in this study. He is also indebted to Mrs. Jeanette Carman for typing the manuscript.

The author is also grateful for the financial support received from the Board of Curators of the University of Missouri and the Monsanto Company, without which this study would not have been possible.

TABLE OF CONTENTS

CHAPTER PAGE

CHAPTER PAGE

LIST OF TABLES

TABLE PAGE

TABLE PAGE

TABLE PAGE

LIST OF FIGURES

FIGURE PAGE

FIGURE PAGE

FIGURE PAGE

FIGURE PAGE

FIGURE PAGE

CHAPTER I

INTRODUCTION

During the past decade a great amount of research has been directed toward the conversion of chemical energy directly into electricity by use of the fuel cell. This increased interest has been generated by a great demand in military and space areas, as well as for commercial and industrial applications.

One of the major advantages of a fuel cell is that no mechanical step is required in the process of the energy conversion. The high efficiency and energy-weight ratios provide light compact sources of electricity. Also, the absence of air pollution such as that caused by gases from internal combustion engines of present vehicles are another point in their favor. A large number of the cells under consideration today have end products of water, carbon dioxide, and/or nitrogen. Unspent fuels and oxidants can be recycled and electrolytes totally enclosed or isolated from the exhaust system.

The purpose of this investigation was to establish a mechanism for the anodic oxidation of acetylene on Pt-Au alloy electrodes in aqueous solutions. Pt and Au are known as effective electro-catalysts, but Au has a higher Tafel limit since it does not tend to passivate as readily as Pt. It is desirable to investigate the combined catalytic influence of these two metals to possibly provide a better

understanding of fuel cell electrode kinetics.

CHAPTER II

LITERATURE REVIEW

In fuel cell research, the anodic behavior of organic substances is of great interest, especially unsaturated hydrocarbons which can be considered as potential fuels. The transition metals have been found to be the most active catalysts for the anodic oxidation of such hydrocarbons as well as for H_2 and alcohols. This literature review includes general information about electro-catalysis and electrode kinetics, and specific information about the anodic oxidation of acetylene.

I. ELECTRO-CATALYSIS

The catalyst in electrode processes functions as an adsorbent, an electron source or sink, and a reaction surface. The adsorption of a reactant should be strong enough to allow complete reaction and fast enough to sustain high currents. Generally, the type of adsorption involved is chemisorption.

Parsons[1] has reported the dependence of electrode reactions on the free energy of adsorption of the reactant He showed that the exchange current for hydrogen evolution is higher on metals having low free energies for atomic hydrogen adsorption. As ΔG°_{ads} approaches zero, the exchange current reaches a maximum. For metals having large negative heats of adsorption, i.e., strong adsorbers, the exchange current decreases with ΔG°_{ads}.

Conway and Bockris[2] discussed the relation of heats and free energies of adsorption to the activation energy and mechanism of hydrogen evolution. They demonstrated the effect of electro-catalysis in two ways. First, a plot of the work functions of the metals versus the logarithm of the exchange current density (Fig. 1) revealed the presence of two distinct groups which are associated with the slow discharge and slow electrochemical desorption mechanisms.

In the second, a plot of D_{MH} (strength of M-H bond) versus the overpotential at a constant current density (Fig. 2) showed the same division between the two groups. For metals on which the slow discharge mechanism is controlling, the overpotential decreased with increasing D_{MH}. The opposite behavior was observed for metals on which the rate determining step is electrochemical desorption.

An analogous relation between log i_o and the d-band character was found by Conway[3] for transition metal alloys (See Fig. 3). The d-band character was defined as the extent to which the d-electron orbitals of a metal or alloy are filled and can be related to the adsorption energy on the metal. Metals which have the lower values of d-band character (more vacancies in the d-band) have more unpaired electrons. These vacant orbitals are capable of forming bonds with electron donors, thus promoting chemisorption of the donor. In general, the lower the percentage of d-band character, the greater is the adsorption tendency and the heat of adsorption. If adsorption is slow, a metal of low d-band

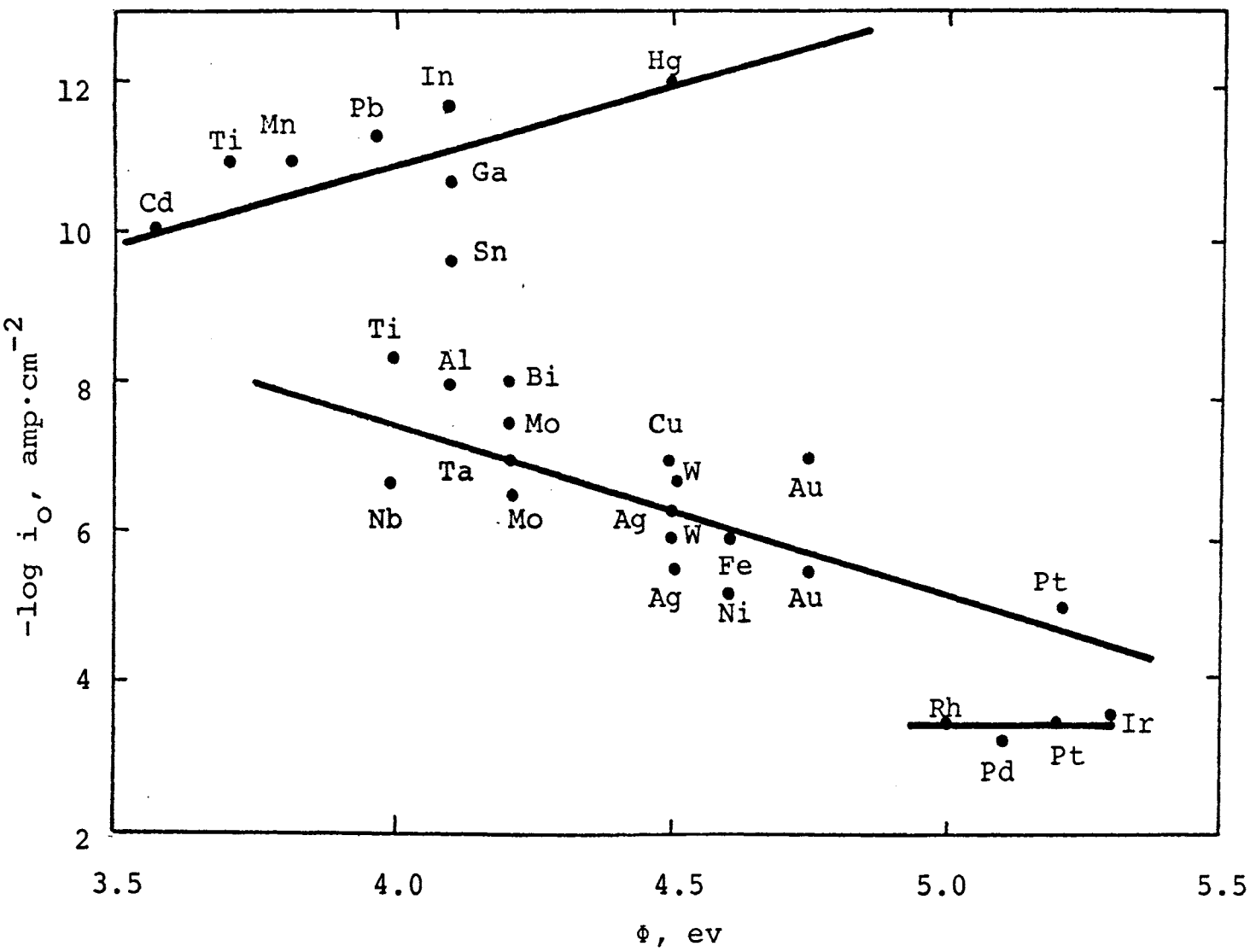

Figure 1. Dependence of exchange current density for hydrogen evolution on the work function of various metals.[2]

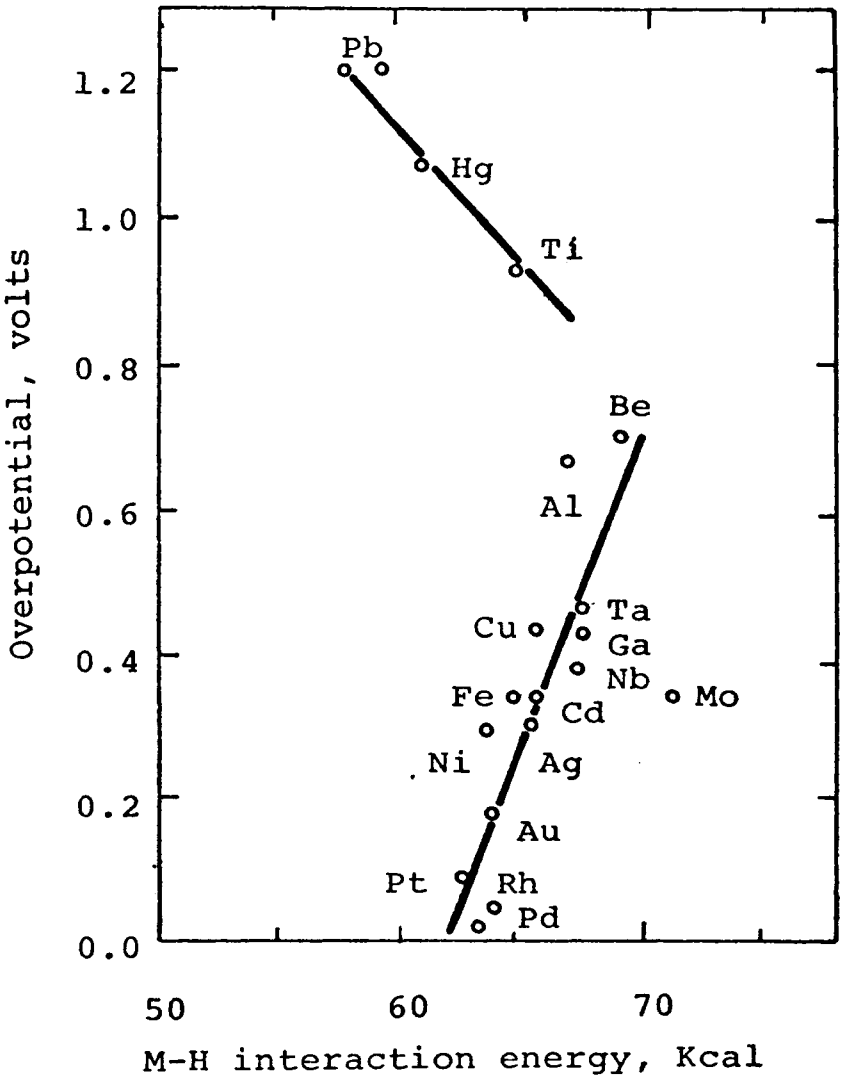

Figure 2. Dependence of hydrogen overpotential on the metal-hydrogen bond strength at a current density of 10^{-3} amp·cm^{-2}.[2]

character will usually be a better catalyst. When desorption is slow, a metal with higher d-band character should be more effective.

The transition metals have been widely used as electrocatalysts. Of these, Pt, Pd, and Rh are the most active for the oxidation of H_2, CO, hydrocarbons, and alcohols. The catalytic properties of these metals have been explained by the formation of covalent bonds with the fuels by means of d-band vacancies.

Young and co-workers[4] have correlated the hydrogen electrode open-circuit potentials on the transition metals with their d-band vacancies. Their data tend to support the electronic theories of fuel cell catalysis. The influence of d-character on alloy electrodes has also been shown with potential measurements (See Fig. 4). Alloying with small quantities of Au decreased the potential of a Pt-H_2 electrode. The Au was thought to have contributed electrons to the vacant d-orbitals of Pt, thus filling the d-band vacancies that are necessary for catalysis. Alloys containing over 60 percent Au showed no further change in potential.

The phase behavior of Au-Pt alloys has been extensively investigated. Johansson and Linde[5] found the existence of a continuous series of solid solutions above 1300°C. Darling and co-workers[6] established the complete equilibrium diagram (Fig. 5) by means of microscopic methods (x-ray diffraction and resistance measurements). A two-phase region was found below the solidus. The lattice parameters (for a

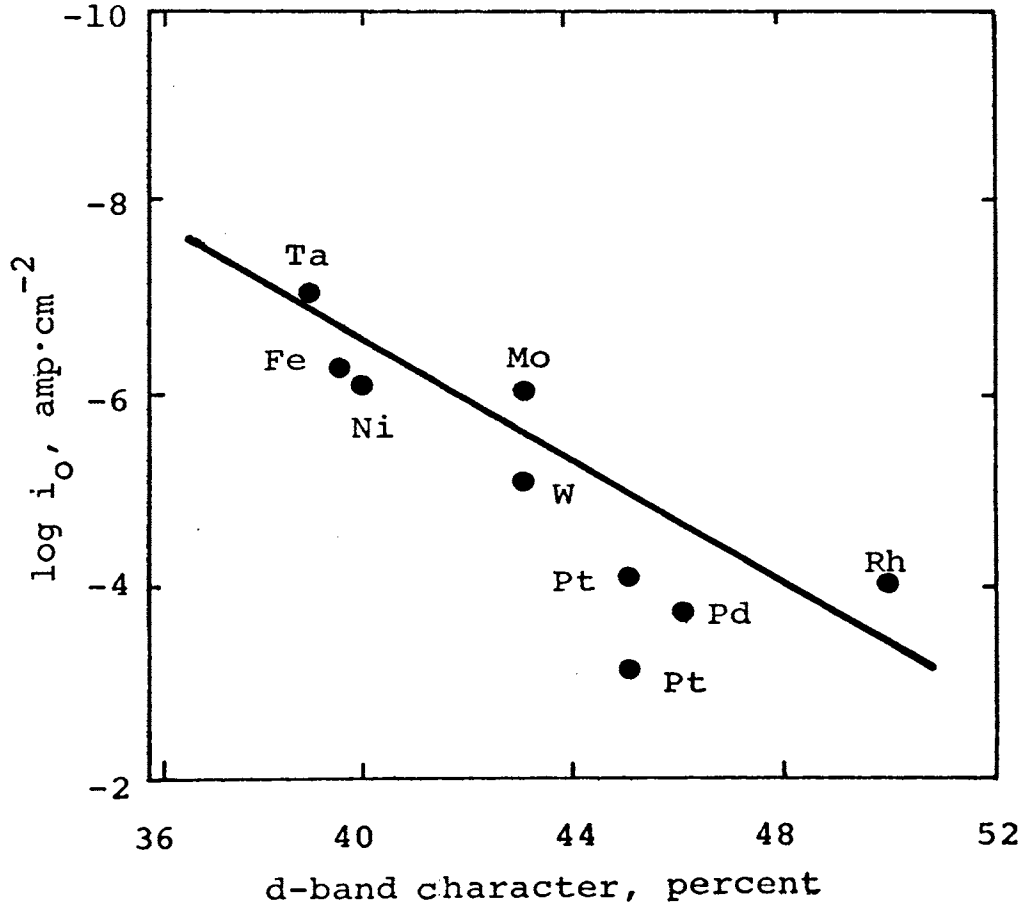

Figure 3. Relation of hydrogen evolution exchange current on d-band character for various transition metals.[3]

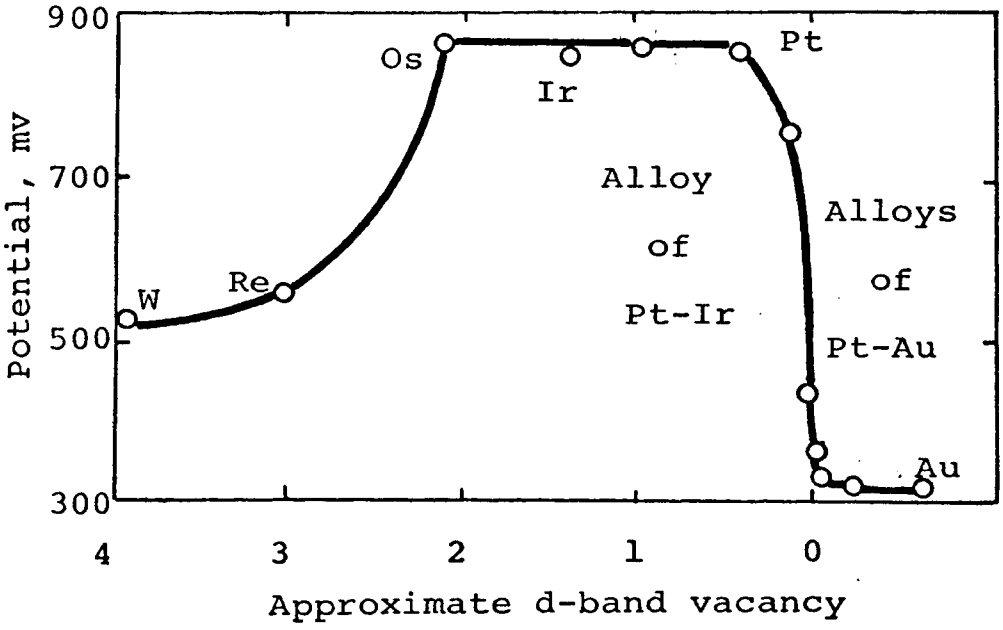

Figure 4. The dependence of H_2 half-cell potentials on d-band vacancy of the electrode.[4]

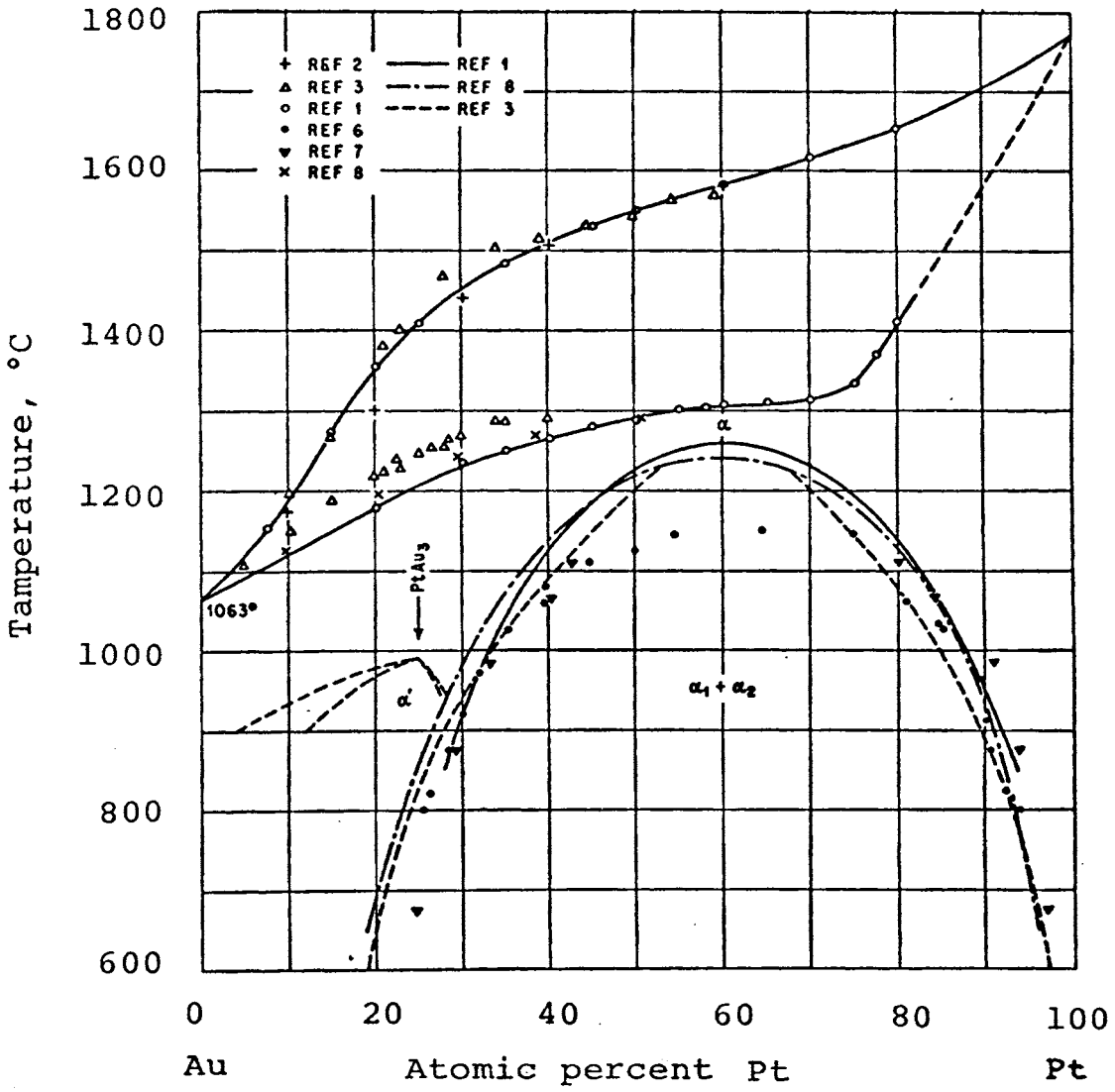

Figure 5. Platinum-Gold phase diagram.[6]

quenching temperature of 1150°C) were 3.931 and 4.062 Å for the Pt-rich (α_1) and the Au-rich (α_2) phases, respectively.

Vogt[7] investigated the magnetic properties of transition metal alloys. In a plot of the susceptibility of Pd-Au alloys against atomic composition (Fig. 6), the susceptibility of a 55 percent Au alloy had decreased to a small negative value comparable to that of Au. For Pt-Au alloys, the transition from paramagnetic to diamagnetic is less sharp. The explanation of this behavior is that Au atoms contribute electrons which go into the d-band of Pd or Pt as long as vacancies remain. When the d-bands of all Pd or Pt atoms have been filled, the alloy is diamagnetic. On the average, there are about 0.55 positive holes in the d-bands of Pt and Pd atoms, thus the similar behavior of the susceptibilities of their alloys.

Oxide formation on the surface of Pt-Au alloys during anodic polarization in sulfuric acid has been studied by Breiter[8]. The surface oxidation of pure Pt began at about 0.8 v (SHE) during the anodic potential sweep. On Au, a small increase of current with potential was observable above 1.2 v. The increase became large above 1.3 v. The reduction of the oxygen layer on Pt occurred mainly below 1.0 v, whereas on Au it was reduced mainly above 1.0 v. An I/V curve resulting from the superposition of the curves for pure Pt and Au was compared to the I/V curve of the heterogeneous Pt-Au alloys. The results suggested the possibility of an electrochemical determination of the relative amounts of Au

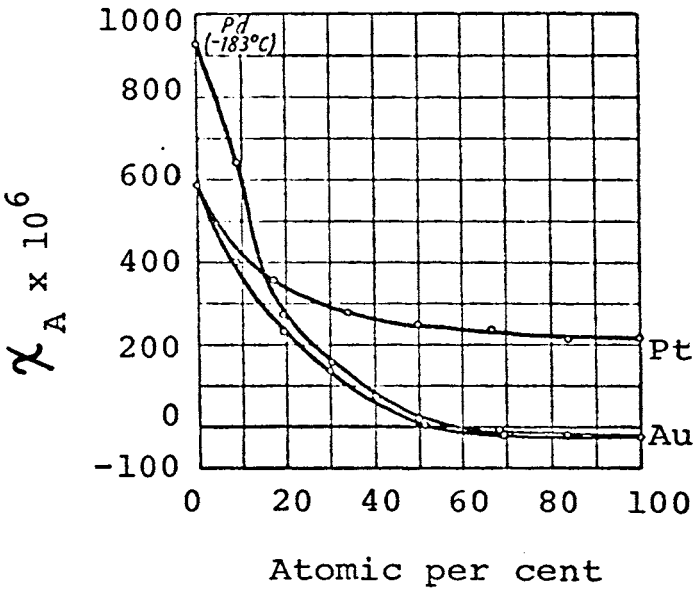

Figure 6. Atomic susceptibility of Au-Pd and Pt-Pd alloys.[7]

and Pt on an active surface by integrating the area under the two reduction waves of the cathodic sweep.

II. ELECTRODE KINETICS

Generally speaking, an electrochemical reaction may be considered to proceed through several or all of the following elementary steps:

1. Transport of the reactants from the electrolyte to the electrode-electrolyte interface (double layer).
2. Adsorption of reactants on the reaction sites.
3. Charge transfer involving adsorbed reactants, discharged species, or other species in the double layer.
4. Surface reactions between adsorbed reactants, discharged species, or other species in the double layer.
5. Desorption of products.
6. Transport of products back into the electrolyte.

An energy barrier (activation energy) is associated with each of the processes. Their magnitudes depend on the properties of the reactants, intermediates, and products for most reactions. In the case of electron transfer steps or charged species, the effects of the electric field must also be considered[9].

A. Concentration Polarization

The transport of reactants and products to and from the electrode is by the mechanisms of diffusion (molecular and turbulent) and/or ionic migration. Overpotentials arising from diffusion limitations are known as concentration polarization[10]. When the diffusion of a reactant is rate controlling, the rate (in terms of the current) may be described as follows:*

$$i = (zFD/\delta)\ (C_B - C_i) \qquad [2.1]$$

The value of the current reaches a limiting value when the concentration of the reactant at the electrode-solution interface falls to zero, i.e.,

$$i_L = zFDC_B/\delta \qquad [2.2]$$

In terms of reversible electrode behavior, concentration polarization (ΔE_{conc}) can be expressed as

$$\Delta E_{conc} = \frac{RT}{zF} \ln\ (C_i/C_B) \qquad [2.3]$$

Eliminating C_i and C_B from Eq. 2.3, the concentration polarization is expressed in terms of i_L as

$$\Delta E_{conc} = \frac{RT}{zF} \ln\ (1 - i/i_L) \qquad [2.4]$$

This shows that a linear relation exists between ΔE_{conc} and i when $i << i_L$, and that the magnitude of ΔE_{conc} increases

---

*See Appendix - for legend.

rapidly when i approaches i_L. If reactant transport were the slow step in a reaction sequence, the potential would not be expected to have a direct effect on the over-all reaction. However, control by preceding electrochemical reactions of the concentration of a reactant in a diffusion step would allow potential to affect the over-all reaction.

B. Chemisorption

In an electrode process, the reactant may be adsorbed at a site on the electrode prior to electron transfer or surface reaction. The activation energy for the adsorption of hydrocarbons varies from 10 to 100 Kcal and often presents a formidable barrier to high currents. It is possible that the rate of chemisorption may be the slowest step in a reaction sequence. Numerous models for chemisorption kinetics have been proposed and differ mainly with the assumptions involving the nature of surface heterogeneity. Langmuir's isotherm[12] is the one most frequently used in the analysis of kinetic data. It is based on the assumption that the heat of adsorption on active sites is constant and that there is no interaction between adsorbed species. It has been well established that these assumptions are not generally applicable, however, the isotherm may be used with reasonable success when sites participating in the reaction have narrow distributions of surface energies and the interactions between adsorbed species are constant. These conditions are often met and hence the Langmuir approach is widely used as it results in relatively simple working expressions.

C. Activation Polarization

In an electrochemical reaction, the rate of the electron transfer step is controlled by the potential difference across the electrical double layer. Under reversible conditions, the potential difference is the reversible value and the magnitudes of the rates of electron transfer in both the forward and reverse directions are the same. These rates are normally referred to as the exchange current, i_o[13].

Under irreversible conditions, the magnitude of the potential difference between the electrode and solution increases, thus accelerating the electron transfer in one direction and decelerating it in the reverse. The overpotential, defined as the difference between the potential of the electrode and its reversible potential, is a measure of this potential difference. The overpotential is positive for anodic and negative for cathodic processes.

$$\eta \equiv V - V_r \qquad [2.5]$$

The general equation for an anodic current in an electrochemical reaction is

$$i = i_o \exp(\alpha\eta F/RT) - i_o \exp[-(1-\alpha)F\eta/RT] \qquad [2.6]$$

When the electron transfer step represented by this equation is rate controlling and η is greater than 0.05 v, the backward reaction is negligible. Thus, only the first term on the right is considered and the equation reduces to the Tafel expression.

III. ANODIC OXIDATION OF ACETYLENE

A. Oxidation of Acetylene on Platinum

The electro-oxidation of acetylene on Pt has been studied by Johnson, Wroblowa, and Bockris[14]. The reaction sequence suggested was

$$C_2H_2 = C_2H_2(ads) \qquad [2.7]$$

$$H_2O = OH^{\cdot}(ads) + H^+ + e \qquad [2.8a)$$

or

$$OH^- = OH^{\cdot}(ads) + e \qquad [2.8b]$$

r.d.s.

$$C_2H_2(ads) + OH^{\cdot}(ads) \rightarrow C_2H_2OH(ads) \qquad [2.9]$$

$$C_2H_2OH(ads) \rightarrow \overset{H_2O}{\cdots} \rightarrow 2\ CO_2 + 9\ H^+ + 9\ e \qquad [2.10]$$

Current-potential relations were determined in solutions with pH's ranging from 0.3 to 12.6. Although the individual plots were displaced as a function of pH, the slope of the linear portion of the Tafel curves remained constant at about 2.3 RT/F, i.e., 70 mv at 80°C. Two other experimental parameters evaluated from the current-potential plots were

$$(\partial \log i/\partial pH)_{V,P,T} = 0.8$$

and

$$(\partial V/\partial pH)_{i,P,T} = -50 \text{ mv}$$

The effect of temperature was studied in 1 N NaOH and 1 N H_2SO_4. The change of apparent activation energy with potential was approximately -25 Kcal/volt compared with -23.06 predicted from the suggested reaction sequence. The

activation energies at the reversible potentials were calculated to be 42 and 48 Kcal for the acid and alkaline solutions, respectively.

Acetylene partial pressure studies in 1 N H_2SO_4 and 1 N NaOH revealed a negative pressure effect, i.e., the current increased with decreasing partial pressure at constant potential. The effect was more pronounced in 1 N NaOH.

Evidence was given that acetylene probably adsorbs with a four-point attachment. The Langmuir adsorption isotherm was successful in correlating the pressure dependencies and was given as

$$\frac{\theta_A}{(1-\theta_A)^4} = K_c C_A = K_p P_A \qquad [2.11]$$

The resulting rate equation for the oxidation was

$$i = nFK_{2.8}k_{2.9}(a_{H^+})^{-1}\theta_A(1-\theta_T)\exp(FV/RT) \qquad [2.12]$$

The total coverage, θ_T, was assumed to be equal to θ_A, or $(1-\theta_T) = (1-\theta_A)$, due to the high values of θ_A. Since step 2.8b would be diffusion limited in acid solutions and since no transition was found in the $(\partial \log i/\partial pH)$ or $(\partial V/\partial pH)$ plots in going from acid to base solutions, step 2.8a was considered to predominate throughout the entire pH range. However, the same pH dependence is exhibited by both steps 2.8a and 2.8b.

K_p values for the isotherm were estimated to be between 10^4 and 10^6. Theoretical current-pressure curves were

constructed using K_p values as parameters. Agreement with experimental data was found in acid solutions for a $K_p = 10^4$. In 1 N NaOH, the change of current with pressure at constant potential was two to three times higher than that predicted by the isotherm for acid solution. It was suggested that this difference might be due to a different type of adsorption in the solutions. Two possibilities presented were: (1) A rearrangement occurs in alkaline solution so that the absorbed species have a decreased occupancy of one per acetylenic radical. (2) Acetylene does not form covalent bonds with d-band vacancies as assumed above, but on the basis of steric considerations will occupy only two adjacent sites. In acid solution, adsorption would occur along with hydration according to the reaction

$$C_2H_2 + H_2O = CH_2CHOH \qquad [2.13]$$

and the resulting species would occupy an area covering approximately four surface sites.

The faradaic efficiency studies were based on the overall reaction

$$C_2H_2 + 4\ H_2O \rightarrow 2\ CO_2 + 10\ H^+ + 10\ e \qquad [2.14]$$

The efficiency for CO_2 production was found to be 100 ± 1 percent in acid and 95 ± 5 percent in alkaline solutions. An analysis was made of the 1 N NaOH anolyte to determine the presence of any organic substances that might be products of branching reactions. An ultraviolet spectrum of the

electrolyte showed no significant absorption, indicating no conjugated unsaturation such as might be suspected for polymerization reactions. Infrared spectrograms of samples obtained by extracting portions of the electrolyte with benzene, ethyl ether, and n-hexane revealed nothing other than sodium carbonate. Thus, it was assumed that no branching leading to products other than CO_2 and H_2O occurred to any appreciable extent.

B. Acetylene Oxidation on Gold

The anodic oxidation of acetylene on gold has been studied by Reed, et.al.[15] Two different sets of reaction parameters were found which depended on the potential region in which the electrode was operating. These regions were separated by an inflection point (transition region) in the Tafel curves. At potentials below the transition region, the reaction sequence was given as

$$C_2H_2 = C_2H_2(ads) \qquad [2.7]$$

r.d.s. $$H_2O \rightarrow OH^{\cdot}(ads) + H^+ + e \qquad [2.8a]$$

or $$OH^- \rightarrow OH^{\cdot}(ads) + e \qquad [2.8b]$$

$$C_2H_2(ads) + OH^{\cdot}(ads) \rightarrow \overset{\cdot\cdot}{H_2O} \rightarrow CO_2, \text{ polymer}, H^+, e \qquad [2.15]$$

Above the transition region, the r.d.s. changed to

$$C_2H_2(ads) + H_2O(ads) \rightarrow C_2H_2OH^{\cdot}(ads) + H^+ + e \qquad [2.16a]$$

$$C_2H_2(ads) + OH^-(ads) \rightarrow C_2H_2OH^{\cdot}(ads) + e \qquad [2.16b]$$

The transition from one sequence to the other was attributed to a pH and potential dependence of the acetylene coverage. Tafel slopes obtained in solutions of various pH's were found to be about 2(2.3 RT/F) or 140 mv both above and below the transition region.

Acetylene partial pressure studies were made in 1 N H_2SO_4 and 1 N NaOH. Langmuir adsorption isotherms were used to correlate the data. As Au has no statistically calculated d-orbitals available for covalent bonding, the number of sites occupied was ascertained from the size of the organic molecules and the inter-atomic distances of the metal atoms (See Fig. 7). The acetylene covers only two sites but possibly blocks two others due its size. Therefore, the adsorption isotherm was taken as

$$\frac{\theta_A}{(1-\theta_A)^n} = K_p P_A \quad . \qquad [2.17]$$

where n can be equal to 2 or more.

In 1 N H_2SO_4, the pressure effect ($\partial i/\partial p$) was negative. In 1 N NaOH below the transition region, the pressure effect started out negative, but became positive for pressures <0.1 atm. In 1 N NaOH above the transition region, the effect was positive at pressures >0.1 atm and approached a constant value at pressures <0.1 atm. The anodic oxidation of acetylene below the transition region (btr) was expressed as

$$i_{btr} = nF(k_{2.8a} a_{H_2O} + k_{2.8b} a_{OH^-})(1-\theta_A)\exp(\alpha FV/RT) \qquad [2.18]$$

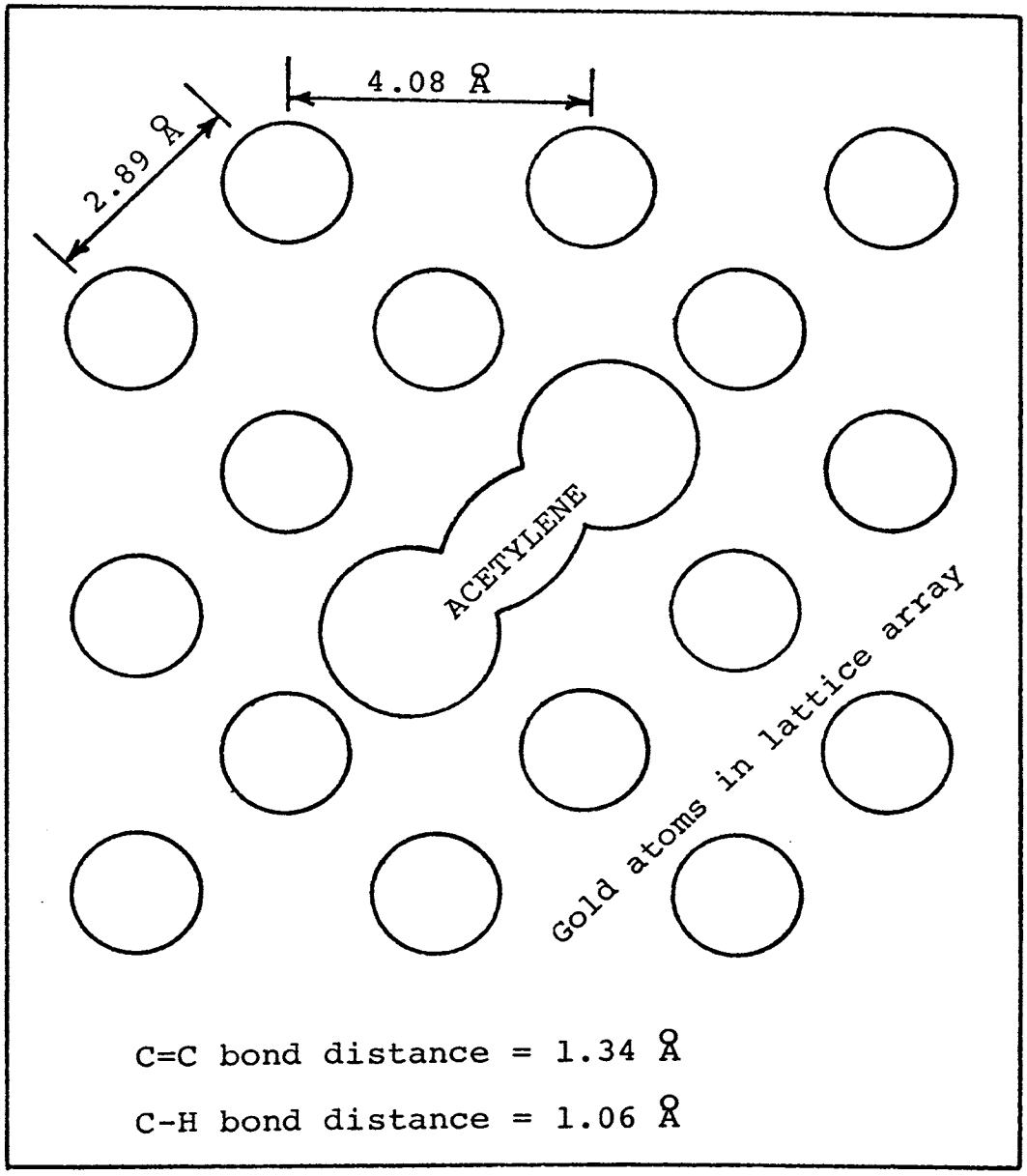

Figure 7. Schematic diagram of an acetylene molecule adsorbed on a gold surface.

The coverage of OH radicals was considered very low[16], and the coverages of all other intermediates were neglected in comparison with θ_A, since they occurred in the reaction sequence after the r.d.s., therefore, $\theta_A \simeq \theta_T$.

Above the transition region (atr), the over-all rate was expressed as

$$i_{atr} = nF(k_{2.16a}a_{H_2O} + k_{2.16b}a_{OH^-})\ \theta_A \exp(\alpha FV/RT) \quad [2.19]$$

The effects of temperature on current in 1 N H_2SO_4 and 1 N NaOH (above and below the transition region) was determined and the variation with potential found to be about 11 Kcal/volt (approximately αF) as predicted from Eqns. 2.13 and 2.14. However, there was an apparent discontinuity in the values in crossing the transition region, thus indicating a change in the mechanism.

The coulombic efficiency was 60 ± 5 percent in 1 N H_2SO_4 and 80 ± 10 percent in 1 N NaOH. The efficiency decreased with decreasing acetylene partial pressure. A resinous film (dark brown in color) was formed on the anode in acidic, but not in basic solutions. The film was found to have a C:H:O ratio of approximately 2:2:1. No carbonyl groups were determined to be present by infrared analysis, but the presence of O-H, C=C, and C-OH was indicated. A polymeric structure was proposed as

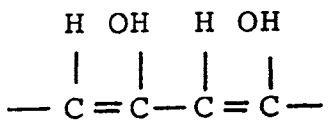

The proposed mechanisms were successful in correlating the data.

CHAPTER III

EXPERIMENTAL

The experimental plan for the investigation consisted of the following major parts: (1) current-potential studies, (2) current-temperature studies, (3) current-pressure studies, and (4) faradaic efficiency studies. The results are presented in this chapter.

I. MATERIALS

The materials used in the investigation are listed and described in Appendix B.

II. PREPARATION OF ELECTRODES

The working electrodes, or anodes, were Pt-Au alloys, and the cathode was platinized Pt. The reference electrodes were calomel (1 N KCl) and mercurous sulfate (1 N H_2SO_4) for basic and acidic solutions, respectively.

A. Anodes

The compositions (Pt-Au atomic ratios) of the anodes were 20-80, 40-60, 60-40, and 80-20. The alloys were subjected to both x-ray and microscopic examinations and all possessed a two-phase microstructure. The relative amounts of the phases were determined by an x-ray diffraction technique. The impurities in the alloys were determined by an atomic absorption analysis. The results are shown in

Tab. I. The anodes were fabricated from foils (0.003 inch thickness) with a width of 3.45 cm and height 4.38 cm giving a geometric area of 15.1 cm^2. A small hole was drilled near the top and a thin alloy wire (same composition, 26 gauge) was looped through it and spot welded. The alloy wire (which led outside the electroytic cell) was sealed in a 5 mm pyrex glass tube.

The anodes were cleaned and activated prior to each experiment. They were cleaned by brief (a few minutes) immersion in boiling 1 N KOH, primarily to dissolve any polymer film adhering to the surface of the electrode from the previous run. The anode was then activated by placing it in 1.0 N H_2SO_4 (along with a small piece of Pt gauze which acted as a counter-electrode) and polarizing cathodically (hydrogen evolution) for 5 minutes at a current density of 0.25 amp/cm^2. After activation, it was immediately removed, rinsed with distilled water and transferred to the electrolytic cell.

B. Cathode

The cathode was made of 52-mesh Pt gauze folded on a Pt wire frame. The Pt wire leading outside the cell was also sealed in a 5 mm glass tube. The electrode was platinized using a platinic chloride solution to which a trace of lead acetate had been added.

TABLE I

X-RAY AND ATOMIC ABSORPTION ANALYSES* OF Pt-Au ALLOYS

Alloy Composition Atomic ratio	Relative amount of phases, percent		Impurity, ppm								
	Pt-rich percent	Au-rich percent	Zn	Ag	Ni	Mn	Cu	Fe	Co	Cr	Pb
80Pt-20Au	82	18	<30	47	<160	<60	<100	93	<250	<170	<150
60Pt-40Au	67	33	<30	75	<160	<60	<100	75	<250	<170	<150
40Pt-60Au	25	75	<30	100	<160	<60	<100	84	<250	<170	<150
20Pt-80Au	2	98	24	240	96	<24	89	79	<110	<70	<70

*The atomic absorption analyses were performed by Continental Oil Company, Ponca City, Oklahoma

III. CURRENT-POTENTIAL STUDIES

A. Apparatus

A schematic diagram of the experimental arrangement is shown in Fig. 8. A list of all apparatus is included in Appendix C.

The cell was constructed of pyrex glass and consisted of three basic compartments, the anodic, cathodic, and reference. The anodic compartment was separated from the cathodic by means of a water-sealed stopcock which was open for potentiostatic and closed for galvanostatic operation. The reference electrode was connected to the anodic compartment through a water-sealed stopcock and a Luggin capillary. This stopcock remained closed. Both compartments were provided with gas inlets for the nitrogen and acetylene purge. The anodic compartment was thermostated by means of a temperature probe which controlled the applied voltage (on-off type) to a heating tape wrapped around the compartment. The heating and cooling cycles were made approximately the same by adjusting the voltage applied to the tape with a variable transformer.

The gas flow-rate through the anodic compartment was controlled with a dual-flow proportioner. It was capable of metering both the nitrogen and acetylene flow rates independently.

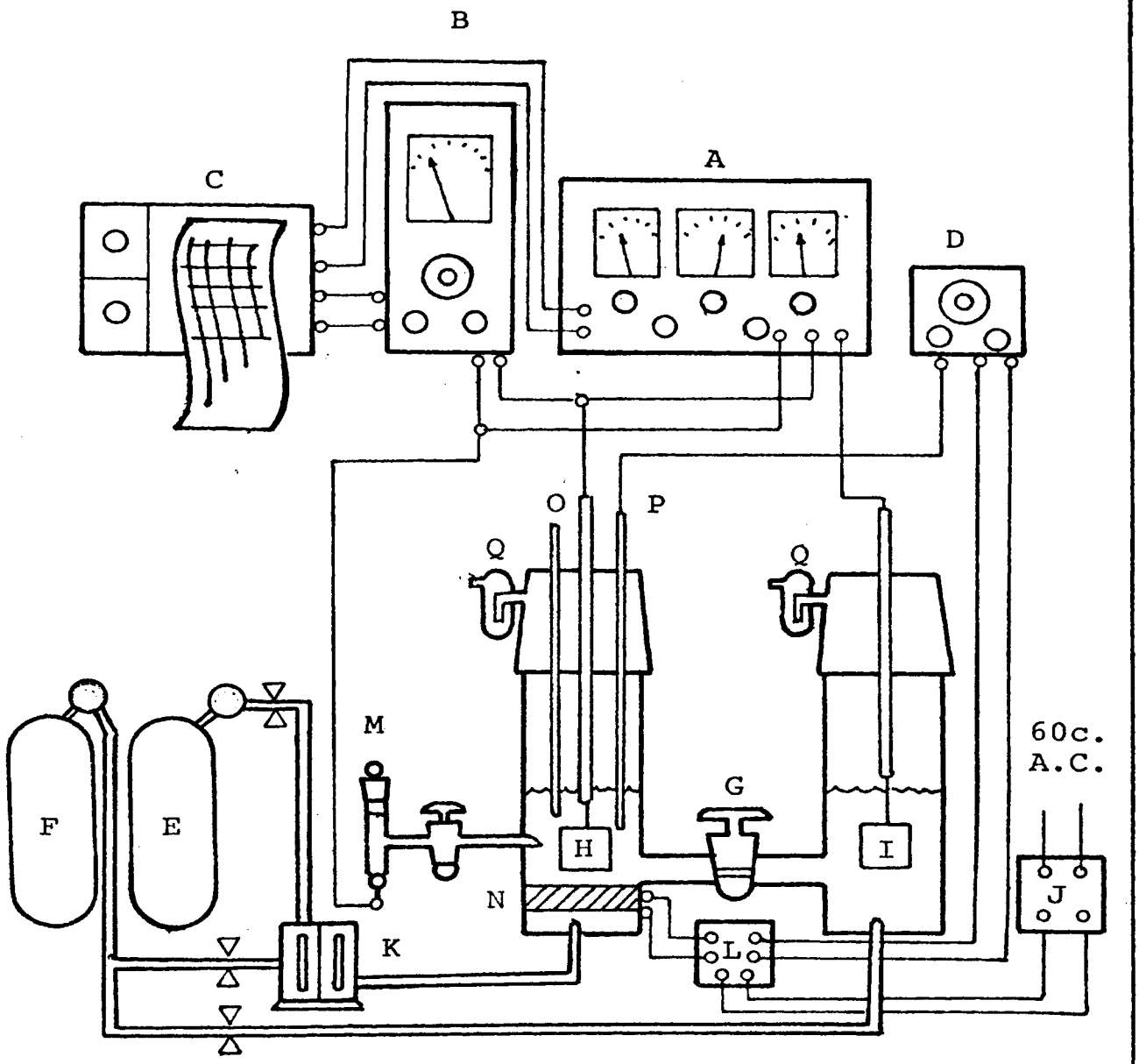

A Potentiostat
B Electrometer
C Recorder
D Temperature controller
E Acetylene tank
F Nitrogen tank
G Glass cell
H Alloy anode
I Platinum cathode
J Variac
K Gas rotameter
L Electrical relay
M Reference electrode
N Heating tape
O Thermometer
P Temperature probe
Q Water-sealed gas exit

Figure 8. Diagram of the apparatus used for current-potential studies.

A constant potential difference between the working electrode (alloy anode) and reference electrode was maintained with a potentiostat. The current, voltage, and rest potentials were recorded on a dual channel recorder. The current and potential values to the recorder were outputs from the potentiostat and electrometer, respectively.

B. Procedure

The activated anode and Pt cathode were placed into their respective compartments and the anode positioned so that its bottom edge just contacted the Luggin capillary. The nitrogen flow and heating were begun and the potential of anode recorded. The potential changed gradually (with no current flowing) and reached a constant value after about 30 minutes. The nitrogen flow to the anodic compartment was then stopped and acetylene introduced. After about one more hour, the potential again came to a steady state (rest potential with acetylene). These values varied with pH and alloy composition. Using the potentiostat, the potential of the anode was then raised to a value approximately 0.2 v above the rest potential and held constant until a steady current (less than a ten percent change per hour) was attained (usually within one hour). When the current had come to a steady value, the potential was increased by an increment of 0.025 to 0.050 v and the procedure continued until a limiting current was reached.

C. Data and Results

The polarization studies were made in solutions of pH 0.3, 2.1, 3.2, 9.8, 11.3, and 12.8. The solutions were prepared using various combinations of H_2SO_4, K_2SO_4, K_2CO_3, KOH, and distilled water. Their normality was held constant at unity. The temperature was held constant at 80 ± 0.5°C, the acetylene pressure was 1.0 atm, and its flow rate was 50 cm^3/min.

The rest potentials of the alloys in the presence of acetylene are shown in Tab. II for the various electrolytes. In acid solutions, the rest potentials of the alloys were less noble than either Pt or Au. In basic electrolytes, they were less noble than Au but more noble than Pt. The approximate pH dependencies are shown in Tab. III.

Tafel curves for the four alloys have been plotted in Figs. 9 to 12, and the data are tabulated in Appendix D. The current values at a constant potential could be reproduced within 5-10 percent. The curves for 80Pt-20Au and 20Pt-80Au are quite similar to those for pure Pt and Au, respectively. The other two alloys, 60Pt-40Au and 40Pt-60Au, have some regions of behavior similar to those of the pure metals and others with an intermediate behavior. Distinct discontinuities are observed in the 40Pt-60Au curves in basic solutions as compared with a transition region (inflection point) for pure Au and the 20Pt-80Au alloy.

In acidic solutions, an orange-brown resinous film became visible on the anode surface toward the end of each experimental run. The anolyte became clear amber in color. Basic solutions were colored similarly, but there was no visible film on the electrode surface.

The slopes of the linear Tafel region for 80Pt-20Au and 60Pt-40Au are quite similar to that of pure Pt in both acidic and basic solutions (70 mv). For the Au-rich alloys; 20Pt-80Au and 40Pt-60Au, the Tafel slopes varied from 100 to 140 mv. A summary of the Tafel slopes is shown in Tab. IV.

The effects of pH on current density are shown in Figs. 13 to 16 for a potential of 0.40 v. The currents densities were obtained by extrapolating the linear Tafel regions with their respective slopes. The pH effects ($\partial \log i / \partial pH$) have been determined and are shown in Tab. V.

TABLE II

REST POTENTIALS ON Pt-Au ALLOYS FOR THE ANODIC OXIDATION OF ACETYLENE AT 80°C

pH	Rest Potential, volts (SHE)			
	80Pt-20Au	60Pt-40Au	40Pt-60Au	20Pt-80Au
0.3	0.126	0.127	0.097	0.187
2.1	0.103	0.078	0.027	0.128
3.2	0.087	0.030	-0.080	0.032
9.8	-0.298	-0.193	-0.291	-0.023
11.3	-0.383	-0.353	-0.373	-0.193
12.6	-0.443	-0.423	-0.417	-0.423

TABLE III

pH DEPENDENCIES OF REST POTENTIALS ON Pt-Au ALLOYS FOR THE ANODIC OXIDATION OF ACETYLENE AT 80°C

Electrode	$-(\partial V_{rest}/\partial pH)$, mv	
	Acidic Electrolyte	Basic Electrolyte
80Pt-20Au	0.10	50-70
60Pt-40Au	50-70	50-70
40Pt-60Au	50-70	50-70
20Pt-80Au	50-70	140

TABLE IV

TAFEL SLOPES FOR THE ANODIC OXIDATION OF ACETYLENE ON Pt-Au ALLOYS AT 80°C

Electrode	Tafel Slope, mv	$(\partial \log i/\partial pH)_{V,T}$
80Pt-20Au	70(a)	∿0
($82\alpha_1, 18\alpha_2$)	70(b)	1
60Pt-40Au	70(a)	∿0
($67\alpha_1, 33\alpha_2$)	70(b)	1
40Pt-60Au	100(a)	∿0.2
($25\alpha_1, 75\alpha_2$)	70(b)*	1.0
	140(b)**	∿0.7
20Pt-80Au	140(a)	∿0
($2\alpha_1, 98\alpha_2$)	100(b)*	∿0.75
	140(b)**	∿0.75

(a) acidic electrolyte

(b) basic electrolyte

* Below transition region

** Above transition region

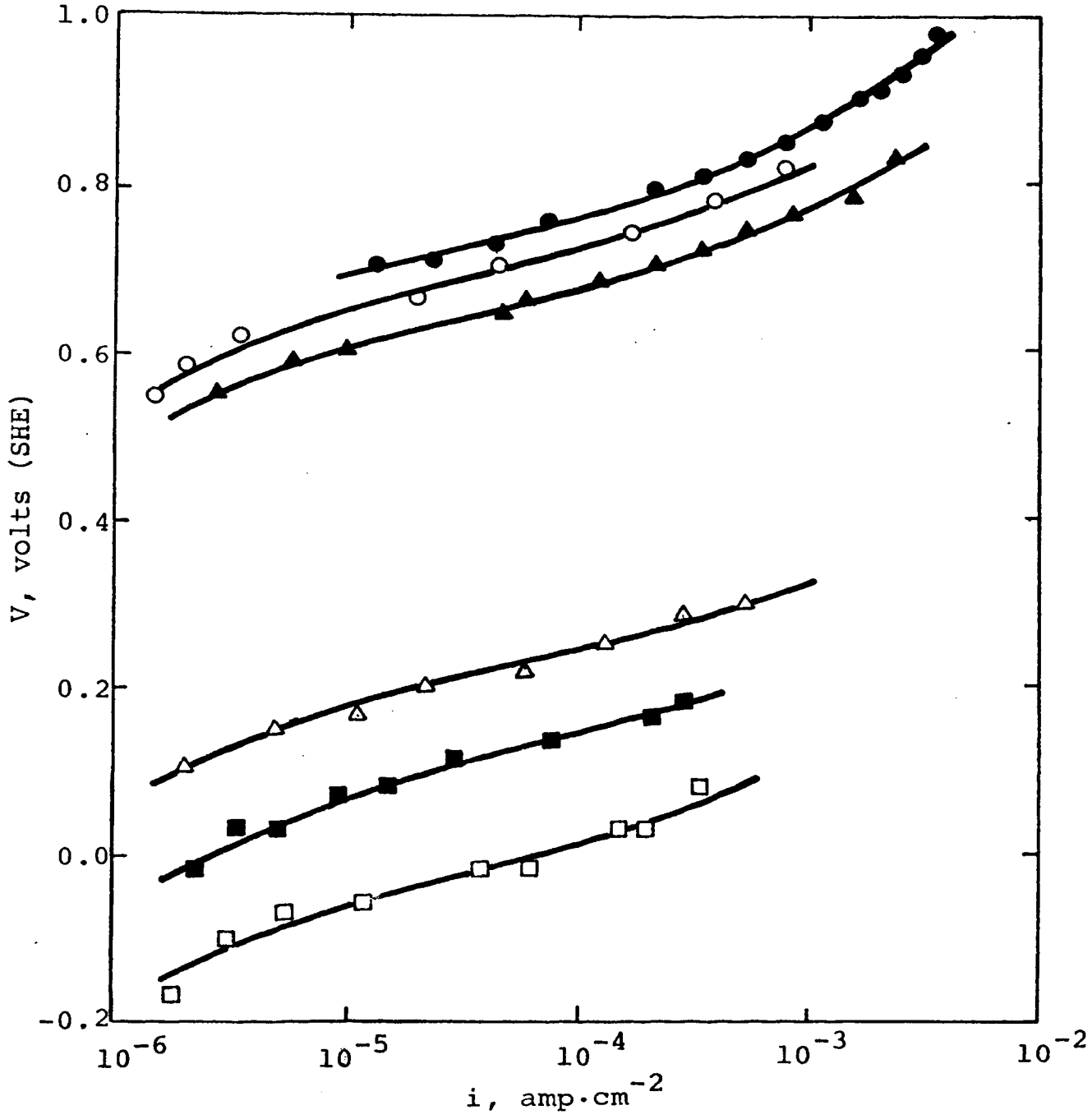

Figure 9. Effect of potential on current density for the anodic oxidation of acetylene on 80Pt-20Au alloy at 80°C (P_A= 1 atm) (●, pH= 0.4; ○ ,2.1; ▲, 4.4; △, 8.8; ■, 10.8; □, 12.8).

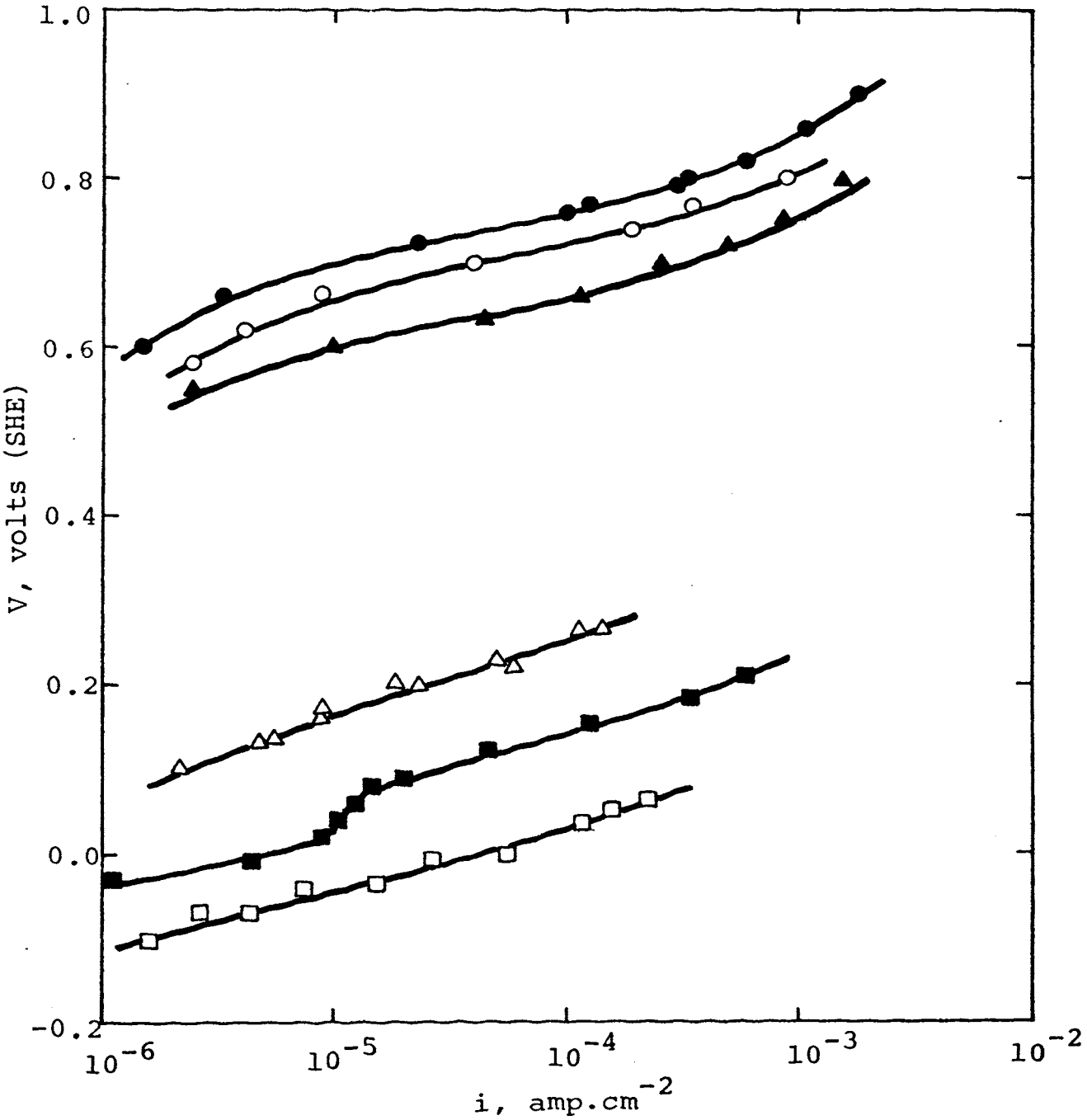

Figure 10. Effect of potential on current density for the anodic oxidation of acetylene on 60Pt-40Au alloy at 80°C (P_A= 1 atm) (●, pH= 0.3; ○,2.2; ▲, 3.3; △, 9.8; ■, 11.3; □, 12.8)

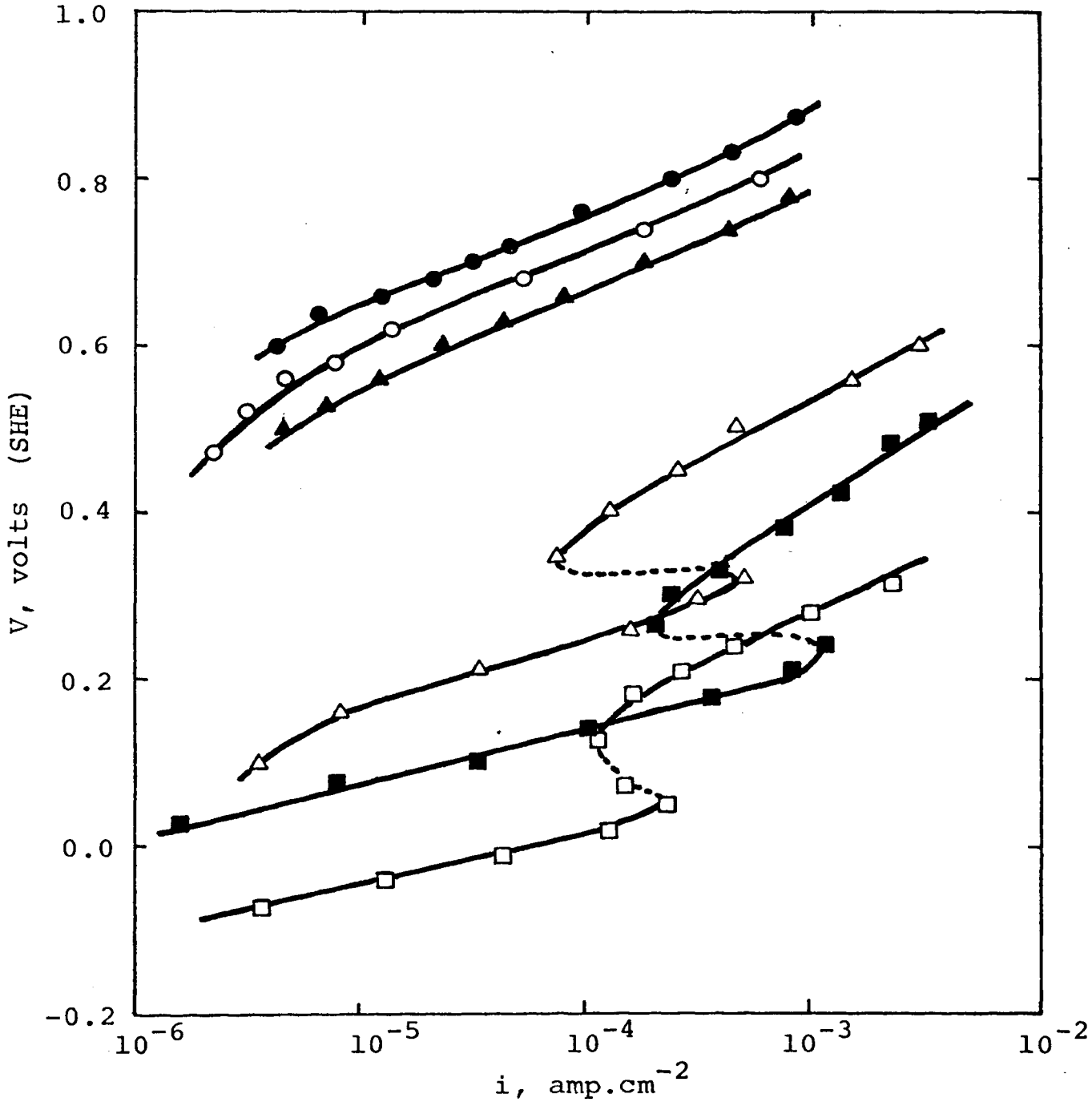

Figure 11. Effect of potential on current density for the anodic oxidation of acetylene on 40Pt-60Au alloy at 80°C (P_A= 1 atm) (●, pH= 0.35; O,2.1; ▲, 3.4; △, 9.8; ■, 11.3; □, 12.8)

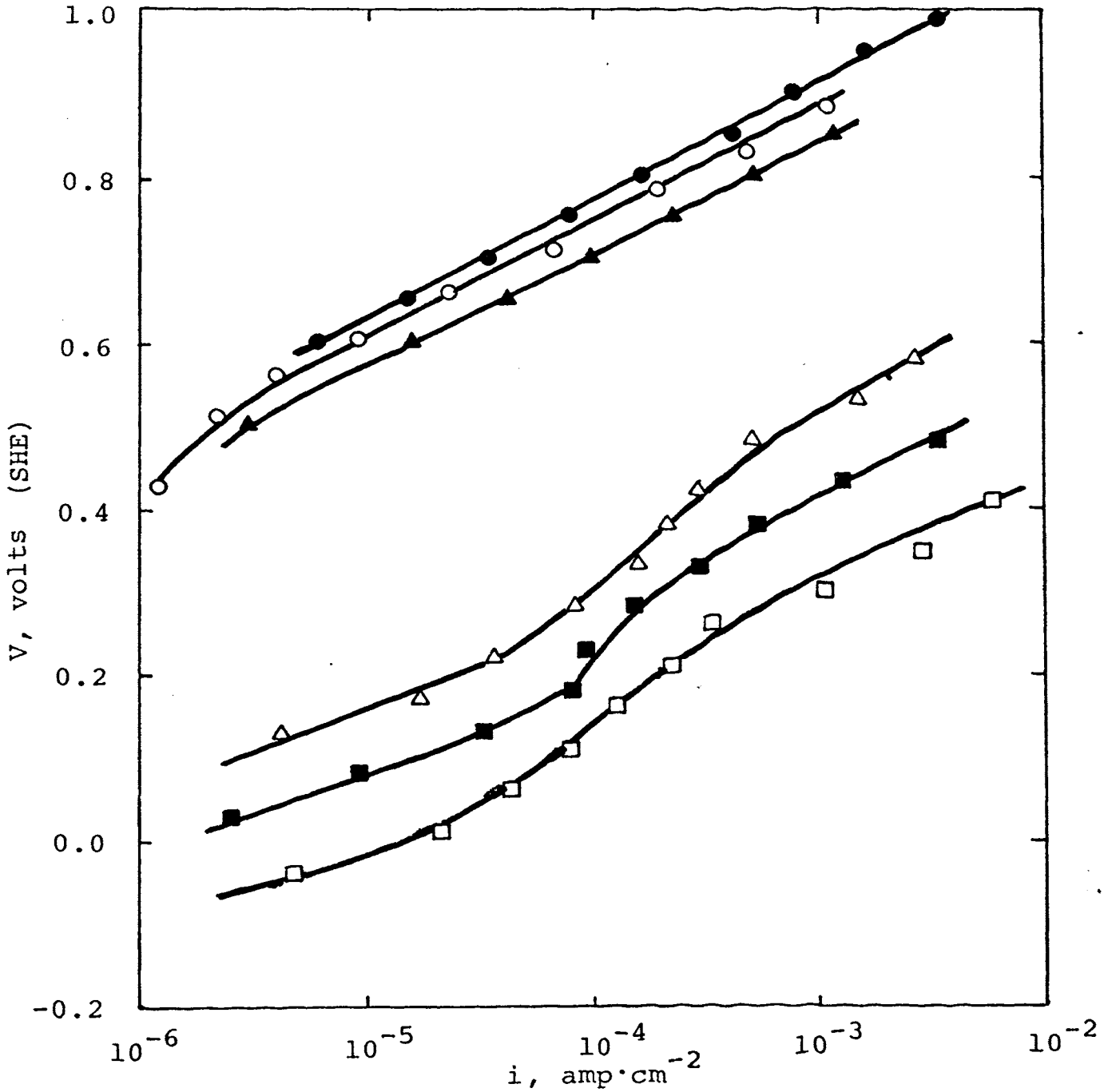

Figure 12. Effect of potential on current density for the anodic oxidation of acetylene on 20Pt-80Au alloy at 80°C (P_A= 1 atm) (●, pH= 0.35; ○,2.1; ▲, 3.4; △, 9.8; ■, 11.3; □, 12.8)

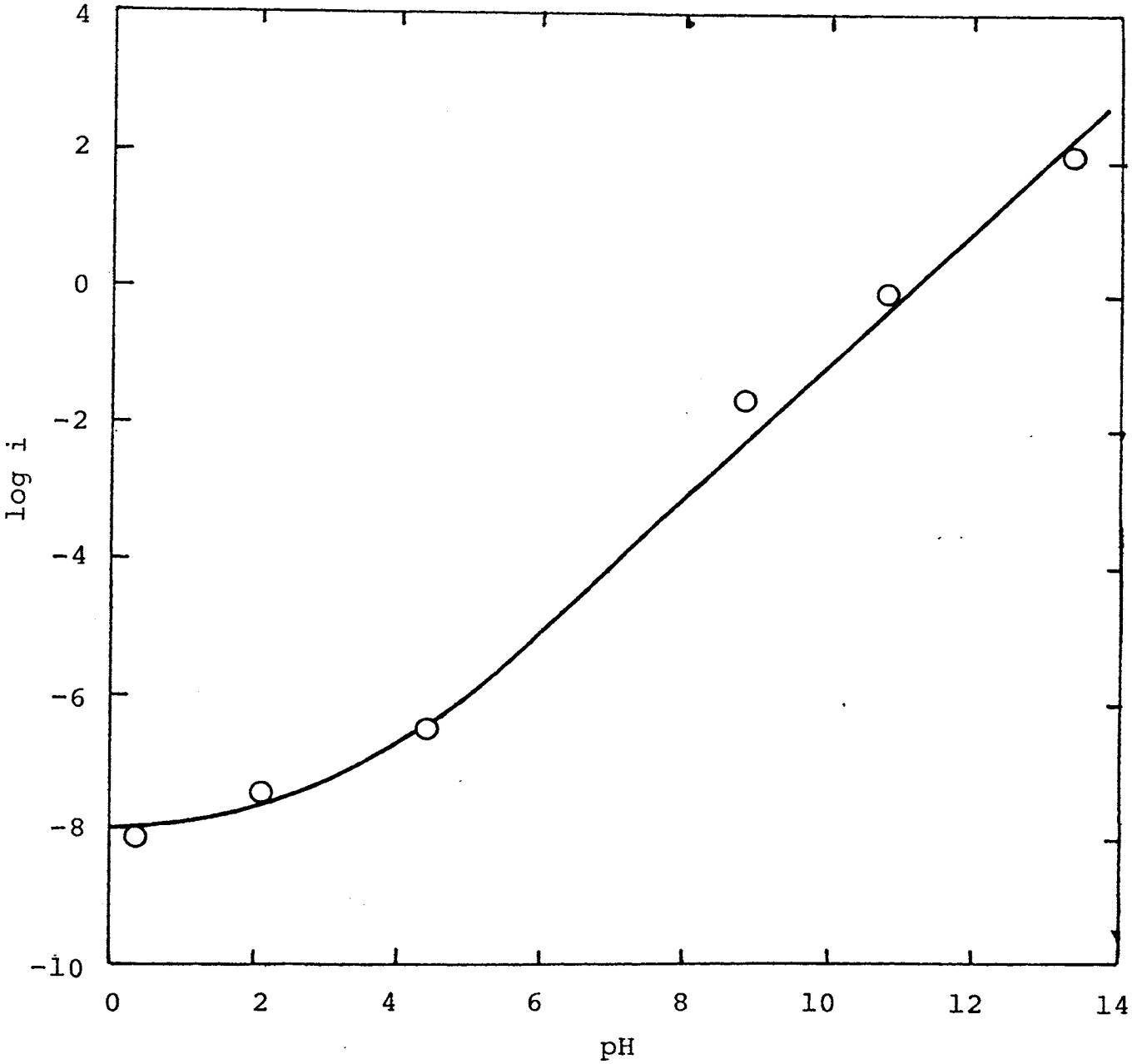

Figure 13. Effect of electrolyte pH on current density for the anodic oxidation of acetylene on 80Pt-20Au alloy at constant potential of 0.40 volts (SHE) at 80°C.

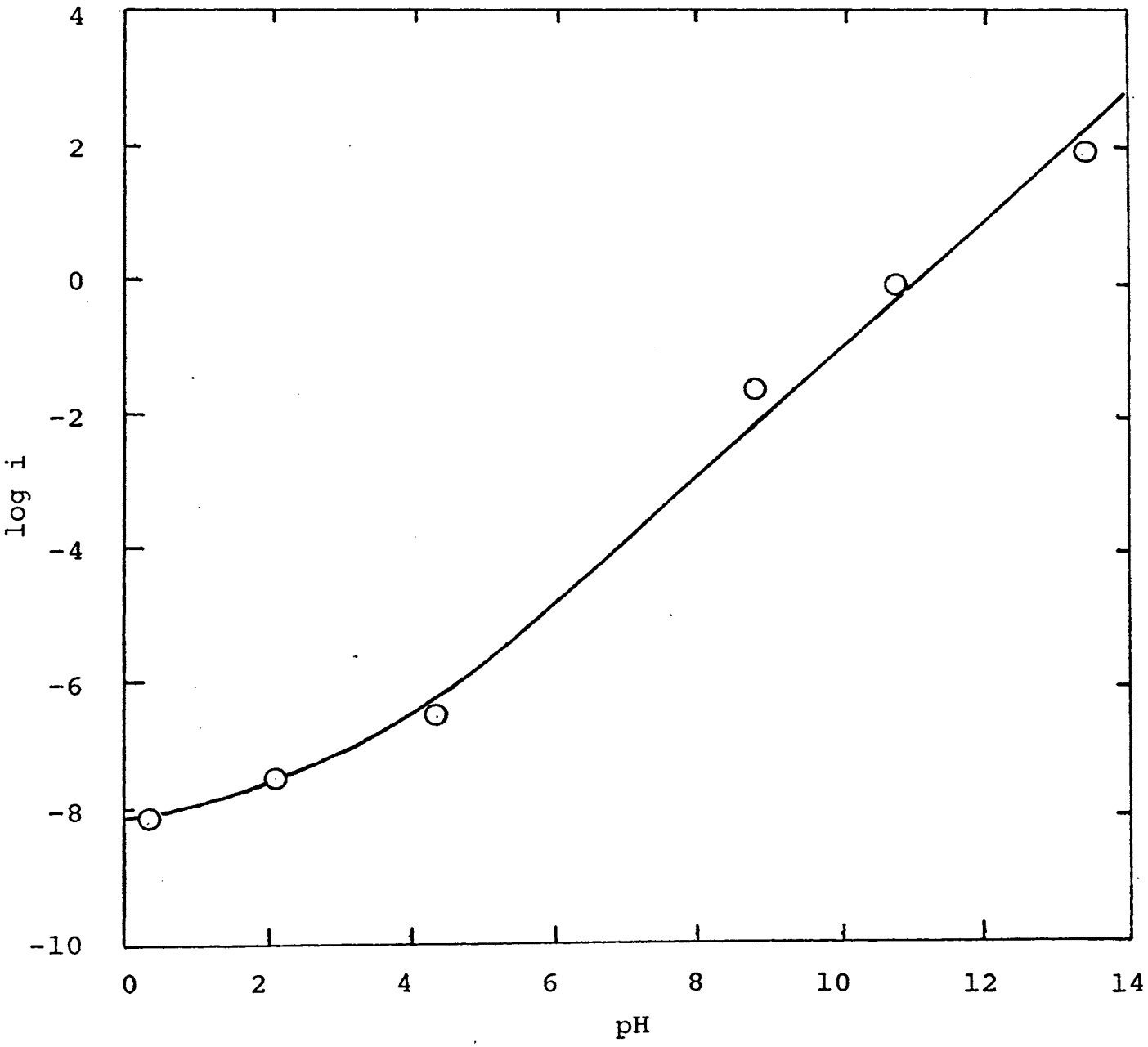

Figure 14. Effect of electrolyte pH on current density for the anodic oxidation of acetylene on 60Pt-40Au alloy at constant potential of 0.40 volts (SHE) at 80°C.

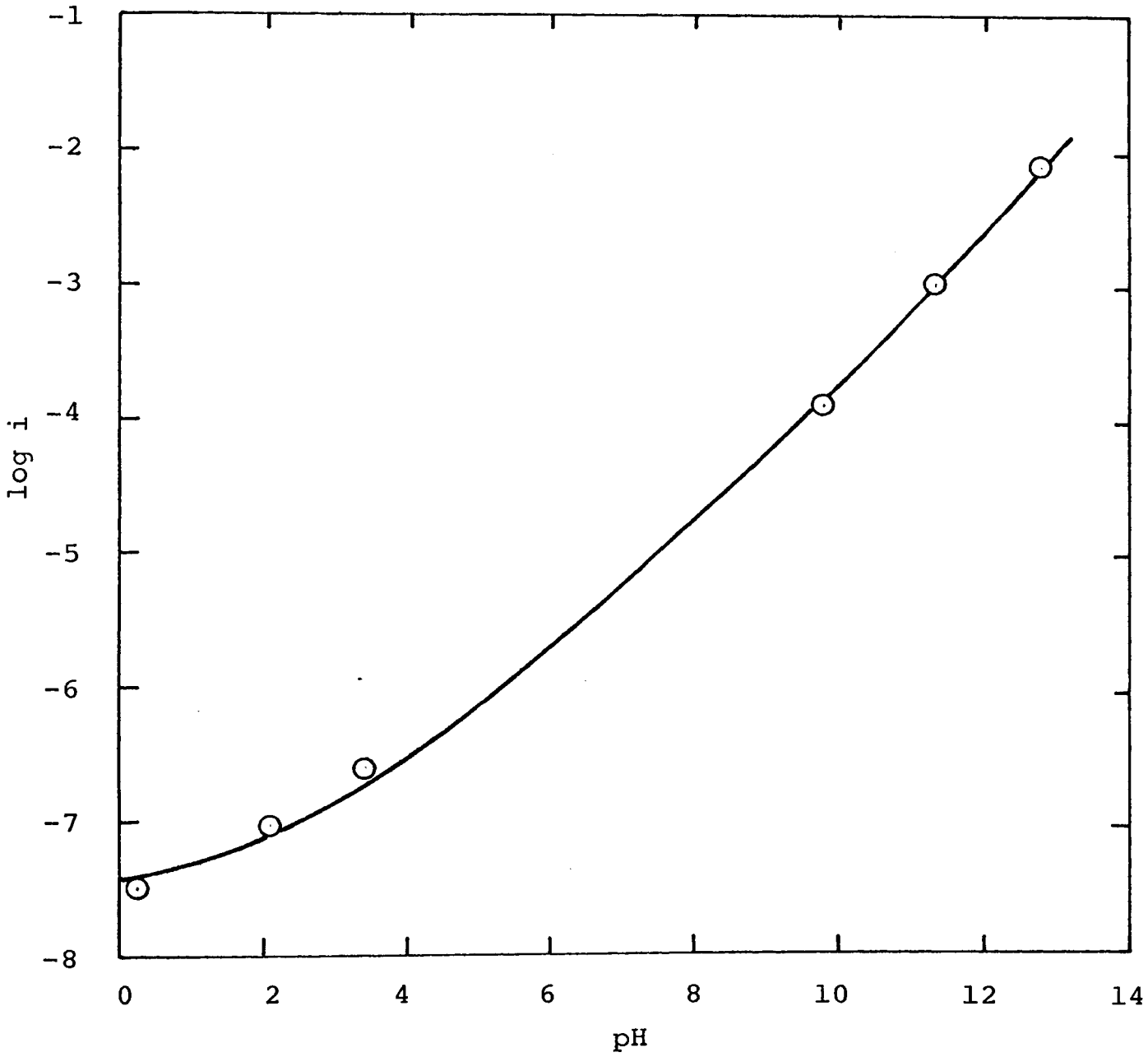

Figure 15. Effect of electrolyte pH on current density for the anodic oxidation of acetylene on 40Pt-60Au alloy at constant potential of 0.40 volts (SHE) at 80°C.

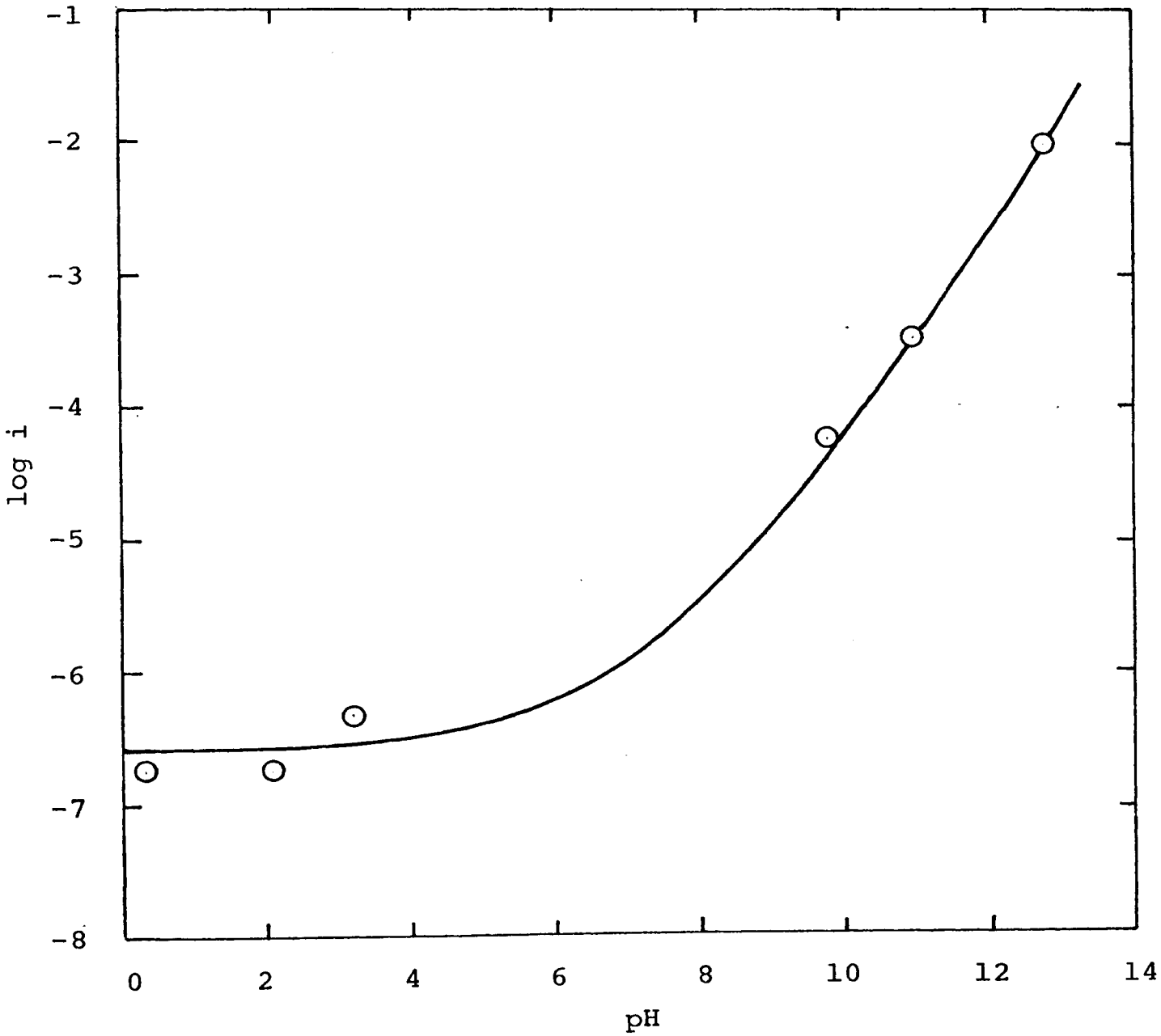

Figure 16. Effect of electrolyte pH on current density for the anodic oxidation of acetylene on 20Pt-80Au alloy at constant potential of 0.40 volts (SHE) at 80°C.

TABLE V

CURRENT-pH RELATION FOR THE ANODIC OXIDATION OF ACETYLENE ON Pt-Au ALLOYS AT CONSTANT POTENTIAL (0.40 v, SHE) at 80°C

Electrode	pH	i amp/cm^3	log i	$\left(\frac{\partial \log i}{\partial pH}\right)_{V,T}$
80Pt-20Au ($82\alpha_1, 18\alpha_2$)	0.4	7.07×10^{-9}	-8.15	0.15
	2.1	3.16×10^{-8}	-7.50	"
	4.4	2.63×10^{-7}	-6.58	"
	8.8	1.95×10^{-2}	-1.71	1
	10.8	7.08×10^{-1}	-0.15	1
	12.8	6.02×10	1.78	1
60Pt-40Au ($67\alpha_1, 33\alpha_2$)	0.3	6.92×10^{-10}	-9.16	0
	2.2	3.02×10^{-9}	-8.52	1
	3.3	1.91×10^{-8}	-7.72	1
	9.8	1.91×10^{-2}	-1.72	1
	11.3	4.78×10^{-1}	-0.32	1
	12.8	2.04×10	1.31	1
40Pt-60Au ($25\alpha_1, 75\alpha_2$)	0.35	3.16×10^{-8}	-7.50	0
	2.1	8.91×10^{-8}	-7.05	0
	3.4	2.51×10^{-7}	-6.60	0
	9.8	1.26×10^{-4}	-3.90	1
	11.3	1.05×10^{-3}	-2.98	1
	12.8	7.07×10^{-3}	-2.15	1
20Pt-80Au ($2\alpha_1, 98\alpha_2$)	0.35	1.78×10^{-7}	-6.75	0
	2.1	2.00×10^{-7}	-6.70	0
	3.4	4.90×10^{-7}	-6.31	0
	9.8	5.62×10^{-5}	-4.25	0.75
	11.3	3.24×10^{-4}	-3.49	0.75
	12.8	7.91×10^{-3}	-2.10	0.75

IV. CURRENT-TEMPERATURE STUDIES

A. Apparatus

The temperature dependence of the anodic oxidation of acetylene was studied under potentiostatic conditions. The apparatus employed was the same as that previously described.

B. Procedure

The electrolyte was charged into the cell, the anode activated and placed in the cell, and the experiment began as described previously. The potential on the anode was held constant at a value near the center of the linear Tafel region and the temperature adjusted to different values by changing the setting of the temperature controller. It was varied from 80 to 40°C by 10 degree increments. A thermometer was inserted into the cell so that the solution temperature could be monitered at all times.

C. Data and Results

The effect of temperature was studied in 1 N H_2SO_4 and 1 N KOH for each of the alloys. The experimental data have been tabulated in Appendix D. The results are also shown in Figs. 17 to 20.

The slopes of the curves, the corresponding apparent activation energies, and the effect of potential on the activation energy are given in Tab. VI.

Figs. 21 and 22 show the variation of activation energy with potential for the gold-rich alloys in 1.0 N KOH. Discontinuities upon crossing the transition region can be observed which suggest a change in the reaction mechanism.

D. Sample Calculations

The calculation of the activation energy is based upon the Arrhenius equation. The data from the current-temperature studies on 80Pt-20Au in 1.0 N H_2SO_4 (Tab. V) are used for the sample calculations.

The Arrhenius equation is,

$$\log k = - \frac{E_a}{2.3\ RT} + \log A \qquad [2.1]$$

Since k is proportional to the current, E_a can be evaluated from the log i versus 1/T plots

$$\text{slope} = \frac{-E_a}{2.3\ R} = \frac{\log i_1 - \log i_2}{(1/T_1 - 1/T_2)} = -4{,}020$$

$$E_a = -(2.3)(1.987)(-4{,}020)$$

$$= 18{,}370 \text{ cal (or } 18.4 \text{ kcal)}$$

TABLE VI

ACTIVATION ENERGIES FOR THE ANODIC OXIDATION OF ACETYLENE ON Pt-Au ALLOYS

Electrode	Electrolyte	Potential	Slope	Activation Energy	$\partial E_a/\partial V$
		v (SHE)	°K	kcal	kcal/v
80Pt-20Au ($82\alpha_1, 18\alpha_2$)	1 N H_2SO_4	0.837	-4020	18.4	-22.0
	"	0.737	-4480	20.6	
	1 N KOH	0.078	-4480	20.6	-22.0
	"	-0.021	-4960	22.8	
60Pt-40Au ($67\alpha_1, 33\alpha_2$)	1 N H_2SO_4	0.857	-4445	20.3	-25.4
	"	0.747	-5000	22.8	
	1 N KOH	0.107	-4823	22.0	-25.1
	"	0.057	-5098	23.3	
40Pt-60Au ($25\alpha_1, 75\alpha_2$)	1 N H_2SO_4	0.797	-4684	21.4	-21.6
	"	0.747	-4920	22.5	
	1 N KOH*	0.257	-2466	11.2	-20.6
	" *	0.207	-2692	12.3	
	1 N KOH**	0.020	-4000	18.3	-21.6
	" **	-0.030	-4236	19.3	
20Pt-80Au ($2\alpha_1, 98\alpha_2$)	1 N H_2SO_4	0.797	-4000	18.3	-11.0
	"	0.747	-4120	18.8	
	1 N KOH*	0.360	-2504	11.4	-12.2
	" *	0.310	-2637	12.0	
	1 N KOH**	0.060	-4353	19.9	- 9.6
	" **	0.010	-4454	20.3	

*Below transition region

**Above transition region

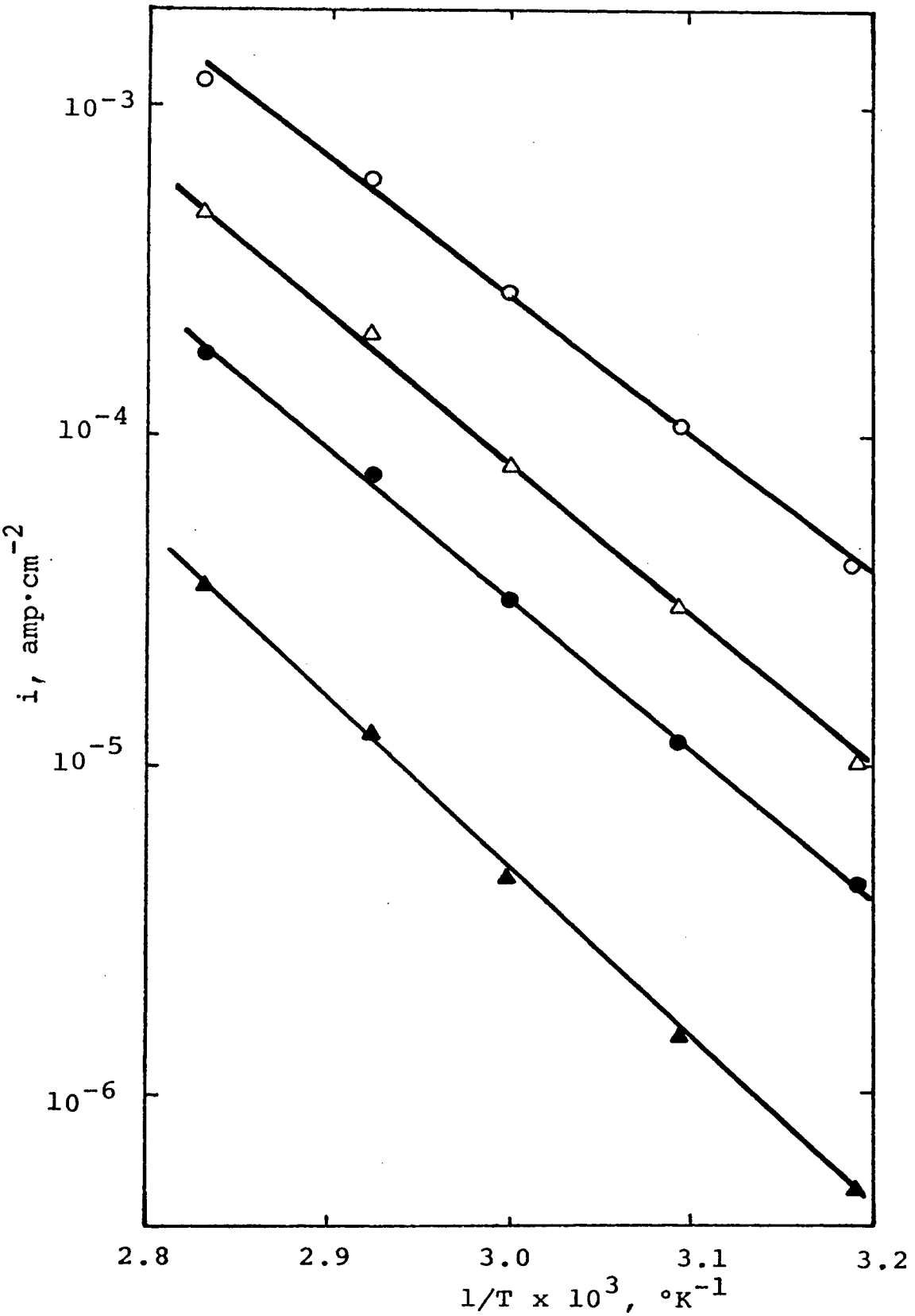

Figure 17. Effect of temperature on current density for the anodic oxidation of acetylene on 80Pt-20Au alloy at constant potential (P_A= 1 atm) (O, 0.837v, 1N H_2SO_4; ●, 0.737v, 1N H_2SO_4; Δ, 0.079v, 1N KOH; ▲, -0.021v, 1N KOH).

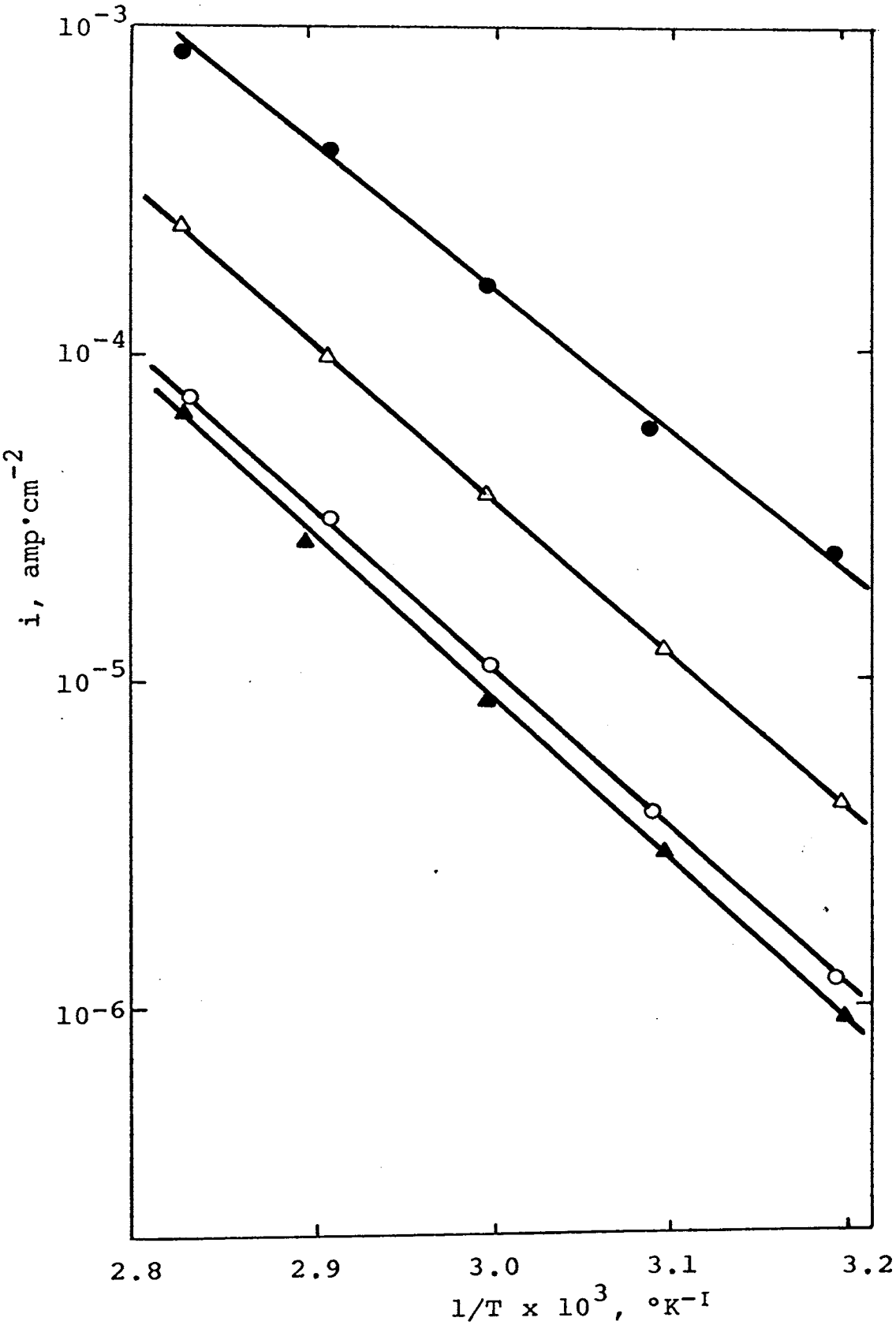

Figure 18. Effect of temperature on current density for the anodic oxidation of acetylene on 60Pt-40Au alloy at constant potential (P_A= 1 atm) (●, 0.857v, 1N H_2SO_4; O, 0.757v, 1N H_2SO_4; △, 0.107v, 1N KOH; ▲, 0.057v, 1N KOH).

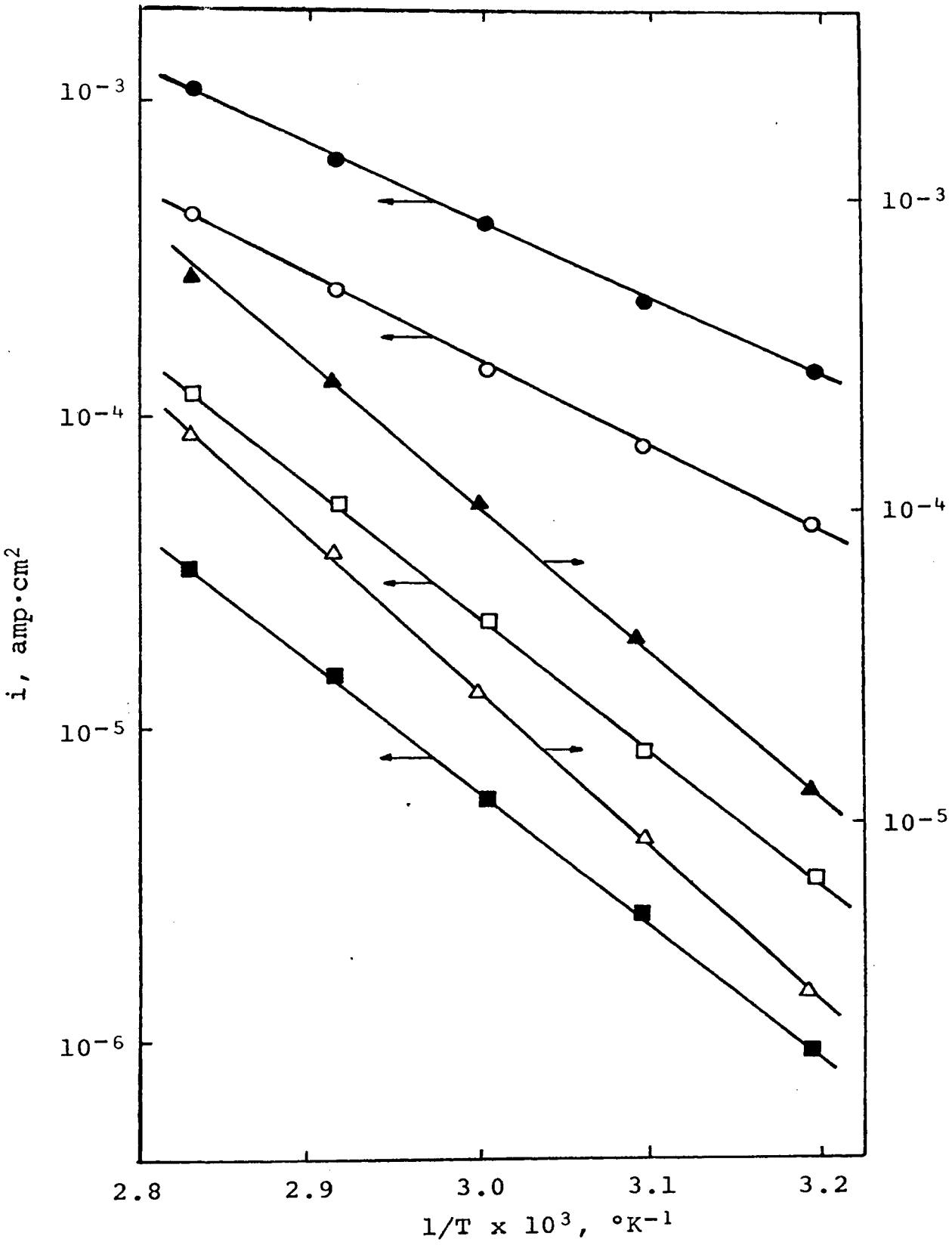

Figure 19. Effect of temperature on current density for the anodic oxidation of acetylene on 40Pt-60Au alloy at constant potential (P_A=1 atm) (▲, 0.80v, 1 N H_2SO_4; △, 0.75v, 1 N H_2SO_4, ●, 0.257v, 1 N KOH; ○, 0.207 v, 1 N KOH; □, 0.02v, 1 N KOH, ■, -0.03v, 1 N KOH).

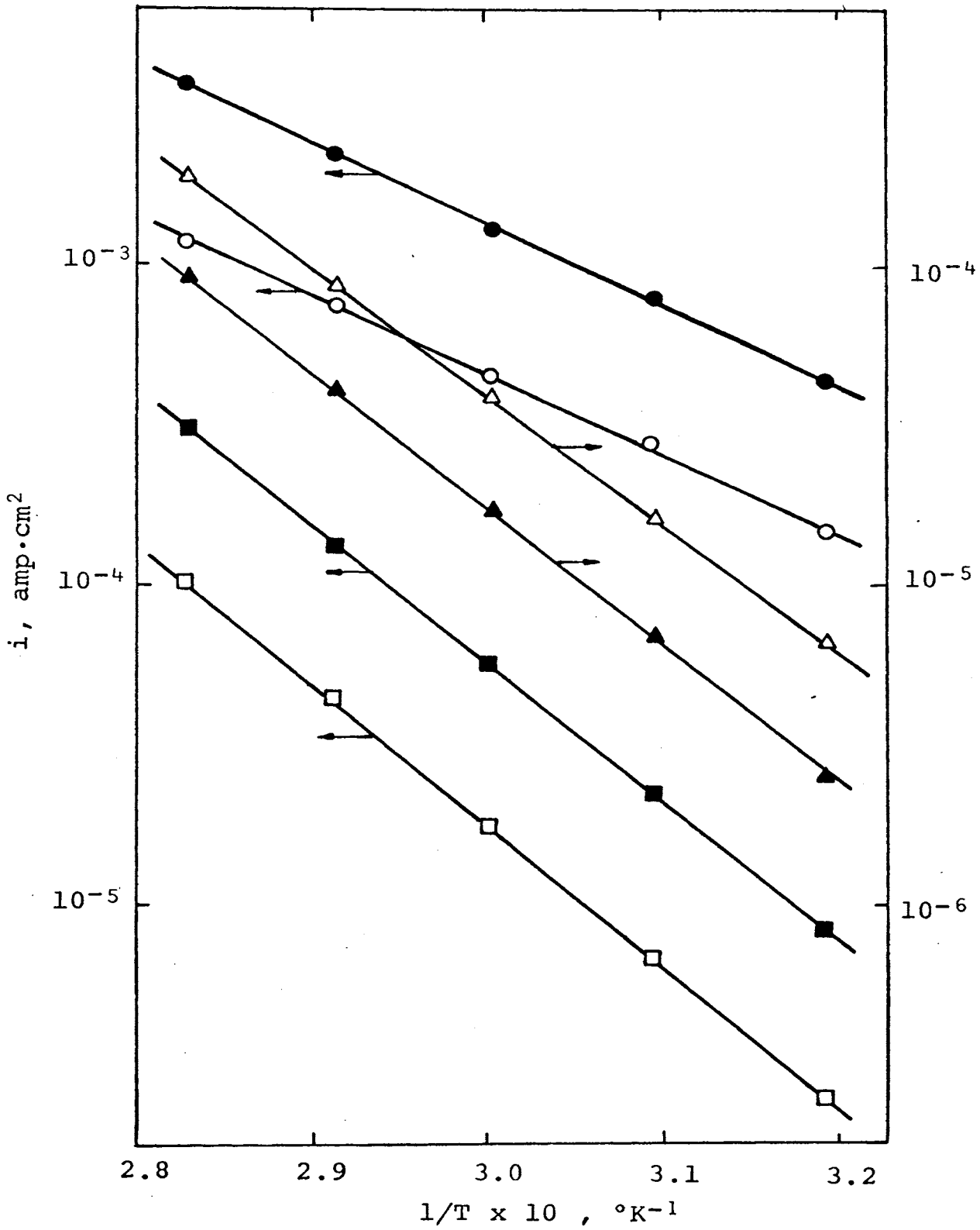

Figure 20. Effect of temperature on current density for the anodic oxidation of acetylene on 20Pt-80Au alloy at constant potential (P_A=1 atm) (△, 0.80v, 1 N H_2SO_4; ▲, 0.75v, 1 N H_2SO_4; ●, 0.36v, 1 N KOH; o, 0.31v, 1 N KOH; ■, 0.06v, 1 N KOH; □, -0.03v, 1 N KOH).

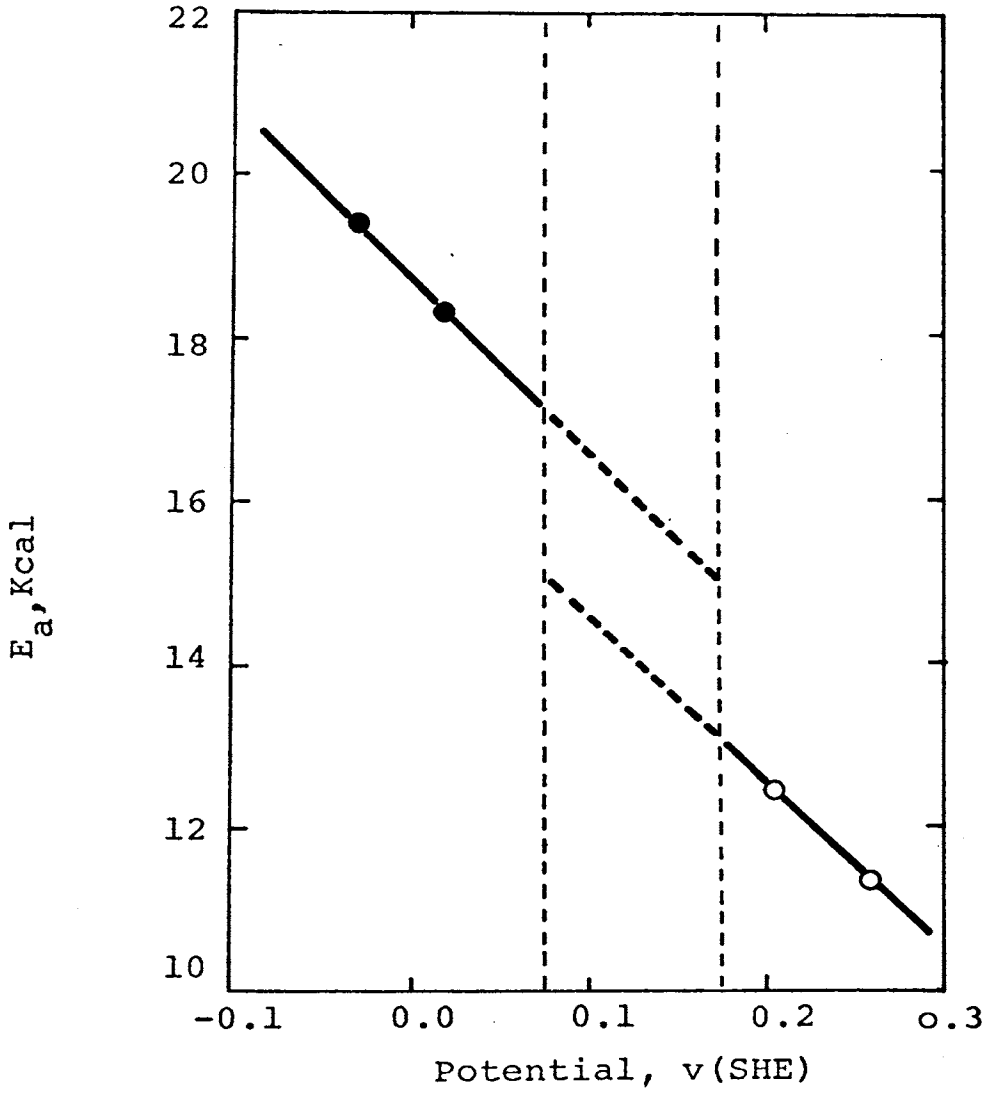

Figure 21. Effect of potential on the activation energy for the anodic oxidation of acetylene on 20Pt-80Au alloy in 1.0 N KOH (●, b.t.r.; o, a.t.r.)

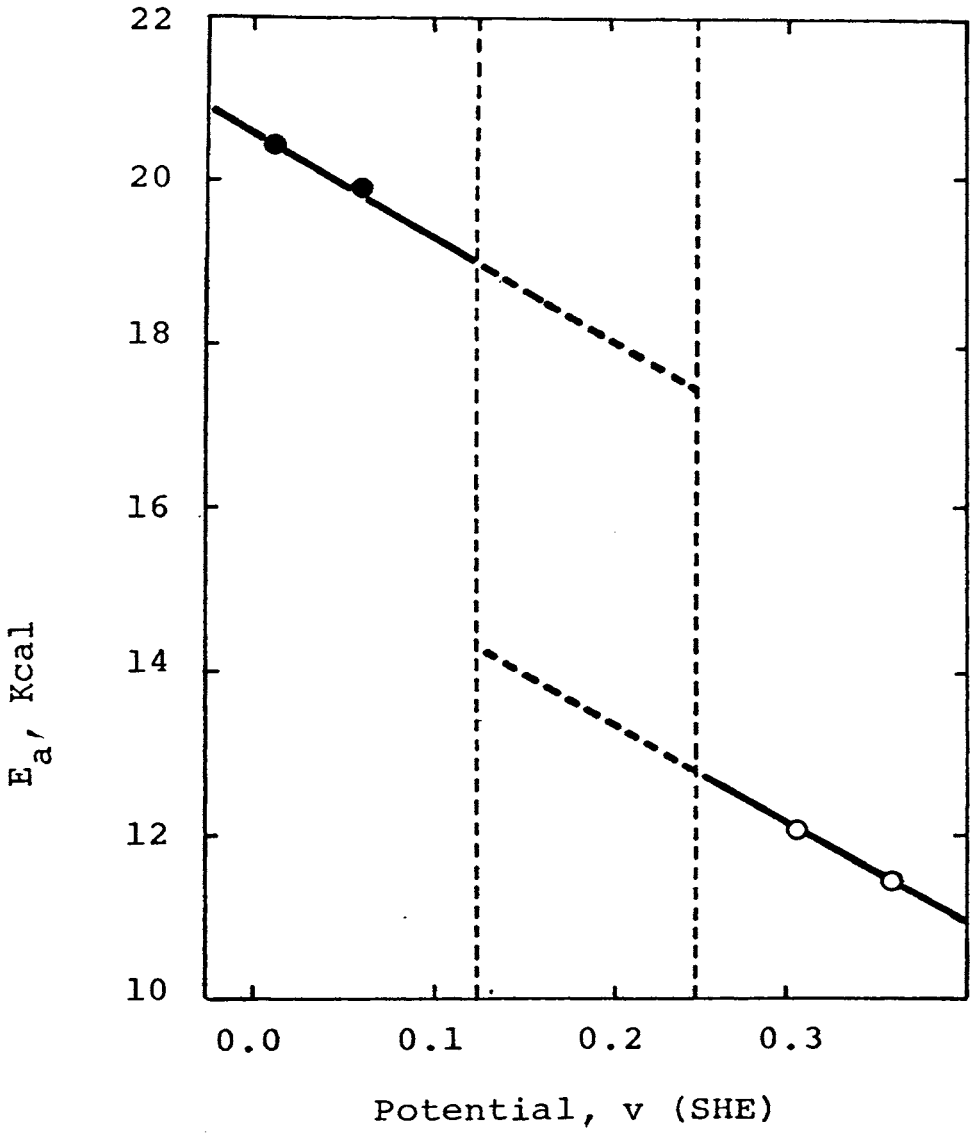

Figure 22. Effect of potential on the activation energy for the anodic oxidation of acetylene on 40Pt-60Au alloy in 1.0 N KOH (●, b.t.r.; o, a.t.r.)

V. CURRENT-PARTIAL PRESSURE STUDIES

A. Apparatus

The apparatus was the same as described previously.

B. Procedure

The procedure was essentially the same as discussed previously. The experiments were began at potentials selected within the linear Tafel region with an acetylene partial pressure of 1 atm. When a steady state current was obtained at 1.0 atm, the acetylene pressure was reduced to 0.5 atm and its steady state current obtained. This procedure was repeated until the partial pressure was reduced to 0.01 atm. The partial pressures were obtained by mixing acetylene and nitrogen with a calibrated gas proportioner. The total gas flow rate through the cell was increased to 100 cm^3/min to facilitate equilibration of the anolyte and the gaseous atmosphere. The increased flow rate did not affect the magnitude of the steady state currents.

C. Data and Results

Partial pressure studies were made in 1 N H_2SO_4 and 1 N KOH at several potentials within the linear Tafel regions. The data are tabulated in Appendix D and have been plotted in Figs. 23 to 26. To facilitate comparisons the results are also summarized in Tab. VII.

In 1 N H_2SO_4, the current increased with decreasing acetylene partial pressure throughout the entire region on all alloys. In 1 N KOH, there were two types of behavior. Those in the first group were the alloys having the higher contents of Pt (80Pt-20Au and 60Pt-40Au). These exhibited a negative effect for partial pressures greater than 0.03 atm; at lower pressures the effect became positive. The second group contained the alloys with the higher Au contents. At potentials above the transition region, the current increased with increasing acetylene partial pressure. This positive effect in 1 N KOH was more pronounced than the corresponding negative effect in 1 N H_2SO_4. At potentials below the transition region, a negative effect was observed on the 40Pt-60Au alloy and a positive effect on the 20Pt-80Au alloy.

TABLE VII

QUALITATIVE EFFECT OF PARTIAL PRESSURE ON CURRENT FOR THE ANODIC OXIDATION OF ACETYLENE ON Pt-Au ALLOYS AT 80°C

Electrode	Electrolyte	Potential v (SHE)	$\left[\frac{\partial i}{\partial p}\right]_{T,V}$ amp/atm
80Pt-20Au ($82\alpha_1, 18\alpha_2$)	1 N H_2SO_4	0.697	neg
	"	0.747	"
	"	0.797	"
	1 N KOH	-0.043	"
	"	0.007	"
	"	0.057	neg→pos
60Pt-40Au ($67\alpha_1, 33\alpha_2$)	1 N H_2SO_4	0.647	neg
	"	0.697	"
	"	0.747	"
	1 N KOH	-0.043	"
	"	0.007	"
	"	0.057	neg→pos
40Pt-60Au ($25\alpha_1, 75\alpha_2$)	1 N H_2SO_4	0.697	neg
	"	0.747	"
	"	0.797	"
	1 N KOH	-0.043*	"
	"	0.007**	neg→pos
	"	0.257*	pos
20Pt-80Au ($2\alpha_1, 98\alpha_2$)	1 N H_2SO_4	0.697	neg
	"	0.747	"
	"	0.797	neg→pos
	1 N KOH	0.007*	pos
	"	0.057*	"
	"	0.257**	pos
	"	0.287**	"

*Below transition region

**Above transition region

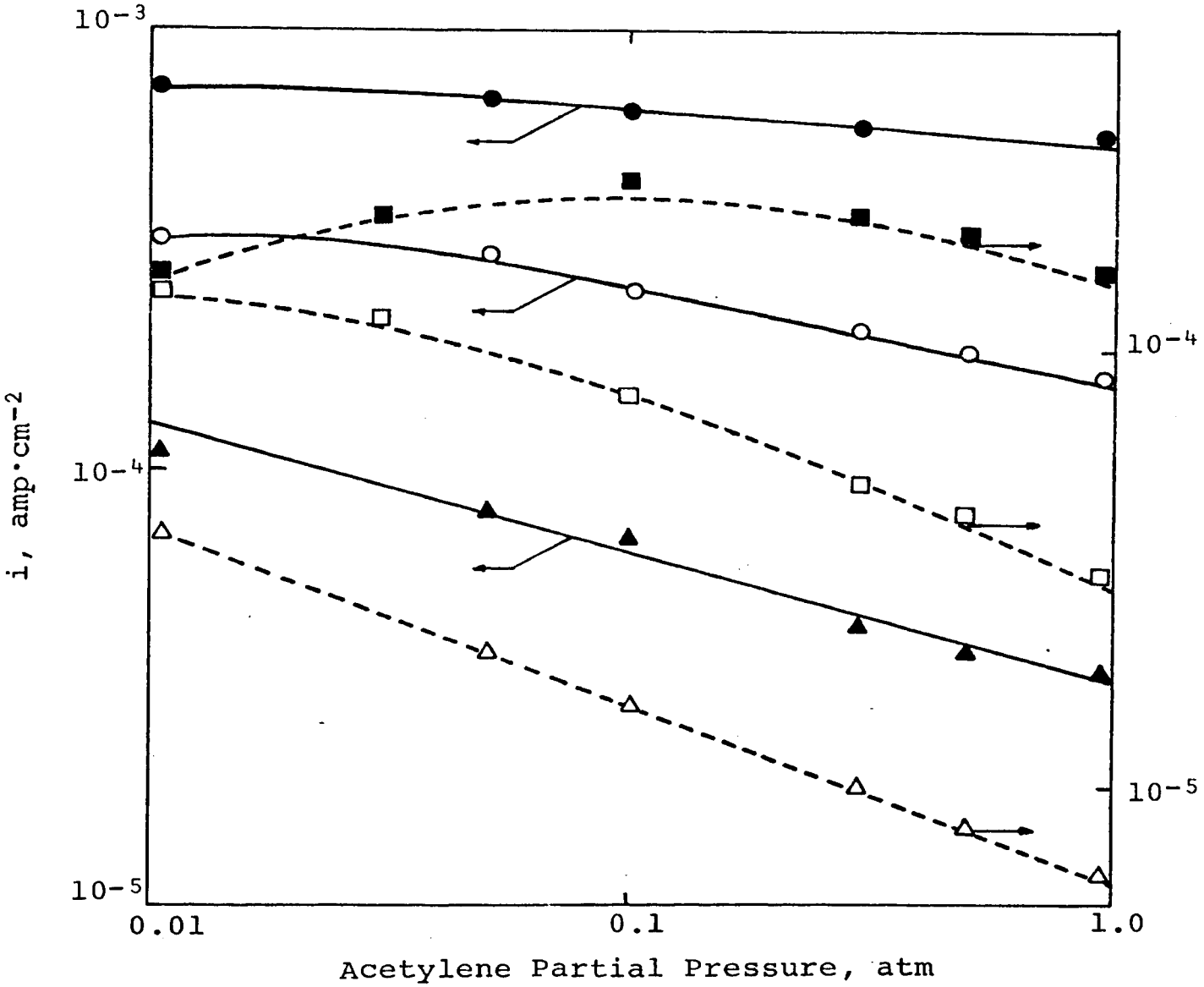

Figure 23. Effect of pressure on current density for the anodic oxidation of acetylene on 80Pt-20Au alloy at 80°C (●, 0.797v, 1 N H_2SO_4; o, 0.747v, 1 N H_2SO_4; ▲, 0.697v, 1 N H_2SO_4; ■, 0.057v, 1 N KOH; □, 0.007v, 1 N KOH; Δ, -0.043v, 1 N KOH).

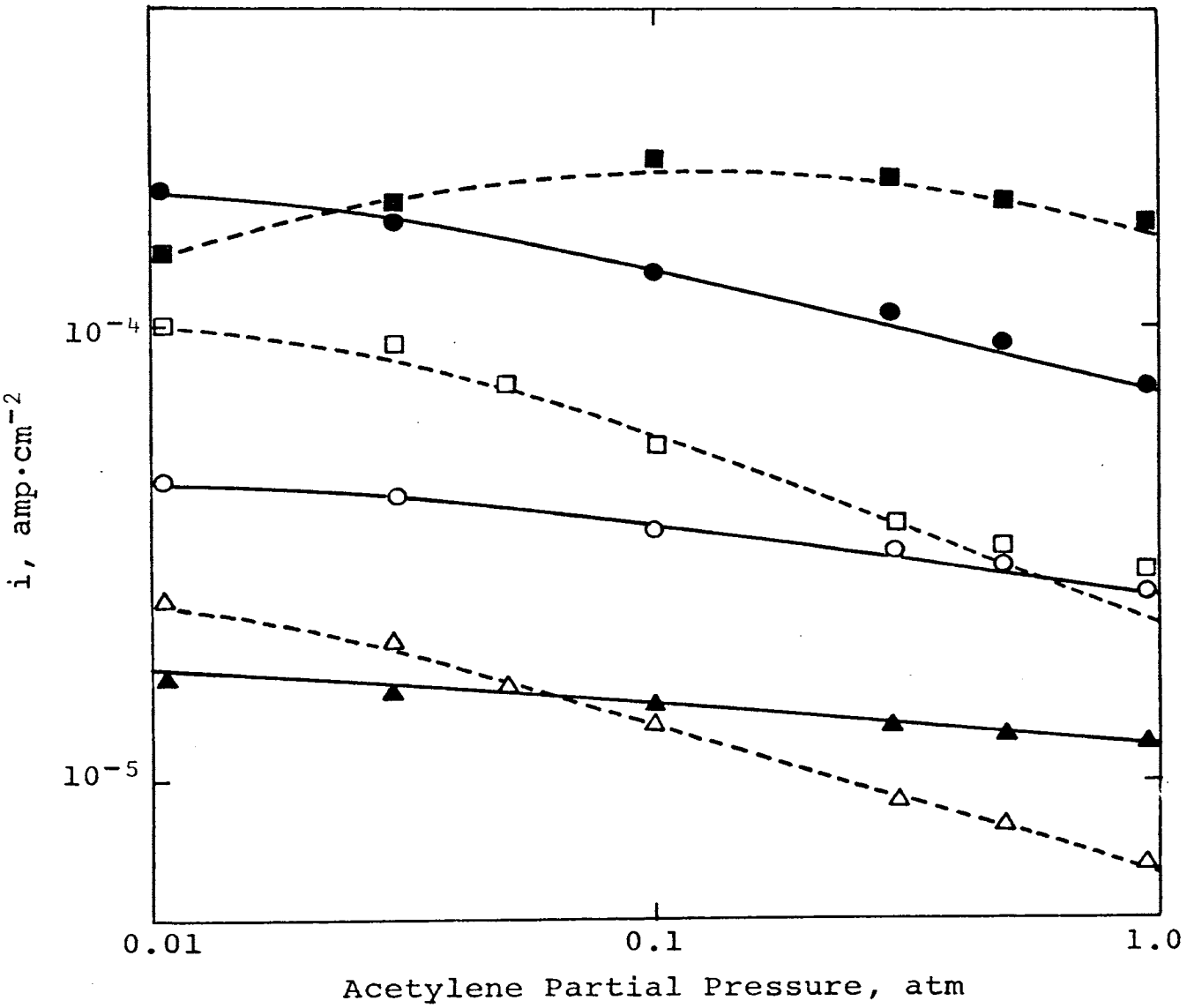

Figure 24. Effect of pressure on current density for the anodic oxidation of acetylene on 60Pt-40Au alloy at 80°C (●, 0.747v, 1 N H_2SO_4; o, 0.697v, 1 N H_2SO_4; ▲, 0.647v, 1 N H_2SO_4; ■, 0.057v, 1 N KOH; □, 0.007v, 1 N KOH; Δ, -0.043v, 1 N KOH).

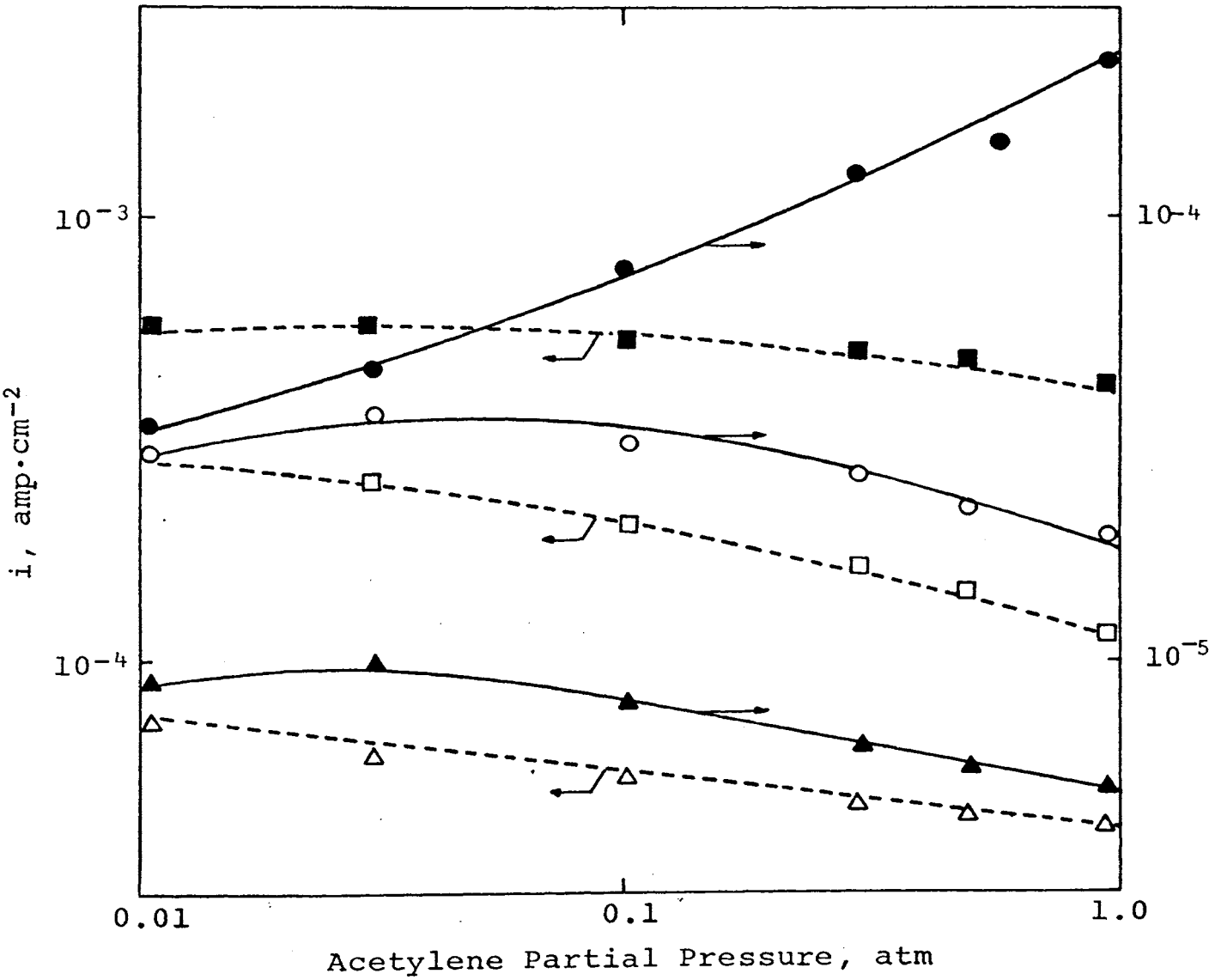

Figure 25. Effect of pressure on current density for the anodic oxidation of acetylene on 40Pt-60Au alloy at 80°C (■, 0.78v, 1 N H_2SO_4; □, 0.75v, 1 N H_2SO_4; Δ, 0.70v, 1 N H_2SO_4; ●, 0.26v, 1 N KOH; o, 0.01v, 1 N KOH; ▲, -0.05v, 1 N KOH).

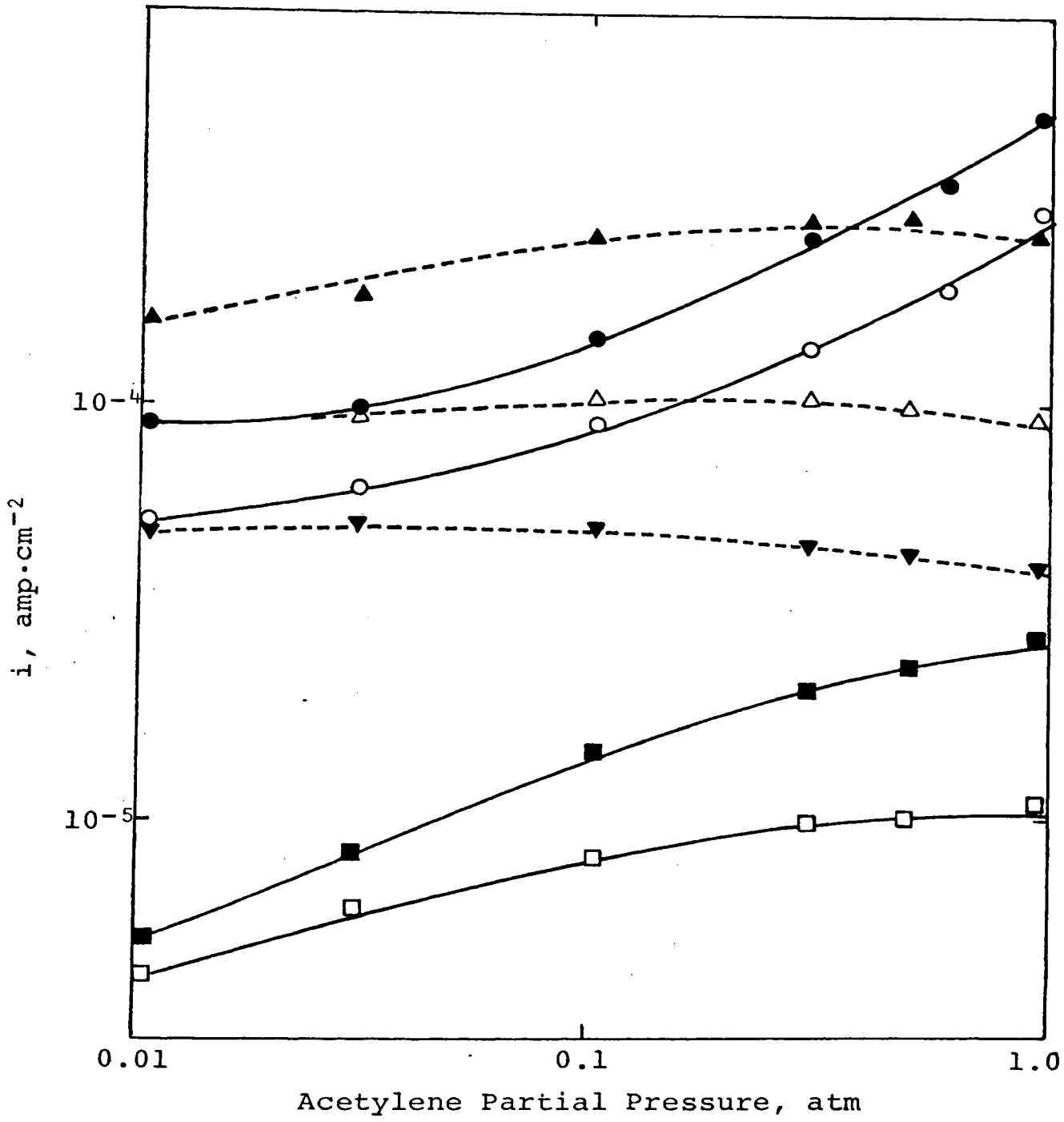

Figure 26. Effect of pressure on current density for the anodic oxidation of acetylene on 20Pt-80Au alloy at 80°C (▲, 0.797v, 1 N H_2SO_4; △, 0.747v, 1 N H_2SO_4; ▼, 0.697v, 1 N H_2SO_4; ●, 0.287v, 1 N KOH; o, 0.257v, 1 N KOH; ■, 0.057v, 1 N KOH, □, 0.007v, 1 N KOH).

VI. FARADAIC EFFICIENCY STUDIES

A. Apparatus

The apparatus used in this section was similar to that used previously. A schematic diagram is shown in Fig. 27. The experiments were run galvanostatically with a constant voltage power supply by including a large resistance in the circuit in series with the cell. The exit gases from the anodic compartment were passed through a train which included concentrated H_2SO_4, ascarite, and a water-sealed outlet. The concentrated H_2SO_4 was used to remove moisture from the gas before it contacted the ascarite. The sealed outlet prevented atmospheric CO_2 from contacting the ascarite.

B. Procedure

The rest potential was obtained in the same manner as for potentiostatic experiments. The stopcock between the compartments was then closed and the current adjusted to a desired value by varying the voltage applied by the power supply. For 1 N H_2SO_4 electrolyte (after the cell had operated several hours to reach a steady state), the exit gases from the anodic compartment were directed through the gas train which contained a weighed amount of ascarite. After a predetermined time interval had elapsed, the experiment was stopped and the weight of CO_2 produced during

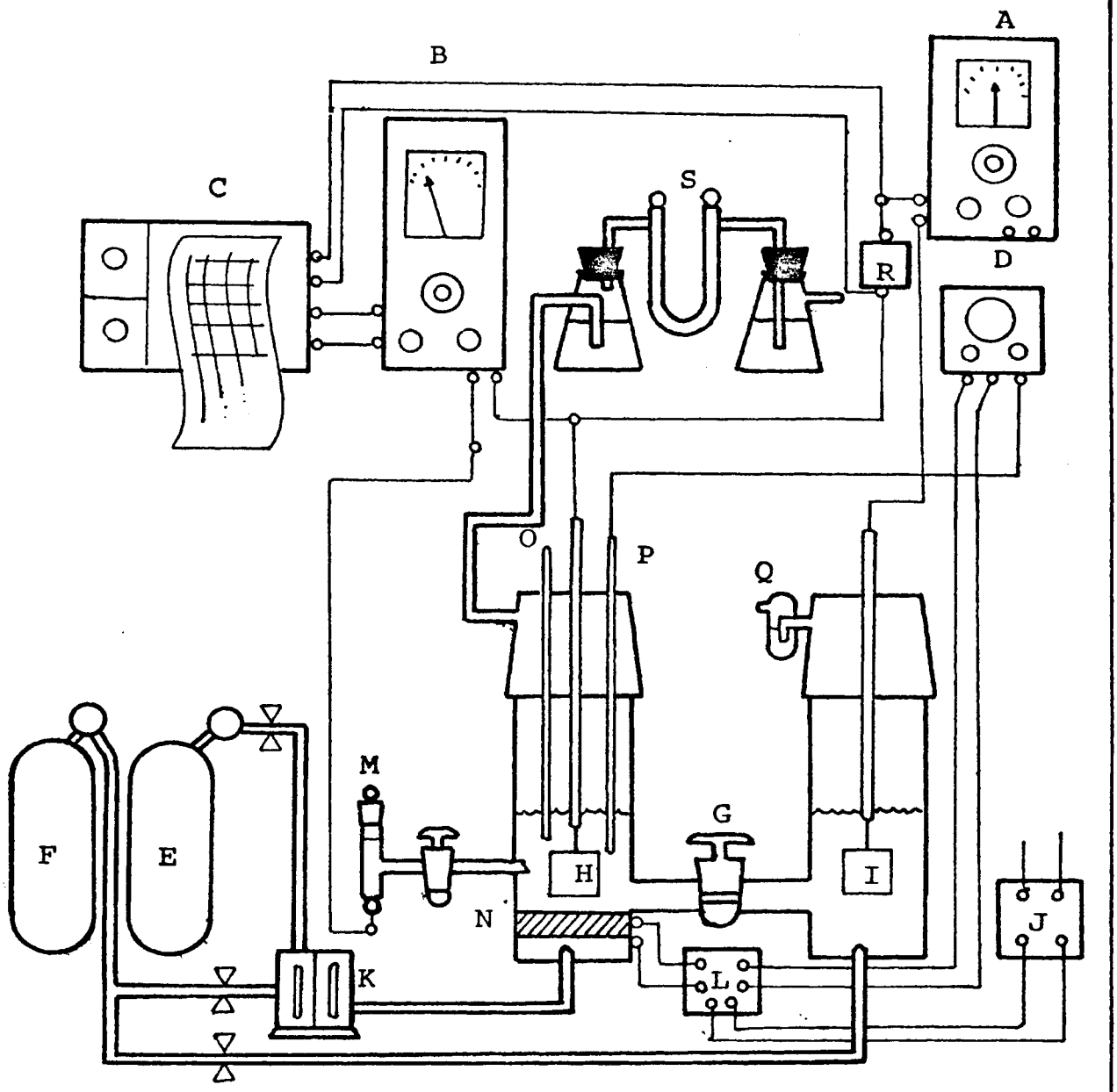

A Potentiostat
B Electrometer
C Recorder
D Temperature controller
E Acetylene tank
F Nitrogen tank
G Glass cell
H Alloy anode
I Platinum cathode
J Variac
K Gas rotameter
L Electrical relay
M Reference electrode
N Heating tape
O Thermometer
P Temperature probe
Q Water-sealed gas exit
R Resistor
S Gas train

Figure 27. Schematic diagram of the apparatus used for the faradaic efficiency studies.

the time interval determined by the weight gain of the ascarite. The efficiency determinations were made at potentials within the linear Tafel region. The potential was monitered continuously to insure that it stayed within the linear region.

The above procedure was modified for 1 N KOH electrolyte since the CO_2 produced was adsorbed by the electrolyte. For this case, the cell was run as usual but with no gas train. After the experiment was concluded, the anolyte was acidified and heated gently to release the CO_2 which was carried into the gas train with a stream of nitrogen. The CO_2 produced was determined as described previously except that a correction was made for the initial carbonate in the electrolyte.

C. Data and Results

The results of the faradaic efficiency studies are shown in Tab. VIII. The anolyte became clear amber in color during the efficiency studies. The electrode became covered with a thin dark-brown resin in 1 N H_2SO_4 anolyte. The resin was also apparently insoluble in carbon tetrachloride, ethyl ether, benzene, and n-hexane, but dissolved appreciably in hot KOH solutions to give amber colored solutions.

D. Sample Calculations

The calculations in this section are based on the complete oxidation of acetylene to CO_2 and H_2O (or H^+) as follows:

$$C_2H_2 + 4\ H_2O \rightarrow 2\ CO_2 + 10\ H^+ + 10\ e \quad \text{(acidic solution)}$$

$$C_2H_2 + 10\ OH^- \rightarrow 2\ CO_2 + 6\ H_2O + 10\ e \quad \text{(basic solution)}$$

Data for the calculations are taken from Tab. VIII for the 72-hour efficiency study on the 80Pt-20Au alloy in 1.0 N H_2SO_4 at 1.0 atm acetylene pressure.

The theoretical amount of CO_2 formed per Faraday of charge passed can be calculated using Faraday's law

$$M_t = \frac{it}{5F} = \frac{(0.005)(72)(3600)}{(5)(96,500)} = 2.682 \times 10^{-3} \text{ moles}$$

The amount of CO_2 actually formed was determined from the difference in weight of the ascarite before and after the experiment,

$$M_a = (M_2 - M_1)/(44) = \frac{0.0891}{44} = 2.021 \times 10^{-3} \text{ moles}$$

The faradaic efficiency, defined as the actual CO_2 formed divided by the theoretical amount for complete oxidation is

$$\frac{M_a}{M_t} = \frac{2.02 \times 10^{-3}}{2.682 \times 10^{-3}} = 0.754 \text{ (or 75 percent)}$$

TABLE VIII

CARBON DIOXIDE FARADAIC EFFICIENCY FOR THE ANODIC OXIDATION OF ACETYLENE ON Pt-Au ALLOYS AT 80°C AND 1 ATM

Electrode	Electrolyte	Current ma	Time hours	Efficiency percent
80Pt-20Au	1 N H_2SO_4	5.0	72	75
($82\alpha_1, 18\alpha_2$)	"	5.0	75	77
	1 N KOH	3.0	72	80
	"	3.0	72	82
60Pt-40Au	1 N H_2SO_4	10.0	32	73
($67\alpha_1, 33\alpha_2$)	1 N KOH	3.0	72	82
40Pt-60Au	1 N H_2SO_4	10.0	32	69
($25\alpha_1, 75\alpha_2$)	1 N KOH	5.0	72	78
20Pt-80Au	1 N H_2SO_4	10.0	32	67
($2\alpha_1, 98\alpha_2$)	1 N KOH	5.0	48	81

*Area of electrode = 15.1 cm^2

E. By Product Analysis

The following analyses were performed to obtain information about the by-products (colored material in the anolyte and film on the anode) from the acetylene oxidation:

1. The 1 N H_2SO_4 anolyte was extracted with ether, carbon tetrachloride, benzene, and n-hexane. Only in ether was there any visible evidence of extraction.
2. The anolyte was subjected to an aldehyde test using Schiff's reagent and a ketone test using a semicarbazide. The results were negative for both cases.
3. Solvation of the resinous material was attempted but it appeared inert to all solvents except base. It dissolved appreciably 1 N KOH, especially when heated slightly.
4. A single beam reflectance spectrum using an infrared spectrophotometer was made of the resin film adhering to the anode. The spectrum indicated the presence of C-C and C=C, but not C=O nor O-H.

These analyses eliminate compounds containing appreciable quantities of carbonyl and hydroxyl groups. Since the bonding is probably conjugated, it is likely that the resin has a polyacetylene structure, i.e.,

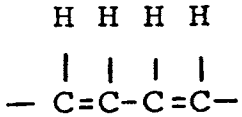

CHAPTER IV

DISCUSSION

The experimental results indicate the alloys can be classified into three categories insofar as acetylene oxidation is concerned. Those in the first and second categories have the higher contents of Pt or Au (80Pt-20Au and 20Pt-80Au) and behave similar to pure Pt and Au, respectively. For the electrodes with intermediate compositions (60Pt-40Au and 40Pt-60Au), separate behaviors were noted. A discontinuity and/or transition region was found in some of the Tafel curves which indicated a change in the reaction mechanism. Due to the nature of the results, those above and below the transition regions will be discussed separately.

The discussion is presented in three major sections, (1) summary of experimental results, (2) postulation of the reaction mechanism, and (3) correlation of experimental data with the proposed mechanism.

I. SUMMARY OF EXPERIMENTAL RESULTS

A. Current-Potential Studies

Tafel slopes obtained in acidic and basic solutions on Pt-rich alloys were found to be 70 mv. This normally indicates a slow surface chemical reaction following the first electron transfer. For the 20Pt-80Au alloy, a Tafel

slope of 140 mv was found in both acidic and basic solutions, which indicated the first electron transfer to be the rate determining step. Discontinuities in the Tafel curves were noted for basic solutions. For the 40Pt-60Au alloy, Tafel slopes of 100 mv were found in acid solutions, but changed to 80 mv below and 140 mv above the transition region in basic solutions. This peculiar behavior was probably due to the heterogeneity of the alloy as will be shown later. Since the products of this study were varied, neither the reversible potentials nor the corresponding exchange currents could be calculated, the pH dependences of current were approximately zero in strong acid solutions and unity in strong basic solutions on all the Pt-Au alloys.

B. Temperature Studies

Apparent activation energies calculated from the temperature studies ranged from 10 to 22 Kcal. They were consistently higher in basic solutions than in acidic. Values of $\partial E_a/\partial V$ fell into two groups corresponding to αF and F Kcal/volt. These values correspond to the different Tafel slopes which indicated changes or alterations in the reaction mechanism. Due to the inability to calculate the reversible potentials, the chemical activation energies (activation energy at zero over-potential) could not be evaluated. The discontinuities in the apparent activation energies (See Figs. 21 and 22) for the Au-rich alloys tends to substantiate the change in the mechanism indicated by the Tafel curves.

C. Partial Pressure Studies

The partial pressure studies conducted at constant potential in 1 N H_2SO_4 revealed that the current increased inversely with pressure, i.e., $(\partial i/\partial p)_{V,T} < 0$. This effect was more pronounced for the Pt-rich alloys than for the Au-rich, and showed that the rate determining step must include species other than adsorbed acetylene or species derived from acetylene.

In basic solutions, the pressure effect can once again be divided into two groups. For Pt-rich alloys, $(\partial i/\partial p)_{V,T} < 0$, and remains negative with increasing potential except at low pressures (0.03 atm) where the current becomes diffusion limited.

The behavior of the Au-rich alloys was similar to pure Au. Above the transition region, a positive pressure effect was noted indicating an acetylenic species in the rate determining step. At potentials below the transition region, a negative effect was observed. The reversal of the pressure effect across the transition region tends to confirm the change of the rate determining step for the Au-rich alloys.

D. Faradaic Efficiency Studies

The efficiency studies confirmed the presence of products other than CO_2 and H^+ (or H_2O). The efficiencies for the Au-containing alloys were appreciably decreased from that of pure Pt.

E. By-Product Analysis

The resinous films formed on the Pt-Au alloys appeared similar to those formed on Au. Qualitative analyses eliminated compounds containing carbonyl groups. The presence of OH, C=C, and C-C from an extract of the basic anolyte (using Au electrodes) was indicated by infrared analysis[15], however, the OH group was not present in the resinous film produced in 1 N H_2SO_4 on the Pt-Au alloy electrodes. It is believed the hydroxyl group referred to in the previous study may have been introduced by the dissolution of the film in the basic anolyte.

A structure consistent with the analyses from this study is the polyacetylene,

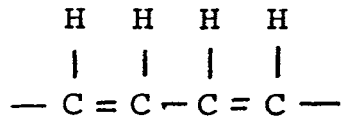

II. POSTULATION OF A REACTION MECHANISM

The reaction sequences for the electro-oxidation of acetylene on Pt and Au have been previously studied[14,15]. The differences in their rate determining steps were related to their relative capabilities for hydrocarbon adsorption, water discharge, and oxide formation on the metal surface. The reaction sequences on the Pt-Au alloys were similar in some respects to the pure metals. A combined influence of Pt and Au was suspected due to the metallurgical heterogeneity of the alloys.

A. Adsorption Isotherm

The adsorption of acetylene on Pt and Au has been postulated to follow the Langmuir adsorption isotherm with the most probable mode of adsorption as[14]

$$C_2H_2\,(sol) \rightarrow \begin{matrix} H & H \\ | & | \\ C & = & C \\ | & & | \\ M & & M \end{matrix} \qquad [4.1]$$

For Pt, it is believed that acetylene forms an immobile layer by means of covalent bonds with d-electron orbitals. Pt is known for its catalytic properties, each atom with 0.55 vacant d-orbitals. Therefore, one molecule of acetylene should require 4 adjacent surface sites for bonding. The adsorption equilibrium constant (K_p) for acetylene has been estimated to be 10^4-10^6 atm^{-1}[15]. These values were obtained by taking into account the energy difference associated with the breaking of one C-C bond in a double and a triple bond, and the difference in free energies of adsorptions due to different adsorbate-solution interactions.

Gold has no d-orbital vacancies available for covalent bonding, and there are no data available that would enable an evaluation of its equilibrium constant for acetylene adsorption. However, some estimations can be made. For the anodic oxidation of ethylene, the mode of adsorption and subsequent oxidation on Au and Pd have been assumed to be the same[16].

Accordingly, the adsorption of acetylene on Au can be hypothesized as having a two-point attachment on adjacent metal atoms. On account of the size of the organic molecules and the interatomic distances of the metal atoms, the acetylene molecule can possibly block two additional sites, thus the values of n could be 2 or 4. A schematic diagram is shown in Fig. 7 for an acetylene molecule adsorbed on a Au surface.

Since there are no vacant d-orbitals in Au, the covalent bond strength between Au and C atoms is much weaker than that between Pt and C. The polymerization product formed during electro-oxidation further indicates that the acetylene does not adsorb on Au as strongly as on Pt. Therefore, the K_p values for Au should be lower than those for Pt.

The adsorption of acetylene on Pt-Au alloys have similarities to both Pt and Au; the relative amounts of α_1 (Pt-rich) and α_2 (Au-rich) phases determine the combined adsorption behavior of the alloys. The α_1 phase is approximately 95 percent Pt, and might be expected to have adsorption characteristics similar to those of pure Pt. The α_2 phase consists of approximately 80 percent Au and behaves similar to pure Au. This is explained by the ability of Au to contribute electrons to the vacant d-orbitals of Pt, thus alloys containing over 60 percent Au show the same electro-catalytic properties as Au.

B. Reaction Mechanism

In accordance with the results reported previously in acidic and basic solutions, the rate determining step for Pt and Pt-rich alloys must exhibit the following characteristics: (1) Be a chemical reaction following the first charge transfer since the Tafel slope is 2.3RT/F, (2) involve a substance other than the adsorbed acetylene or a species derived therefrom because $\partial i/\partial p < 0$, and (3) exhibit no pH dependence in the lower pH region but show a unit pH dependence in basic solutions.

For the Au and Au-rich alloys, below the transition region the rate determining step must: (1) Be associated with the first electron discharge since the Tafel slope is 2(2.3RT/F), (2) involve something other than the adsorbed acetylene or a species derived therefrom since $\partial i/\partial p < 0$, and (3) exhibit no pH dependence in acidic solutions but show a unit pH dependence in basic solutions. Above the transition region, the rate determining step must: (1) Be the first electron discharge step because the Tafel slope is again 2(2.3RT/F), (2) involve adsorbed acetylene, or a substance derived therefrom, since $\partial i/\partial p > 0$, and (3) exhibit a decreasing pH dependence in going from strongly basic to acidic solutions.

In regard to the formation of the partial oxidation product (polymer on the alloy surface) and the total oxidation products (CO_2, H^+, and/or water), there is an apparent competition (parallel reactions) involving intermediate species

on the alloy surface. The experimental data indicate that the competing reactions occur after r.d.s., thus they have no direct effect on the overall rate. Therefore, in the analysis of a series of sucessive reactions, we can assume that only one reaction is rate determining and that those preceding it are effectively at equilibrium. The reactions following the r.d.s. normally need not be considered.

For Pt and Pt-rich alloys, the Tafel slopes indicate the surface reaction is controlling and the reaction sequence can be assumed the same as previously postulated for Pt[14]

$$C_2H_2 = C_2H_2(ads) \qquad [4.2]$$

$$H_2O = OH^{\cdot}(ads) + H^+ + e \qquad [4.3a]$$

or

$$OH^- = OH^{\cdot}(ads) + e \qquad [4.3b]$$

$$C_2H_2(ads) + OH^{\cdot}(ads) \xrightarrow{r.d.s.} C_2H_2OH(ads) \qquad [4.4]$$

$$C_2H_2OH(ads) \ldots \xrightarrow{H_2O} \ldots 2\ CO_2 + 9\ H^+ + 9e \qquad [4.5]$$

Thus, the rate of anodic oxidation of acetylene on Pt and Pt-rich alloys can be expressed as

$$i = nFK_{4.3}k_{4.4}(a_{H^+})^{-1}\ \theta_A(1-\theta_A)\ \exp\ (FV/RT) \qquad [4.6]$$

For the Au-rich alloys, the experimental results indicate a change in the mechanism. Here, the reaction sequence as previously postulated below the transition region for Au can be used[15]

$$C_2H_2 = C_2H_2(ads) \quad [4.2]$$

$$H_2O \xrightarrow{\text{r.d.s.}} OH^{\cdot}(ads) + H^+ + e \quad [4.3a]$$

or $$OH^- \xrightarrow{\text{r.d.s.}} OH^{\cdot}(ads) + e \quad [4.3b]$$

$$C_2H_2(ads) + OH^{\cdot}(ads) \longrightarrow C_2H_2OH(ads) \quad [4.7]$$

$$C_2H_2OH(ads) \ldots \xrightarrow{H_2O} \ldots \text{resin, } CO_2\text{, and } H^+ \quad [4.8]$$

These allow the rate of anodic oxidation of acetylene on Au and Au-rich alloys below the transition region to be expressed as

$$i = nF(k_{4.3a}a_{H_2O} + k_{4.3b}a_{OH^-})(1-\theta_A) \exp(\alpha FV/RT) \quad [4.9]$$

Above the transition region, a surface reaction associated with the first electron discharge is again the rate determining step and the reaction sequence is postulated as

$$C_2H_2 = C_2H_2(ads) \quad [4.2]$$

$$C_2H_2(ads) + H_2O \xrightarrow{\text{r.d.s.}} C_2H_2OH(ads) + H^+ + e \quad [4.10a]$$

or $$C_2H_2(ads) + OH^- \xrightarrow{\text{r.d.s.}} C_2H_2OH(ads) + e \quad [4.10b]$$

$$C_2H_2OH(ads) \ldots \xrightarrow{H_2O} \ldots \text{resin, } CO_2\text{, and } H^+ \quad [4.11]$$

Accordingly, the rate for the anodic oxidation of acetylene on Au and Au-rich alloys above the transition region can then be expressed as

$$i = nF(k_{4.10a}a_{H_2O} + k_{4.10b}a_{OH^-})\,\theta_A \exp(\alpha FV/RT) \quad [4.12]$$

In the Pt-Au system, the mutual solubility of Au and Pt becomes limited below 1260°C, and the solid solution separates into Pt-rich (α_1) and Au-rich (α_2) phases[6]. At temperatures

in the vicinity of 600°C*, the compositions of the two phases are 98 percent Pt for the α_1 phase and 20 percent Pt for the α_2 phase. Because of this heterogeneity, the over-all reaction rate of the oxidation of acetylene is probably affected by the relative amounts of the two phases as their electrocatalytic properties are different. Thus, the total reaction rate may be represented as

$$i = i_1 + i_2 \qquad [4.13]$$

Eqs. 4.6, 4.9, 4.12, and 4.13 can now be used with the experimental data to test this model. In the absence of experimental data for solid solutions representing the α_1 and α_2 phases, data for pure Pt and 20Pt-80Au will be used. These compositions more nearly approximate the composition of the solid solutions than any other available. (Data for smooth Pt were determined experimentally and are shown in Appendix D.)

---

*This is apparently the temperature (or within the temperature range) at which the alloys used in this study were annealed.

III. CORRELATION OF EXPERIMENTAL RESULTS WITH THE THEORETICAL RATE EQUATIONS

In this section, the mechanistic equations will be used to describe separate (parallel) reactions occurring on the distinct metallic phases of the anode and will be tested with the experimental data.

A. Current-Potential Relationships

Substituting Eqs. 4.6 and 4.9 into Eq. 4.13 gives

$$i_t = n_1 F K_{4.3} k_{4.4} (a_{H^+})^{-1} \theta_{A_1}(1-\theta_{A_1}) \exp(FV/RT) + n_2 F (k_{4.3a} a_{H_2O} + k_{4.3b} a_{OH^-})(1-\theta_{A_2}) \exp(\alpha FV/RT) \quad [4.14]$$

The partial derivative with respect to potential of Eq. 4.14 is

$$\frac{\partial i_t}{\partial V} = [n_1 F K_{4.3} k_{4.4} (a_{H^+})^{-1} \theta_{A_1}(1-\theta_{A_1}) \exp(FV/RT)](F/RT) + [n_2 F (k_{4.3a} a_{H_2O} + k_{4.3b} a_{OH^-})(1-\theta_{A_2}) \exp(\alpha FV/RT)](\alpha F/RT) \quad [4.15]$$

Dividing both side of Eq. 4.15 by i_t gives

$$\frac{1}{i_t} \frac{\partial i_t}{\partial V} = \frac{\partial \ln i_t}{\partial V} = \frac{i_1}{i_t}(F/RT) + \frac{i_2}{i_t}(\alpha F/RT) \quad [4.16]$$

Since i_1 and i_2 are proportional to the relative amounts of the phases,

$$i_1/i_t = \beta_1 \quad \text{and} \quad i_2/i_t = \beta_2 \qquad [4.17]$$

For the Pt-rich alloy, $i_1 >> i_2$, so $i_1 \sim i_t$

$$\partial V/\partial \log i = 2.3RT/F = 70 \text{ mv (for 80°C)} \qquad [4.18]$$

For the Au-rich alloy, $i_2 >> i_1$, so $i_2 \sim i_t$

$$\partial V/\partial \log i = 2(2.3RT/F) = 140 \text{ mv (for 80°C)} \qquad [4.19]$$

Eq. 4.16 can now be rearranged to give a general expression

$$\partial V/\partial \log i = 2.3RT/F \left(\frac{1}{\beta_1 + \beta_2 \alpha}\right) \qquad [4.20]$$

Tab. IX shows the Tafel slopes for the different alloys as calculated from Eq. 4.20 and the corresponding experimental values. Figs. 28 and 29 show the experimental data for the two-phase alloys together with the Tafel curves constructed using the weighted values referred to the separate phases of the alloy.

The increase in the Tafel slopes in going from Pt-rich to Au-rich alloys can thus be explained on the basis of separate reactions occurring on the different phases. The composition of the phases remains the same but their relative amounts change with the overall composition of the alloys.

TABLE IX

THEORETICAL AND EXPERIMENTAL TAFEL SLOPES FOR THE ANODIC OXIDATION OF ACETYLENE ON Pt-Au ALLOYS AT 80°C

Electrode		Relative Amount of Phases %		Theoretical Slope mv	Experimental Slope mv	
Pt	Au	α_1	α_2			
100	0	100	0	70	70	(a,b)
80	20	82.3	17.7	76.3	70	(a,b)
60	40	67	33	83.0	70-80	(a,b)
40	60	25	75	111	110-115	(a)
40	60	25	75	111	80	(b)
40	60	25	75	140.0	120-140	(b)
20	80	2	98	137	140	(a)
20	80	2	98	137	100	(b)*
20	80	2	98	140	120-140	(b)**
0	100	0	100	140	140	(a,b)

(a) Acidic solution

(b) Basic solution

* Below transition region

** Above transition region

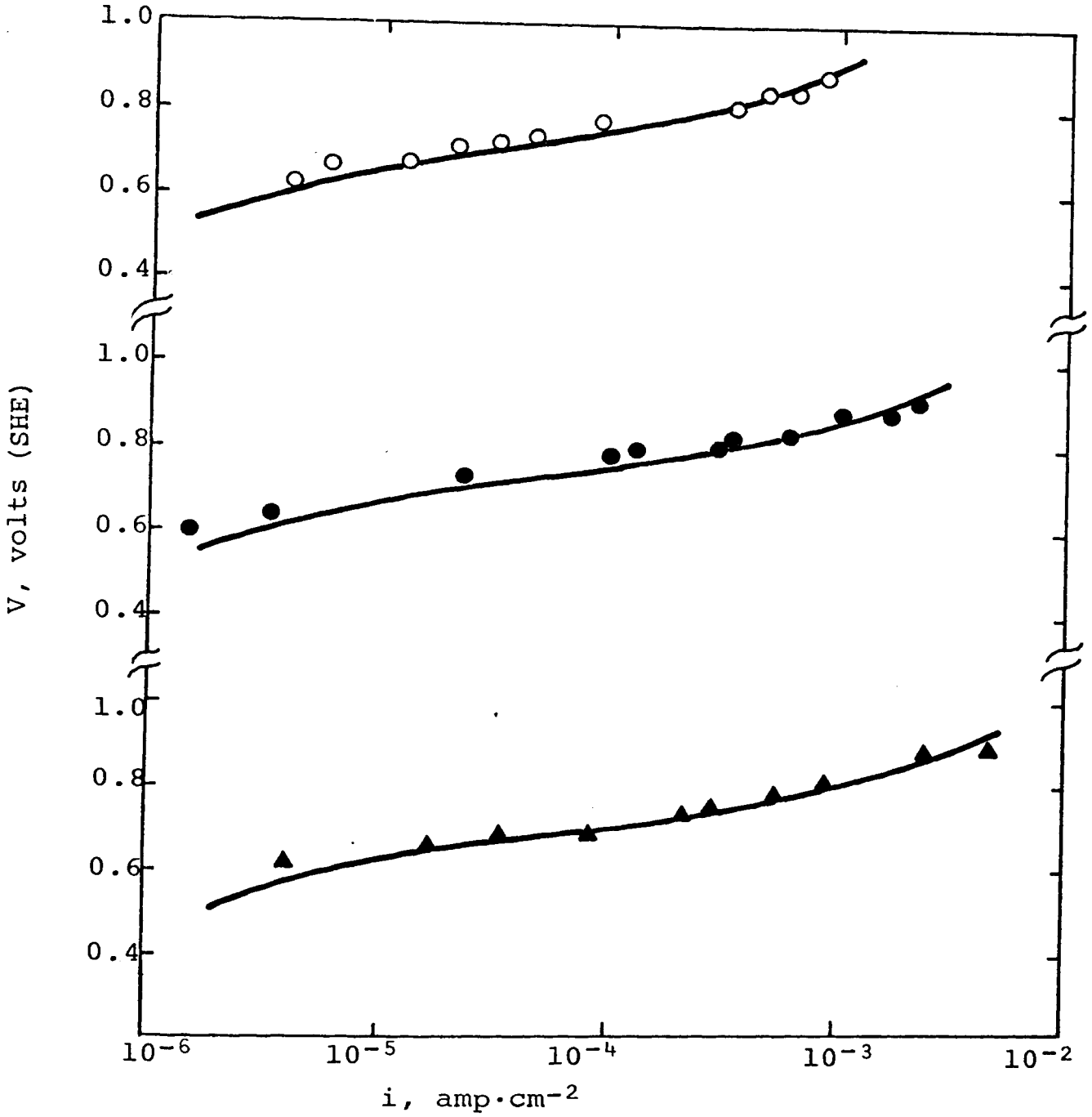

Figure 28. Comparison of the experimentally measured current-potential relationship for the anodic oxidation of acetylene on Pt-Au alloy in 1 N H_2SO_4 at 80°C, with that calculated using weighted values from pure Pt and the 20Pt-80Au alloy. (o, 40Pt-60Au; ●, 60Pt-40Au; ▲, 80Pt-20Au; —, calculated value)

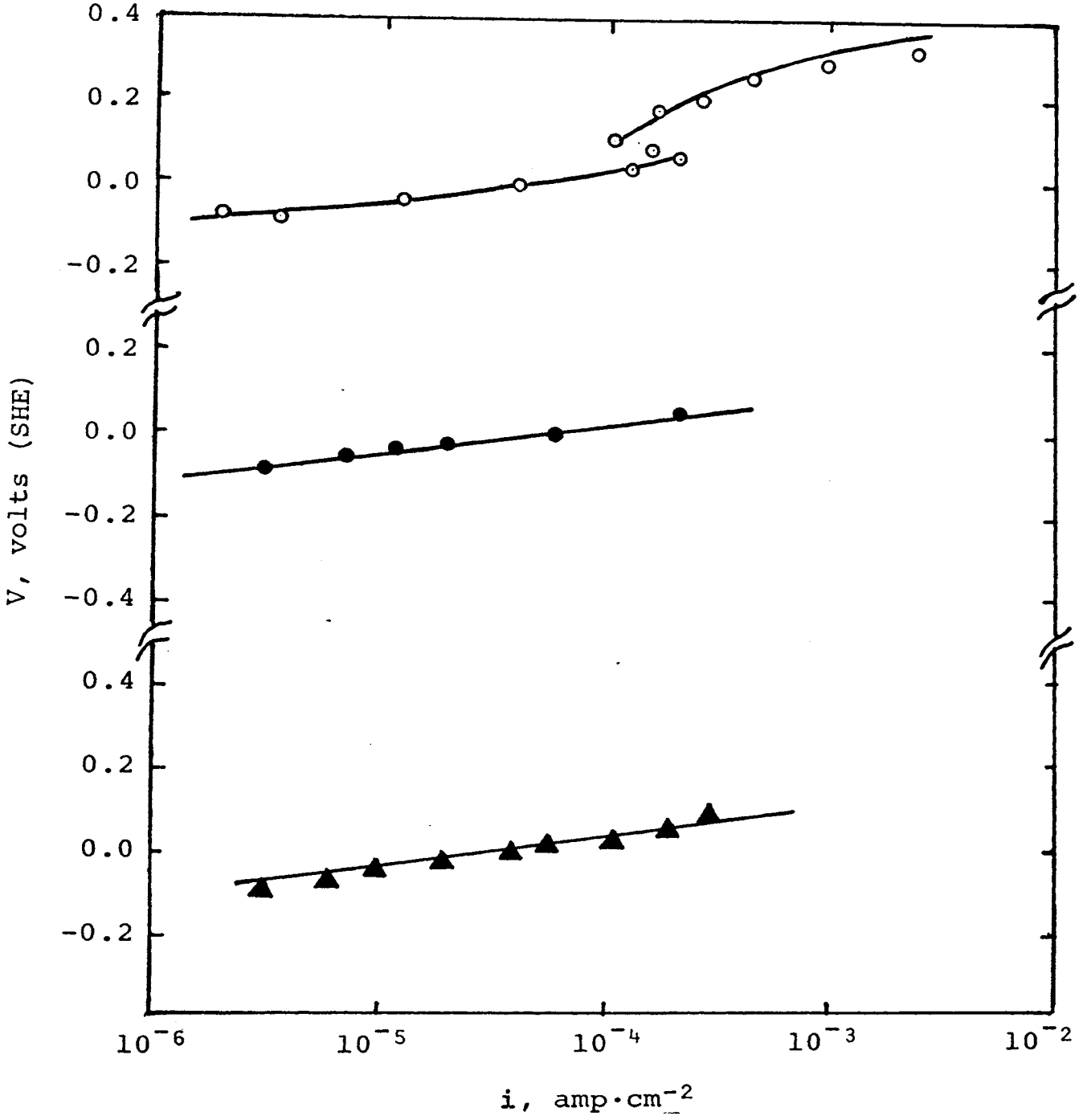

Figure 29. Comparison of the experimentally measured current-potential relationship for the anodic oxidation of acetylene of Pt-Au alloy in 1 N KOH at 80°C, with that calculated using weighted values from pure Pt and the 20Pt-80Au alloy. (○, 40Pt-60Au; ●, 60Pt-40Au; ▲, 80Pt-20Au; —, calculated value)

In basic solutions for the Au-rich alloys, the adsorption of acetylene apparently depends on potential. This is consistent with the discontinuities in the Tafel curves which occur on all the Au-rich alloys and with a greater ease of formation of passivating oxides on the Pt-rich phases. The change in the reaction parameters in crossing the transition region arise when the rate determining step changes from the first electron transfer involving only the discharged species to an electron transfer involving both the discharged and an adsorbed species.

Below the transition region, the acetylene is adsorbed on both α_1 and α_2 phases and H_2O (or OH^-) is discharged adjacent to adsorbed acetylene molecules and further reacts with them. When the potential is increased to a certain point, the $OH^\cdot$ coverage on the α_1 (Pt-rich) phase increases to such an extent that it inhibits the oxidation of the acetylene. At this point, the current decreases appreciably (the transition region) and a further increase in potential is necessary to produce sizeable currents on the α_2 (Au-rich) phase. In other words, below the transition region, reaction is occurring on both α_1 and α_2 phases. Above the transition region, the α_1 phase is passivated and the reaction is occurring only on the α_2 phase. The transition region is a consequence of the passivation of the α_1 phase.

The summation of the currents on the individual phases which have Tafel slopes of 70 and 140 mv gives Tafel curves with slopes varying between 70 and 140 mv in going from predominately α_1 phase to predominately α_2 phase and is consistent with the experimental observations.

B. Current-pH Relationships

Values of current density determined from the experimental data on the alloys and the corresponding pH's for a potential of 0.4 v are shown in Figs. 13 to 16. Current-pH values calculated from Eq. 4.14 are shown in Figs. 30 to 33. The terms,

$$n_1 F\theta_{A_1}(1-\theta_{A_1}) \exp(FV/RT) \quad \text{and} \quad n_2 F(1-\theta_{A_2}) \exp(\alpha FV/RT)$$

from Eq. 4.14 were considered constant at a given potential over the entire pH range. Eq. 4.14 then becomes

$$i = C_1 k_{4.4}(a_{H^+})^{-1} + C_2(k_{4.3a}a_{H_2O} + k_{4.3b}a_{OH^-}) \qquad [4.21]$$

The contribution of the first term was calculated from experimental currents on pure Pt. The contribution of the second term was calculated from the experimental current on Au-rich alloy in 1 N H_2SO_4 and 1 N KOH, respectively. It should be noted the term $k_{4.3b}a_{OH^-}$ is insignificant for the acidic solution as is the term $k_{4.3a}a_{H_2O}$ for the basic solution.

The pH relationship from Eq. 4.21 can be summarized as follows

$$\partial \log i/\partial pH = 0 \quad \text{for acidic solutions}$$
$$= 1 \quad \text{for basic solutions}$$

The experimental values differ slightly from the theoretical ones, however, the trend is correct and errors of these magnitudes could easily arise from the extrapolation of the Tafel curves, error in the relative amounts of the phases, errors in the rates on the phases, and from the assumption that θ_A was independent of potential.

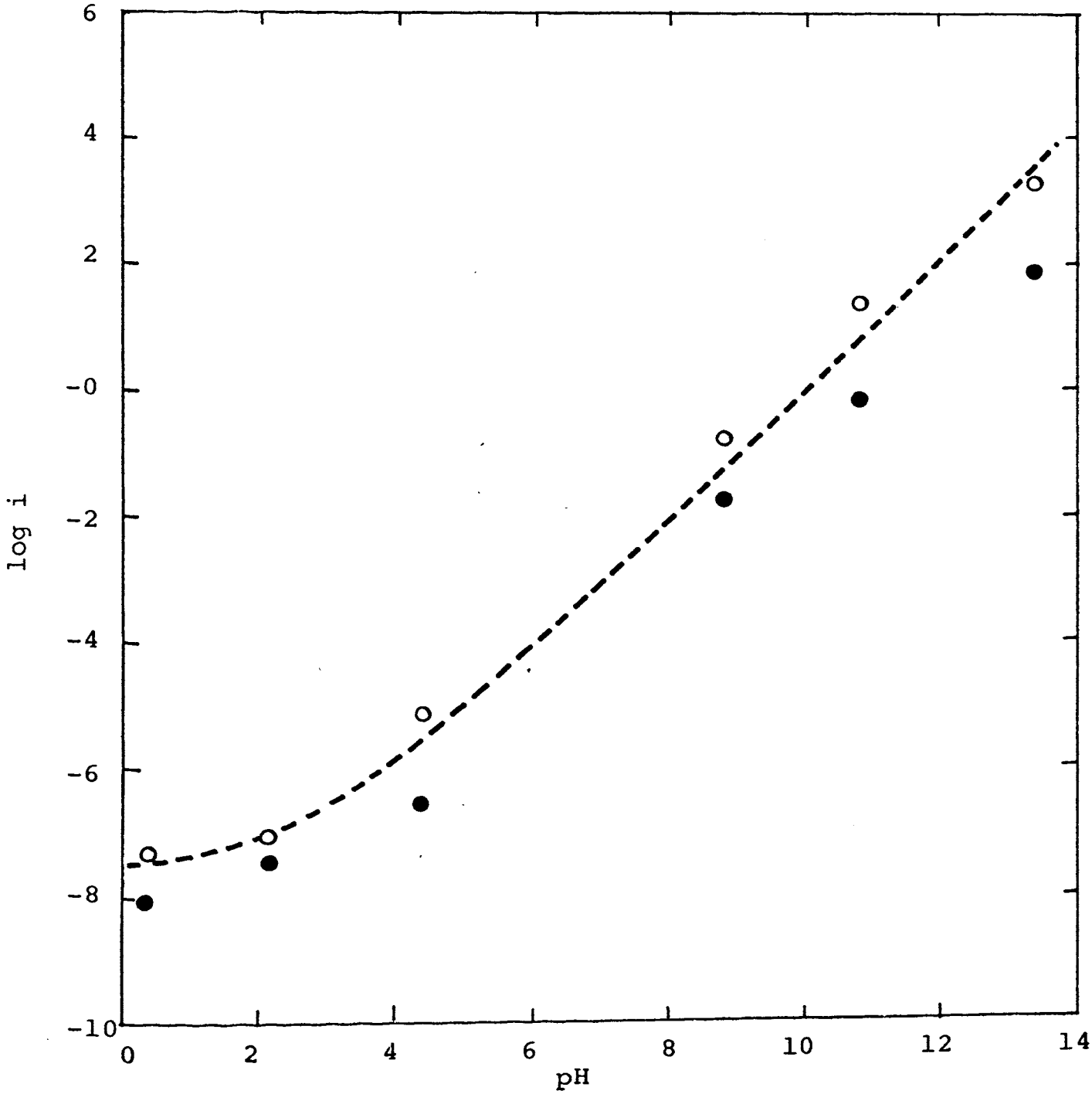

Figure 30. Comparison of the theoretical and experimental effect of pH on current density for the anodic oxidation of acetylene on 80Pt-20Au alloy at 80°C for a constant potential of 0.4 v. (●, Expt.; o, calc. value)

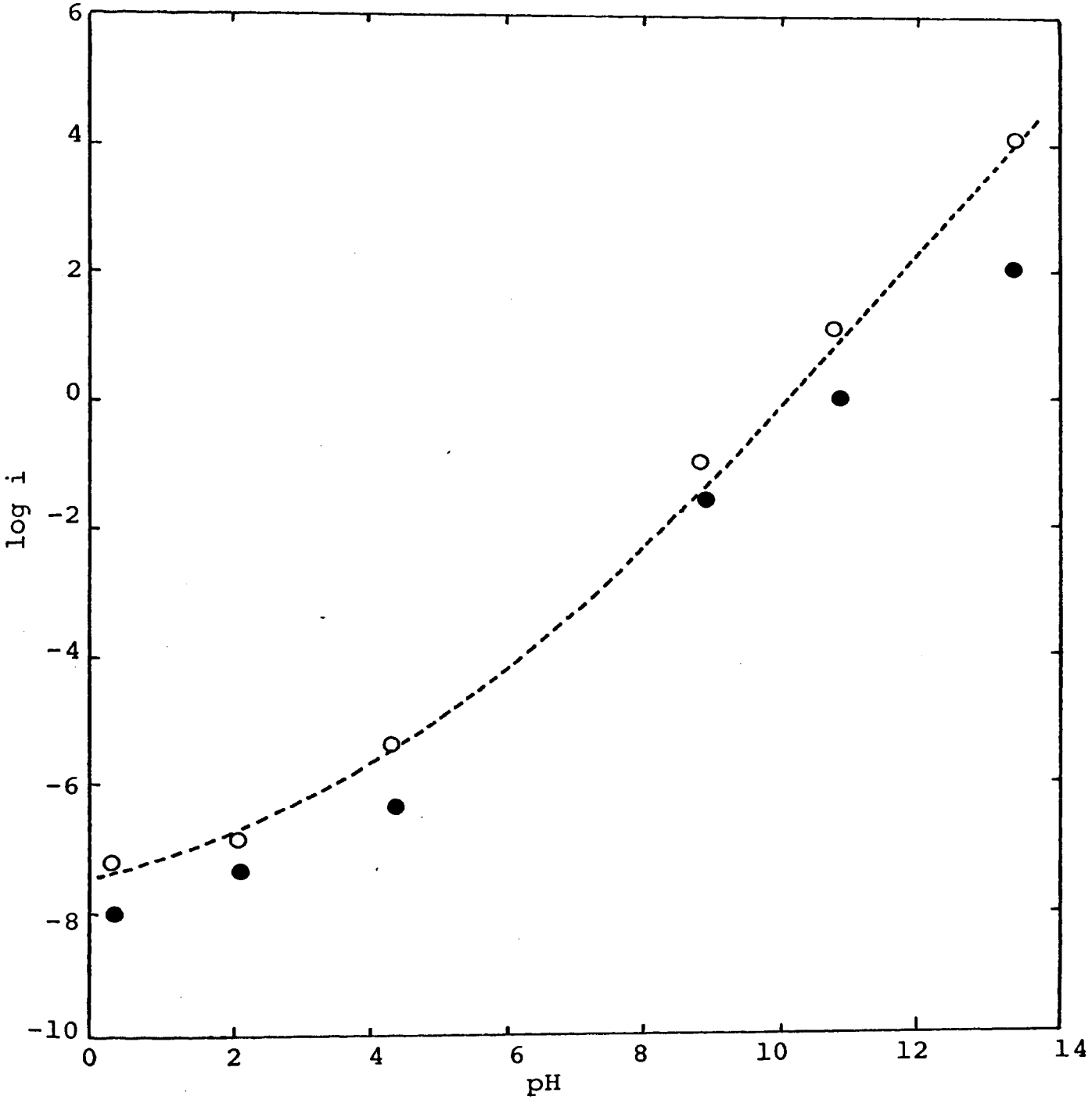

Figure 31. Comparison of the theoretical and experimental effect of pH on current density for the anodic oxidation of acetylene on 60Pt-40Au alloy at 80°C for a constant potential of 0.4 v. (●, Expt.; o, calc. value)

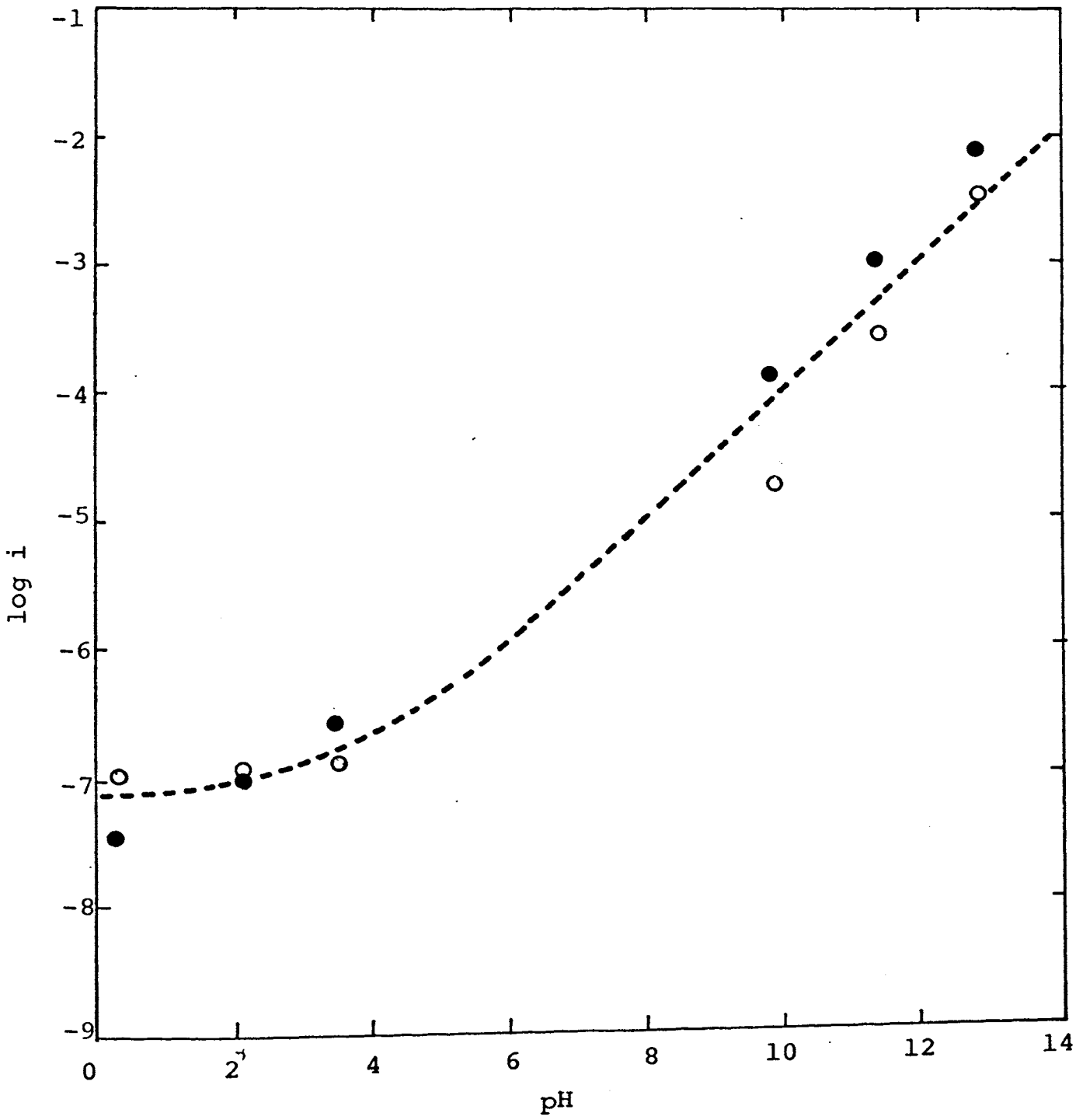

Figure 32. Comparison of the theoretical and experimental effect of pH on current density for the anodic oxidation of acetylene on 40Pt-60Au alloy at 80°C for a constant potential of 0.4 v. (●, Expt.; o, calc. value)

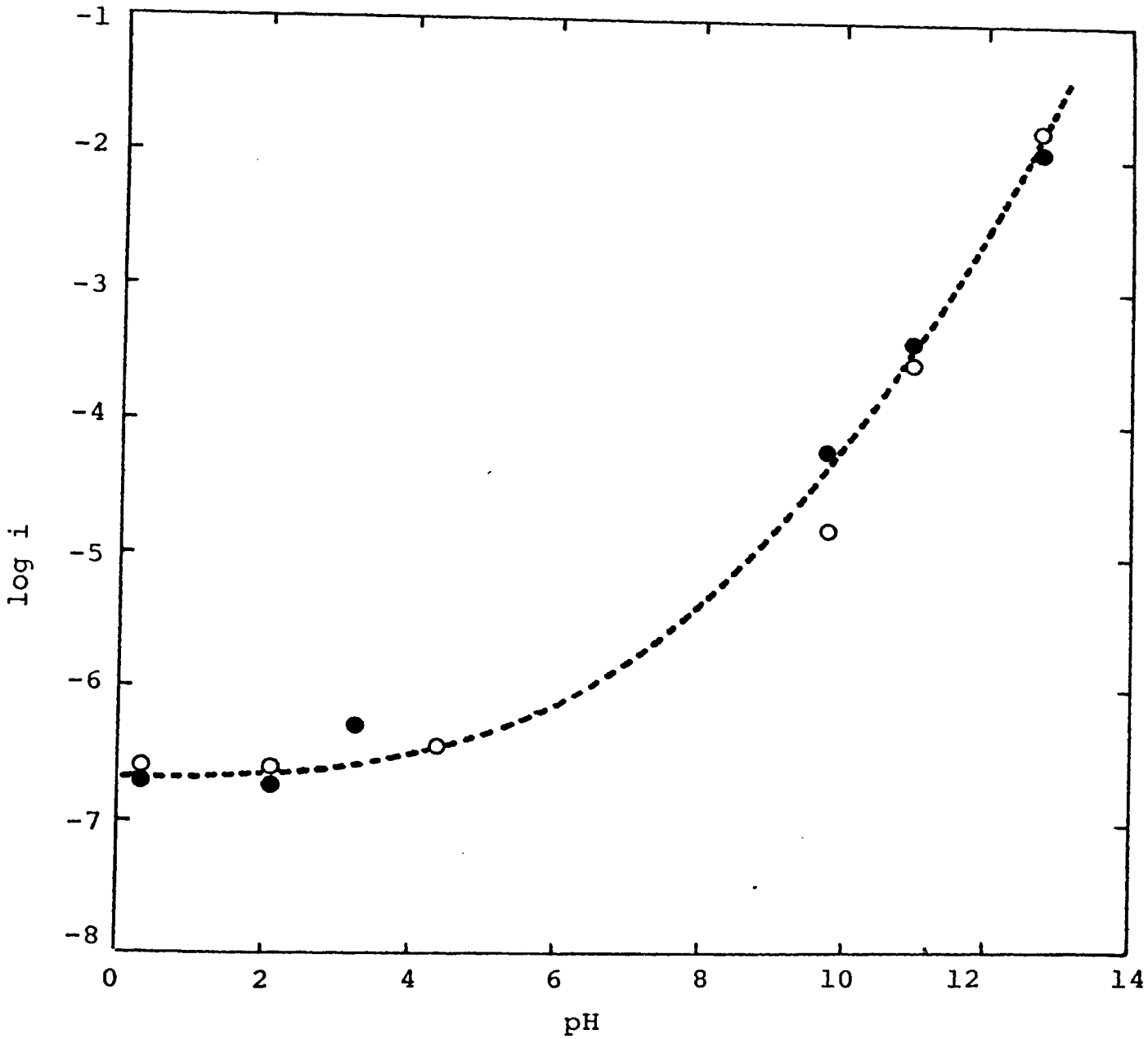

Figure 33. Comparison of the theoretical and experimental effect of pH on current density for the anodic oxidation of acetylene on 20Pt-80Au alloy at 80°C for a constant potential of 0.4 v. (●, Expt.; o, calc. value)

C. Temperature Studies

The predicted variation of activation energy with potential can be found from Eq. 4.14 using the terms $k_{4.3}$, $k_{4.3a}$, and $k_{4.3b}$. They are equivalent to the chemical rate constants, and by use of the Arrehenius relationship, can be expressed as $A \cdot \exp(E_a/RT)$. Substituting for $k_{4.3}$, $k_{4.3a}$, and $k_{4.3b}$, gives

$$i_t = A_1 \exp(E_{a_1}/RT) \exp(FV/RT) + A_2 \exp(E_{a_2}/RT) \exp(\alpha FV/RT) + A_3 \exp(E_{a_3}/RT) \exp(\alpha FV/RT) \quad [4.22]$$

It should be noted the third term of Eq. 4.22 is insignificant for the acidic solution as is the second term for the basic solution. For the acidic solution, taking the partial derivative with respect to 1/T, and dividing both sides by i_t gives

$$\frac{1}{i_t}\frac{\partial i_t}{\partial \frac{1}{T}} = \frac{\partial \log i_t}{\partial \frac{i}{T}} = \beta_1 \frac{E_{a_1}+FV}{2.3\ R} + \beta_2 \frac{E_{a_2}+\alpha FV}{2.3\ R} \quad [4.23]$$

From this expression, the variation of the apparent activation energy with potential on Pt and Pt-rich alloys ($\beta_1 >> \beta_2$) is found to be

$$\frac{\partial E_a}{\partial V} = -F = -23.06 \text{ Kcal} \quad [4.24]$$

On Au and Au-rich alloys ($\beta_2 >> 1$),

$$\frac{\partial E_a}{\partial V} = -\alpha F = 11.53 \text{ Kcal} \qquad [4.25]$$

Similar values are obtained for the basic solution both above and below the transition region. These theoretical values agree well with those obtained experimentally (See Tab. VI).

D. Partial Pressure Studies

The mode of acetylene adsorption during the reaction has already been discussed. Qualitatively, a negative pressure effect was observed on all the alloys with the exception of the Au-rich alloy in basic solutions above the transition region.

For the case represented by Eq. 4.6 (in acidic and basic solutions on Pt-rich alloys), the reaction rate depends on the term $\theta_A(1-\theta_A)$. Since the α_1 phase is dominant in these alloys, the number of points of attachment for the adsorbed acetylene can be assumed to be four (the same as for Pt). For $K_p = 10^4$ to 10^6, $\theta_A(1-\theta_A)$ increases inversely with pressure over the range studied.

In the case of Eq. 4.9 (in acidic and basic solutions below the transition region on the Au-rich alloys), the acetylene coverage can be assumed to follow that of gold.

At a high acetylene coverage almost every vacant site is adjacent to an adsorbed acetylene molecule, thus any water molecule (or OH^-) adsorbing could undergo discharge[15]. The over-all rate depends, therefore, on $(1-\theta_A)$ and the rate would be related to pressure through the adsorption isotherm. Either two-or four-point attachment satisfactorily correlates the data.

In the case of Eq. 4.12 (above the transition region on Au-rich alloys in basic solutions), the coverage of the acetylene is low. In this case, only those water molecules (or OH^-) adsorbing adjacent to adsorbed acetylene molecules react, thus the rate of reaction depends on θ_A[15]. The θ_A term must include not only the sites on which the acetylene molecule is adsorbed, but it must also include the adjacent vacant sites on which water can discharge and further react. It is thus most likely that a four-point attachment would be the minimum feasible for the isotherm.

In order to correlate the acetylene partial pressure with current, θ_A was calculated for various K_p's as a function of pressure using Eq. 2.11. (For illustration, the results calculated using a four-point attachment, n = 4, are shown in Fig. 34.) Using Eq. 4.7 for this example, at constant potential and pH, the following terms can be considered constant with respect to changes in acetylene partial pressure

$$n\ F\ [K_{4.3}k_{4.4}(a_{H^+})^{-1}]\ \exp\ (FV/RT)$$

Thus, Eq. 4.7 simplifies to

$$i = (\text{constant})\ \theta_A\ (1-\theta_A)$$

With this expression, the current can be calculated with the appropriate values of θ_A (from Fig. 35), and compared to experimental values. The appropriate values of n and K_p were found by trial and error. Fig. 35 shows the results of such calculations for the 80Pt-20Au alloy in 1 N H_2SO_4 and the comparison with the experimental data. Values of $K_p = 10^2$ and n = 4 gave the best agreement.

For Eqs. 4.9 and 4.11, it was found that the four-point attachment was still best, but the K_p values (10 to 10^2) were much lower than those for Pt and Pt-rich alloys (10^4 to 10^6).

It was shown earlier that the reaction rate on the heterogeneous alloys could be determined from the rate on the individual phases for 1 atm acetylene partial pressure. This also implies the total reaction rate as the sum of the rates of the individual phases for other acetylene partial pressures. A set of such i/P curves, constructed from the curves for pure Pt and the 20Pt-80Au alloy, are shown in Fig. 36 to 38 along with experimental data for comparison. Though the experimental values differ from the theoretical ones, the trend is correct and errors of such magnitude could easily arise as mentioned previously regarding the pH effect.

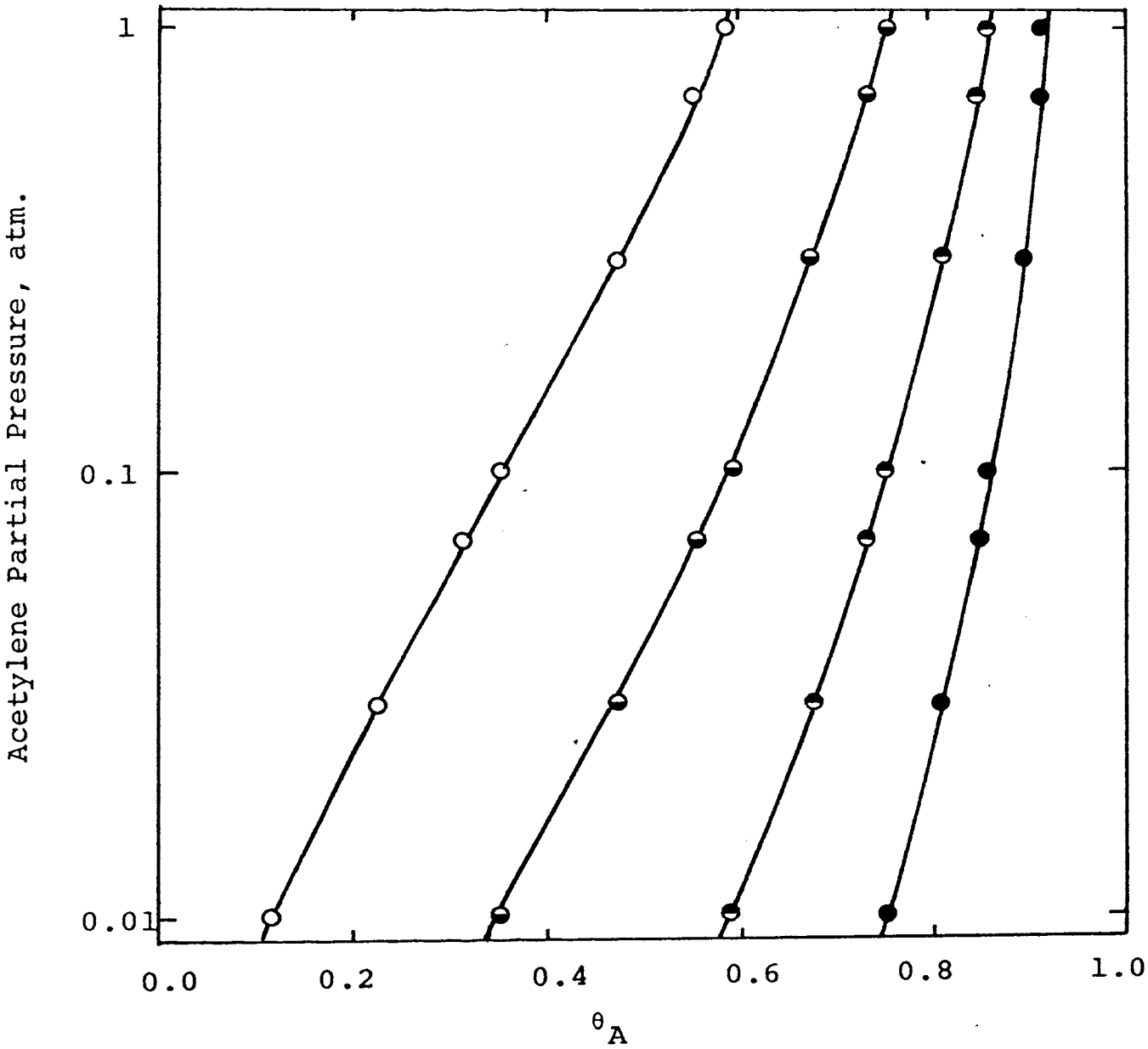

Figure 34. Langmuir adsorption isotherms for acetylene assuming a four point attachment on a Pt-Au alloy surface. (K_p = ●, 10^4; ◓, 10^3; ◒, 10^2; ○, 10).

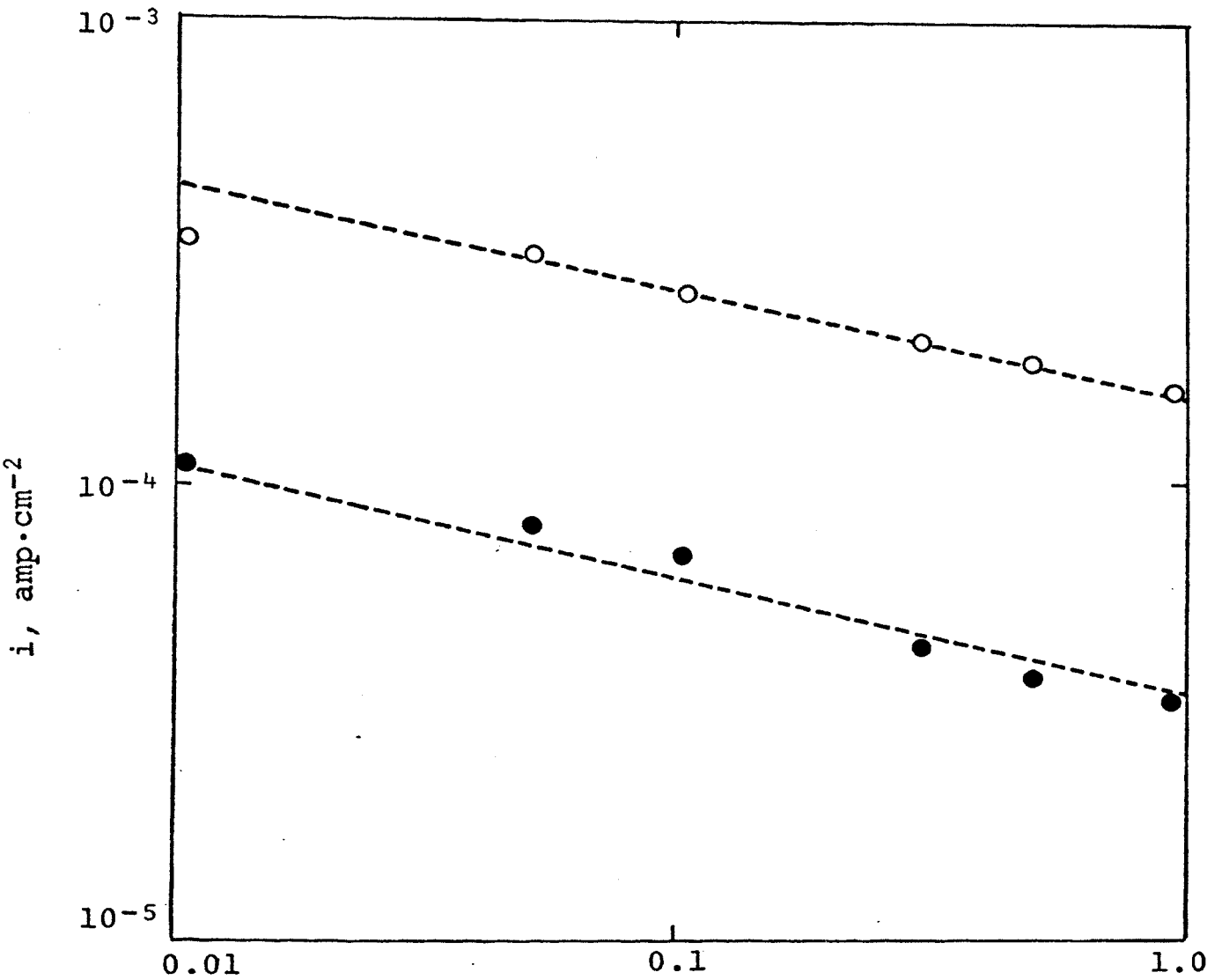

Figure 35. Comparison of the theoretical and experimental effect of acetylene partial pressure on current density for the anodic oxidation of acetylene on 80Pt-20Au in 1 N H_2SO_4 at 80°C (●, 0.7v; o, 0.75v).

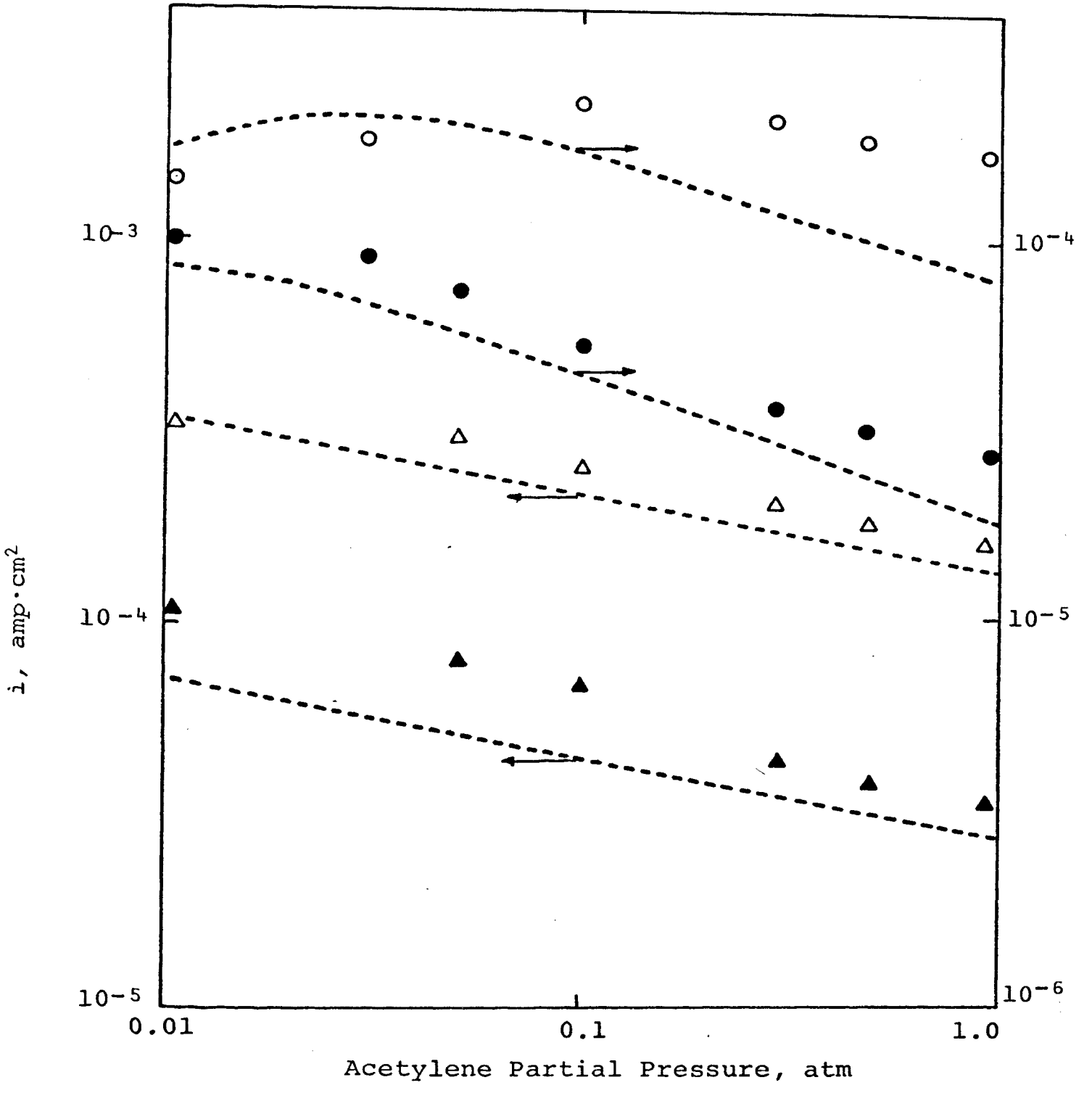

Figure 36. Comparison of the experimentally measured current-pressure relationship for the anodic oxidation of acetylene on 80Pt-20Au alloy at 80°C with that calculated using weighted values from pure Pt and the 20Pt-80Au alloy (▲, 0.7 v, 1 N H_2SO_4; △, 0.75 v, 1 N H_2SO_4; ●, 0.01 v, 1 N KOH; o, 0.06 v, 1 N KOH; ---, calc. value).

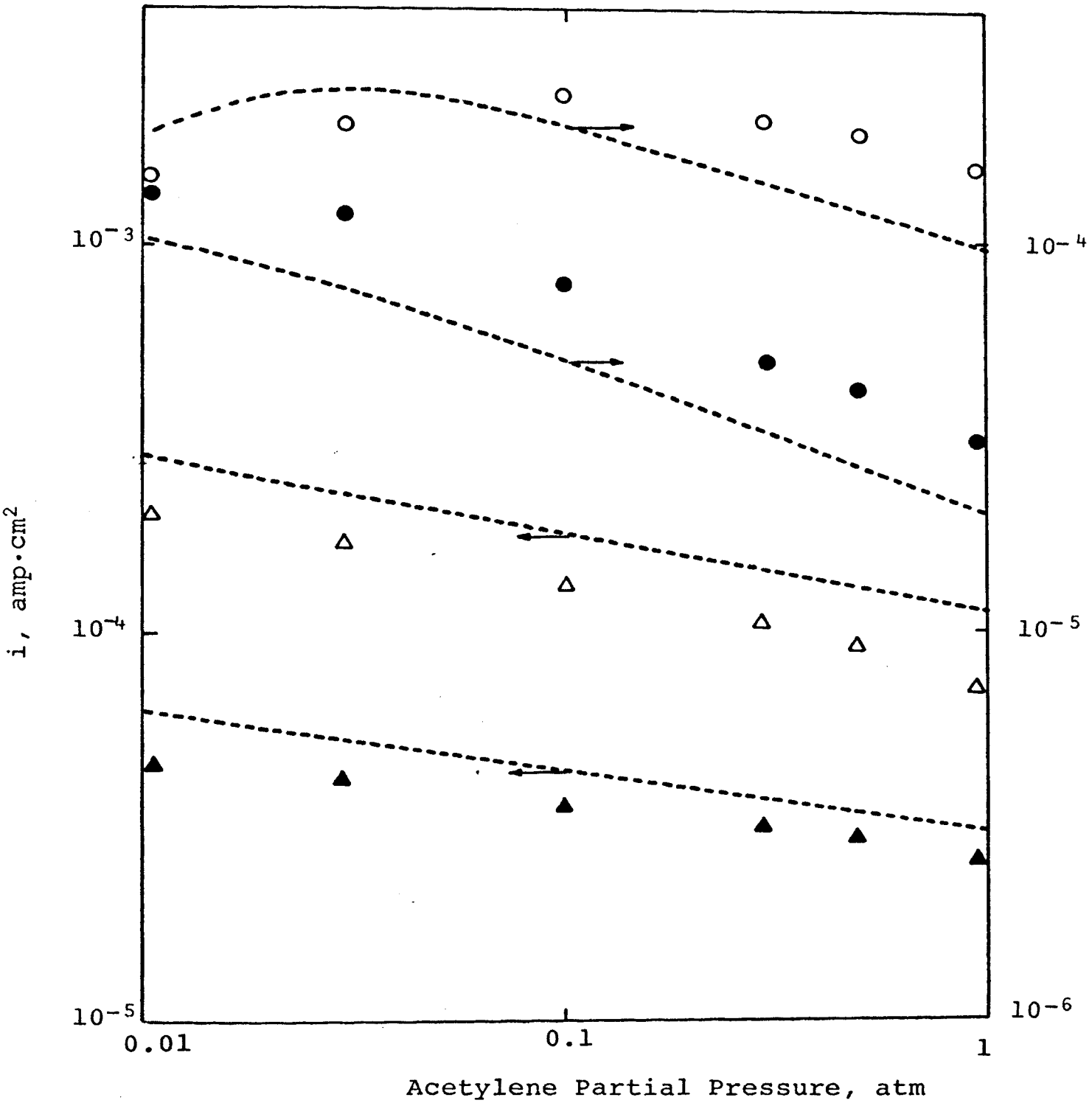

Figure 37. Comparison of the experimentally measured current-pressure relationship for the anodic oxidation of acetylene on 60Pt-40Au alloy at 80°C with that calculated using weighted values from pure Pt and the 20Pt-80Au alloy (▲, 0.7 v, 1 N H_2SO_4; Δ, 0.75 v, 1 N H_2SO_4; ●, 0.01 v, 1 N KOH; o, 0.06 v, 1 N KOH; ---, calc. value).

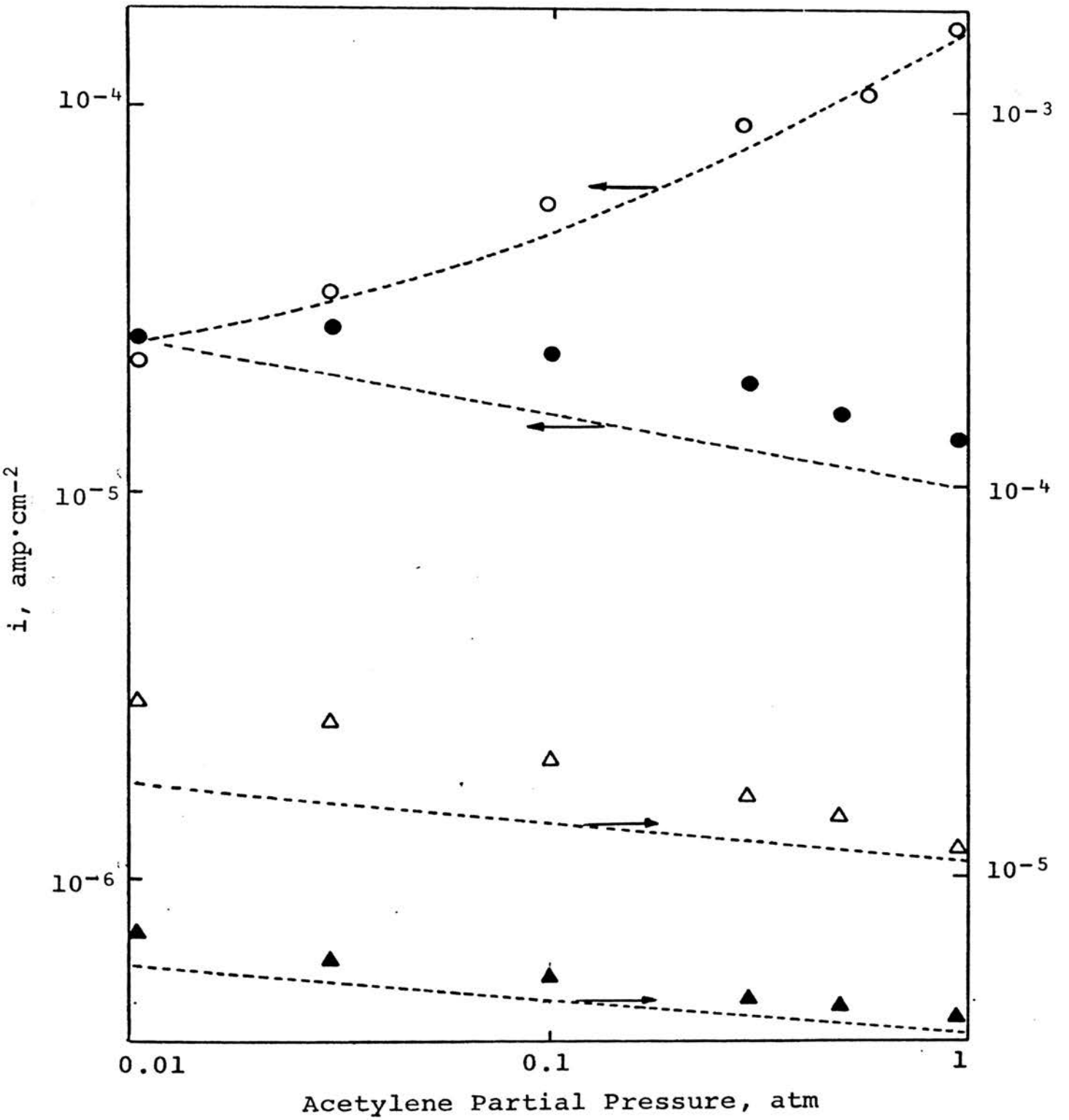

Figure 38. Comparison of the experimentally measured current-pressure relationship for the anodic oxidation of acetylene on 40Pt-60Au alloy at 80°C with that calculated using weighted values from pure Pt and the 20Pt-80Au alloy (▲, 0.7v, 1 N H_2SO_4; △, 0.75, 1 N H_2SO_4; ●, 0.01v, 1 N KOH; o, 0.26v, 1 N KOH).

E. Reaction Products

The explanation for the incomplete oxidation of acetylene on Au-rich alloys is essentially that proposed previously by Reed, et al[15]. The Pauling equation for the covalent bond strength between a metal and a carbon atom is[17]

$$E_{M-C} = \tfrac{1}{2} (E_{M-M} + E_{C-C}) + 2.306 (X_C - X_M)^2 \qquad [4.26]$$

The heats of sublimation for Pt and Au (125 and 84 Kcal, respectively)[18] can be used to approximate the metallic bond energies. The electro-negativities of Pt, Au, and C are 2.2, 2.3, and 2.5, respectively[19]. Acetylene has two π bonds and one σ bond whose respective bond strengths are 54, 63, and 83 Kcal. Assuming the first π bond is broken when acetylene is adsorbed, the strengths of the M-C bonds for Pt and Au are

$$E_{Pt-C} = \tfrac{1}{2}(125 + 54) + 23.06 (2.5 - 2.2)^2 \qquad [4.27]$$
$$= 91.5 \text{ Kcal}$$
$$E_{Au-C} = \tfrac{1}{2}(84 + 54) + 23.06 (2.5 - 2.3)^2 \qquad [4.28]$$
$$= 70 \text{ Kcal}$$

Two M-C bonds are formed in each case from the ruptured acetylene π bond. This leaves one C-C π bond, one C-C σ bond, and two C-M bonds for the adsorbed acetylene molecule. The C-C π bond is the weakest of the three, therefore, it is likely that it would be broken next. Thus the initial attack

on an adsorbed acetylene molecule on Au is the same as on Pt. The next most probable bond rupture on Pt would be the C-C σ bond (83 versus 91.5 Kcal for the Pt-C bond), but for Au, the Au-C bond strength (70 Kcal) is slightly less that of the C-C σ bond. Therefore, the M-C bond for Au is more likely to be broken than the C-C σ bond and allow a partially oxidized acetylene molecule (radical) to desorb and react with other acetylene molecules to form a polymer.

CHAPTER V

RECOMMENDATIONS

A further investigation of the anodic oxidation of acetylene on solid solution Pt-Au alloys might lead to a better understanding of the reaction mechanism and would provide data for correlating electro-catalytic properties with the d-band character of the alloys.

The adsorption of acetylene should be studied in detail to ascertain the mode of adsorption, the potential dependencies of the adsorption, and the real coverage of the adsorbed species. Also, a study of the current-potential relationships under reduced acetylene partial pressure might be useful in determining the correctness of the adsorption isotherm.

It is conceivable that anodic reaction of other unsaturated hydrocarbons might yield partially oxidized compounds of significant commercial value. This could be one of the more interesting areas and is relatively unexplored.

CHAPTER VI

SUMMARY AND CONCLUSIONS

The anodic oxidation of acetylene on Pt-Au alloys of four compositions (80-20, 60-40, 40-60, and 20-80 Pt-Au) was studied at 80°C in solutions of constant pH and unit normality. Currents were measured as a function of potential and partial pressure of acetylene. The coulombic efficiencies for CO_2 production were determined. The experimental results gave reaction parameters falling into three groups; Pt-rich, Au-rich, and intermediate compositions.

The following parameters were found for the Pt-rich alloys

$$(\partial V/\partial \log i)_{V,T,pH} \sim 70 \text{ mv}, \quad (\partial i/\partial p)_{V,T,pH} < 0$$

$$(\partial \log i/\partial pH)_{V,T,P} \sim 0 \quad (pH \sim 0)$$

$$\sim 1 \quad (pH > 6) \quad \left(\frac{\partial E_a}{\partial V}\right)_{P,pH} \sim -23 \text{ Kcal/volt}$$

For the Au-rich alloys, a transition region (an apparent change of the mechanism) was found in the Tafel plots. The parameters below the transition region were

$$(\partial V/\partial \log i)_{V,T,pH} \sim 140 \text{ mv}, \quad (\partial i/\partial p)_{V,T,pH} < 0$$

$$(\partial \log i/\partial pH) \sim 0 \quad (pH < 4)$$

$$\sim 1 \quad (pH > 6), \quad (\partial E_a/\partial v)_{P,pH} \sim -11 \text{ Kcal/volt}$$

Above the transition region, all parameters remained the same as below the transition region except the pressure dependence. It was

$$(\partial i/\partial p)_{V,T,pH} > 0$$

For the intermediate compositions (60Pt-40Au and 40Pt-60Au), the reaction parameters were

$$(\partial v/\partial \log i)_{V,T,pH} = \frac{1}{(\beta_1 + \beta_2\alpha)} \quad (RT/F)$$

$$(\partial i/\partial p)_{V,T,pH} \begin{cases} < 0 & \text{(b.t.r.)} \\ > 0 & \text{(a.t.r.)} \end{cases}, \quad \left(\frac{\partial \log i}{\partial pH}\right)_{V,T,P} \begin{cases} \sim 0 & (pH<6) \\ \sim 1 & (pH>6) \end{cases}$$

$$\left(\frac{\partial E_a}{\partial v}\right)_{P,pH} \begin{cases} \sim F & \text{(Pt-rich)} \\ \sim \alpha F & \text{(Au-rich)} \end{cases}$$

A polymer product was formed during the oxidation which was soluble in the basic electrolytes. The coulombic efficiency for CO_2 production was 70 ± 5 percent in 1 N H_2SO_4 and 80 ± 5 percent in 1 N KOH at 1.0 atm acetylene partial pressure.

The oxidation on the Pt-Au alloys can be interpreted in terms of two mechanisms. For Pt-rich alloys and Au-rich alloys below the transition region, the reaction sequence consists of the following steps

$$C_2H_2(sol) \longrightarrow C_2H_2(ads) \qquad [6.1]$$

$$H_2O\ (sol) \longrightarrow OH^{\cdot}(ads) + H^+ + e$$
$$OH^-\ (sol) \longrightarrow OH^{\cdot}(ads) + e \qquad [6.2]$$

$$C_2H_2(ads) + OH^{\cdot}(ads) \longrightarrow \text{products} \qquad [6.3]$$

The rate determining step depends on the composition of the alloy. For the Pt-rich alloys, Step 6.3 is the r.d.s. For the Au-rich alloys, the r.d.s. is changed to Step 6.2.

Above the transition region (for the Au-rich alloys), the mechanism consists of the following steps

$$C_2H_2(sol) \longrightarrow C_2H_2(ads) \qquad [6.1]$$

$$C_2H_2(ads) + H_2O(sol) \longrightarrow C_2H_2OH^{\cdot}(ads) + H^+ + e \qquad [6.4a]$$

$$C_2H_2(ads) + OH^-(sol) \longrightarrow C_2H_2OH^{\cdot}(ads) \qquad [6.4b]$$

$$C_2H_2OH^{\cdot}(ads) \longrightarrow \text{products} \qquad [6.5]$$

Step 6.4 is the rate determining step.

The corresponding rate equations are:

For the Pt-rich alloy,

$$i = nFK_{6.1}(k_{6.2a}a_{H_2O} + k_{6.2b}a_{OH^-})\theta_A(1-\theta_A) \exp (FV/RT \qquad [6.6]$$

For the Au-rich alloy below the transition,

$$i = nF(k_{6.2a}a_{H_2O} + k_{6.2b}a_{OH^-})(1-\theta_A) \exp (\alpha FV/RT) \qquad [6.7]$$

For the Au-rich alloy above the transition region,

$$i = nF(k_{6.4a}a_{H_2O} + k_{6.4b}a_{OH^-})\theta_A \exp (\alpha FV/RT) \qquad [6.8]$$

The change in mechanism of Au-rich alloys is attributed to a decrease in the acetylene coverage. The total current on the heterogeneous phases can be represented as the sum of the currents on the separate phases:

$$i = i_1 + i_2 \qquad [6.9]$$

BIBLIOGRAPHY

1. R. Parsons, Trans. Faraday Soc. 54, 1053 (1958).
2. B. E. Conway, J. O'M. Bockris, J. Chem. Phys. 26, 532 (1957).
3. B. E. Conway, E. Beatty, P.A.D. de Maine, Electrochim. Acta, 7, 39 (1962).
4. G. J. Young, R. B. Rozelle, "Fuel Cells", p. 23, Reinhold, New York (1960).
5. C. H. Johansson, J. O. Linde, Ann. Physik, [V], 5, 762 (1930).
6. A. S. Darling, R. A. Mintern, J. C. Chaston, J. Inst. Metals, 81 (1952-1953).
7. Vogt, Ann. d. Physik, 1, 14 (1931).
8. M. W. Breiter, Electrochim. Acta, 10, 543 (1965).
9. J. O'M. Bockris, "Modern Aspects of Electrochemistry", Vol. 1, p. 180, Academic Press, New York (1954).
10. E. C. Porter, "Electrochemistry", p. 133, Cleaver Hume Press, London (1956).
11. A. Hickling, Quartery Rev. 3, 95 (1949).
12. I. Langmuir, J. Am. Chem. Soc., 38, 221 (1916).
13. J. O'M. Bockris, H. Dahms, J. Electrochem. Soc., 111, 728 (1964).
14. J. O'M. Bockris, J. W. Johnson, and H. Wroblowa, J. Electrochem. Soc., 111, 863 (1964).

15. J. W. Johnson, J. L. Reed, and W. J. James, J. Electrochem. Soc., 114, 572 (1967).

16. J. O'M. Bockris and H. Dahms, J. Electrochem. Soc., 111, 728 (1964).

17. L. Pauling, "The Nature of the Chemical Bond", p. 92 Cornell University Press, Ithaca, New York (1960).

18. L. Pauling, ibid., p. 93 ,

19. F. A. Cotton, and G. Wilkinson, "Advanced Inorganic Chemistry", p. 88, Interscience Publishers, New York(1962).

APPENDIX A

NOTATIONS

A = frequency factor in Arrhenius equation

A_1, A_2, A_3 = constants

a.t.r. = above transition region

b.t.r. = below transition region

C_A = concentration of acetylene in solution

C_B = concentration of reactant in the bulk of the solution

C_i = concentration of reactant at the interface

D = diffusivity of reactants

E_A = apparent activation energy, Kcal

E_{C-C} = carbon-carbon bond energy, Kcal

E_{M-C} = metal-carbon bond energy, Kcal

F = Faraday constant, 96,500 coulombs/equiv. (=23.06 Kcal/volt·equiv)

β_1 = fraction of α_1 phase in solid solution

β_2 = fraction of α_2 phase in solid solution

i_L = limiting current density, amp/cm^2

i_T = total current density, amp/cm^2

i_1 = current density contributed by α_1 phase, amp/cm^2

i_2 = current density contributed by α_2 phase, amp/cm^2

k = rate constant

K_C = concentration equilibrium constant, cm^3/mole

K_p = pressure equilibrium constant, atm^{-1}

M_A = experimental CO formed for oxidation, gm

P_A = partial pressure of acetylene, atm

R = gas constant, 1.987 cal/gmole·°K

r.d.s. = rate determining step

SHE = standard hydrogen electrode

T = absolute temperature, °K

V = potential, volt

V_r = reversible potential, volt

α = fraction of overpotential assisting anodic reaction, (0.5)

α_1 = Pt-rich phase in solid solution

α_2 = Au-rich phase in solid solution

θ_A = fraction of total active sites covered with acetylene

θ_T = fraction of total active sites covered with chemisorbed species

η = overpotential

APPENDIX B

MATERIALS

The following is a list of the materials and reagents used in this investigation. A detailed analysis of the reagents may be obtained from the chemical catalogue of the respective supplier.

1. Acetylene. Purified, Matheson Co., Joliet, Illinois.

2. Acid, Sulfuric. Reagent grade, Fisher Scientific Co., Fairlawn, N. J.

3. Ascarite. Arthur H. Thomas Co., Philadelphia, Pa.

4. Mercurous Chloride. Reagent grade, Fisher Scientific Co., Fairlawn, N. J.

5. Mercurous Sulfate. Reagent grade, Fisher Scientific Co., Fairlawn, N. J.

6. Nitrogen. Prepurified grade, Matheson Co., Joliet, Illinois.

7. Platinum-Gold Alloy. Engelhard Industries Inc., Newark, N. J.

8. Potassium Chloride. Reagent grade, Fisher Scientific Co., Fairlawn, N. J.

9. Potassium Hydroxide. Reagent grade, Fisher Scientific Co., Fairlawn, N. J.

10. Potassium Sulfate. Reagent grade, Fisher Scientific Co., Fairlawn, N. J.

APPENDIX C

APPARATUS

The following is a list of the principal components used in this investigation.

1. Electrometer. Multi-range type, Model 610B, Keithley Instruments Inc., Cleveland, Ohio.

2. Gas Proportioner. Matheson Model 665, Dual-flow control, Matheson Company, East Rutherford, N. J.

3. Potentiostat. Anotrol, Model 4100, Anotrol Division of Continental Oil Co., Ponca city, Oklahoma.

4. Power Supply. 0-500 v, 0-100 ma, Model 711A, Hewlett-Packard Company, Palo Alto, California.

5. Recorder. Moseley Autograph, Model 7100A strip chart recorder, F. L. Moseley Co., 433 No. Fair Oaks Ave., Pasadena, California.

6. Temperature Controller. YSI Thermistemp Model 71, Yellow Springs Instrument Co., Yellow Springs, Ohio.

APPENDIX D

DATA

The following tables include the data obtained in the current-potential studies, current-temperature studies, and current-acetylene partial pressure studies. The potential listed is that actually measured. The electrode potential, with respect to the normal hydrogen scale, may be found by adding the potential of the reference electrode to that listed in the table. The listed current can be converted to current density by dividing by the geometric surface area of the electrode (15.1 cm^2).

TABLE X

CURRENT-POTENTIAL VALUES FOR THE ANODIC OXIDATION OF ACETYLENE ON 80Pt-20Au ALLOY AT 80°C (P_A=1 atm)

1 N H_2SO_4 pH=0.4		H_2SO_4-K_2SO_4 Mixture pH=2.1		H_2SO_4-K_2SO_4 Mixture pH=4.4	
Potential v (SHE)	Current ma	Potential v (SHE)	Current ma	Potential v (SHE)	Current ma
0.697	0.21	0.537	0.022	0.547	0.043
0.707	0.35	0.577	0.031	0.587	0.089
0.727	0.49	0.617	0.053	0.597	0.148
0.767	1.20	0.657	0.220	0.637	0.570
0.797	3.30	0.697	0.680	0.657	0.730
0.817	5.70	0.737	2.75	0.677	2.05
1.827	8.15	0.777	6.10	0.697	3.30
0.857	12.50	0.797	12.10	0.717	5.30
0.877	18.10			0.737	8.60
0.907	26.00			0.757	13.10
0.917	31.00			0.777	25.60
0.937	38.00			0.827	34.70
0.957	47.00				
0.987	53.00				

TABLE XI

CURRENT-POTENTIAL VALUES FOR THE ANODIC OXIDATION OF ACETYLENE ON 80Pt-20Au ALLOY AT 80°C (P_A=1 atm)

K_2SO_4-K_2CO_3 Mixture pH=8.8		1 N K_2CO_3 pH=10.8		1 N KOH pH=12.8	
Potential v (SHE)	Current ma	Potential v (SHE)	Current ma	Potential v (SHE)	Current ma
0.1	0.031	0.08	0.032	-0.17	0.028
0.15	0.074	0.13	0.048	-0.11	0.048
0.16	0.174	0.14	0.082	-0.07	0.085
0.20	0.339	0.17	0.140	-0.06	0.175
0.22	0.910	0.18	0.240	-0.02	0.580
0.25	2.20	0.21	0.45	0.0	1.01
0.28	4.50	0.23	1.20	0.03	2.46
0.30	8.50	0.26	3.20	0.04	3.05
		0.28	4.50	0.08	5.0

TABLE XII

CURRENT-POTENTIAL VALUES FOR THE ANODIC OXIDATION OF ACETYLENE ON 60Pt-40Au ALLOY AT 80°C (P_A=1 atm)

1 N H_2SO_4 pH=0.32		H_2SO_4-K_2SO_4 Mixture pH=2.1		H_2SO_4-K_2SO_4 Mixture pH=3.8	
Potential v (SHE)	Current ma	Potential v (SHE)	Current ma	Potential v (SHE)	Current ma
0.597	0.023	0.577	0.038	0.547	0.038
0.647	0.051	0.617	0.062	0.597	0.15
0.717	0.350	0.657	0.135	0.627	0.68
0.757	1.58	0.697	0.63	0.657	3.90
0.767	1.88	0.717	3.72	0.687	7.55
0.787	4.53	0.757	5.32	0.707	7.55
0.797	4.90	0.787	13.6	0.737	13.2
0.827	9.5			0.787	24.5
0.857	15.5				
0.897	27.5				

TABLE XIII

CURRENT-POTENTIAL VALUES FOR THE ANODIC OXIDATION OF ACETYLENE ON 60Pt-40Au ALLOY AT 80°C (P_A=1 atm)

K_2SO_4-K_2CO_3 Mixture pH=9.8		1 N K_2CO_3 pH=11.2		1 N KOH pH=12.8	
Potential v (SHE)	Current ma	Potential v (SHE)	Current ma	Potential v (SHE)	Current ma
0.1	0.032	-0.03	0.016	-0.11	0.024
0.13	0.075	-0.01	0.068	-0.08	0.043
0.14	0.083	0.03	0.12	-0.07	0.065
0.16	0.135	0.04	0.16	-0.04	0.11
0.17	0.14	0.06	0.20	-0.01	0.42
0.19	0.28	0.08	0.25	-0.00	0.80
0.20	0.35	0.09	0.31	0.03	1.65
0.22	0.75	0.12	0.71	0.05	2.1
0.23	0.91	0.15	2.05	0.06	3.3
0.25	1.65	0.18	5.3	0.10	7.55
0.26	2.42	0.21	9.1		

TABLE XIV

CURRENT-POTENTIAL VALUES FOR THE ANODIC OXIDATION OF ACETYLENE ON 40Pt-60Au ALLOY AT 80°C (P_A=1 atm)

1 N H_2SO_4 pH=0.34		H_2SO_4-K_2SO_4 Mixture pH=2.1		H_2SO_4-K_2SO_4 Mixture pH=3.8	
Potential v (SHE)	Current ma	Potential v (SHE)	Current ma	Potential v (SHE)	Current ma
0.600	0.064	0.47	0.032	0.50	0.068
0.640	0.097	0.52	0.046	0.53	0.105
0.660	0.195	0.56	0.071	0.56	0.185
0.680	0.318	0.58	0.113	0.60	0.348
0.700	0.47	0.63	0.22	0.63	0.628
0.720	0.70	0.68	0.79	0.66	1.24
0.760	1.42	0.74	2.87	0.70	2.86
0.800	3.62	0.80	9.1	0.74	6.5
0.830	6.80			0.78	12.5
0.870	12.70				

TABLE XV

CURRENT-POTENTIAL VALUES FOR THE ANODIC OXIDATION OF ACETYLENE ON 40Pt-60Au ALLOY AT 80°C (P_A=1 atm)

K_2SO_4-K_2CO_3 Mixture pH=8.8		1 N K_2CO_3 pH=10.8		1 N KOH pH=12.8	
Potential v (SHE)	Current ma	Potential v (SHE)	Current ma	Potential v (SHE)	Current ma
0.11	0.055	0.03	0.024	-0.07	0.056
0.16	0.12	0.07	0.12	-0.04	0.185
0.21	0.49	0.11	0.36	-0.01	0.63
0.25	2.63	0.14	1.6	0.02	0.195
0.29	4.65	0.18	5.5	0.05	3.15
0.32	7.36	0.21	12.5	0.08	2.5
0.34	1.15	0.24	16.5	0.13	1.6
0.41	1.88	0.26	3.1	0.18	2.6
0.45	3.7	0.30	3.9	0.21	4.2
0.50	7.2	0.33	5.9	0.24	7.1
0.55	23.5	0.38	11.6	0.28	15.2
0.60	45.0	0.43	18.5	0.32	33.2
		0.48	33.0		
		0.51	48.0		

TABLE XVI

CURRENT-POTENTIAL VALUES FOR THE ANODIC OXIDATION OF ACETYLENE ON 20Pt-80Au ALLOY AT 80°C (P_A=1 atm)

1 N H_2SO_4 pH=0.35		H_2SO_4-K_2SO_4 Mixture pH=2.1		H_2SO_4-K_2SO_4 Mixture pH=3.2	
Potential v (SHE)	Current ma	Potential v (SHE)	Current ma	Potential v (SHE)	Current ma
0.60	0.091	0.45	0.018	0.60	0.045
0.65	0.23	0.51	0.032	0.70	0.265
0.70	0.54	0.56	0.061	0.75	0.63
0.75	1.20	0.61	0.14	0.80	1.5
0.80	2.8	0.67	0.35	0.85	3.6
0.85	6.4	0.71	1.05	0.90	8.5
0.90	12.0	0.78	3.10	0.95	17.5
0.95	28.0	0.83	7.55		
1.00	53.0	0.88	16.5		

TABLE XVII

CURRENT-POTENTIAL VALUES FOR THE ANODIC OXIDATION OF ACETYLENE ON 20Pt-80Au ALLOY AT 80°C (P_A=1 atm)

K_2SO_4-K_2CO_3 Mixture pH=9.8		1 N K_2CO_3 pH=11.3		1 N KOH pH=12.8	
Potential v (SHE)	Current ma	Potential v (SHE)	Current ma	Potential v (SHE)	Current ma
0.13	0.065	0.03	0.038	-0.04	0.073
0.17	0.27	0.08	0.14	0.01	0.32
0.22	0.58	0.13	0.51	0.06	0.71
0.28	1.3	0.18	1.25	0.11	1.20
0.33	2.4	0.23	1.4	0.16	1.90
0.38	3.3	0.28	2.6	0.21	3.32
0.42	4.6	0.33	4.5	0.26	5.65
0.48	8.5	0.38	8.4	0.30	16.5
0.53	23.2	0.43	19.5	0.35	45.0
0.58	42.0	0.48	51.5	0.41	90.5

TABLE XVIII

CURRENT-POTENTIAL VALUES FOR THE ANODIC OXIDATION OF ACETYLENE ON SMOOTH Pt* AT 80°C (P_A=1 atm)

1 N H_2SO_4 pH=0.32		1 N KOH pH=12.8	
Potential v (SHE)	Current ma	Potential v (SHE)	Current ma
0.60	0.038	-0.07	0.029
0.63	0.055	-0.04	0.054
0.66	0.098	-0.01	0.23
0.69	0.27	0.02	0.62
0.72	0.69	0.05	2.05
0.75	1.9	0.08	4.75
0.78	4.7	0.11	9.5
0.81	8.9	0.14	15.0
0.84	17.0		
0.87	27.0		
0.90	36.0		
0.95	54.5		

*Electrode area = 13.6 cm^2

TABLE XIX

CURRENT-TEMPERATURE VALUES FOR THE ANODIC OXIDATION OF ACETYLENE ON 80Pt-20Au ALLOY (P_A=1 atm)

Potential v (SHE)	Temperature °C	Current ma
	1 N H_2SO_4	
0.737	80	2.64
	70	1.15
	60	0.47
	50	0.17
	40	0.067
0.837	80	18.2
	70	9.05
	60	4.08
	50	1.58
	40	0.61
	1 N KOH	
-0.02	80	0.53
	70	0.19
	60	0.068
	50	0.023
	40	0.008
0.08	80	7.25
	70	3.1
	60	12.5
	50	0.47
	40	0.16

TABLE XX

CURRENT-TEMPERATURE VALUES FOR THE ANODIC OXIDATION OF ACETYLENE ON 60Pt-40Au ALLOY (P_A=1 atm)

Potential v (SHE)	Temperature °C	Current ma
	1 N H_2SO_4	
0.757	80	1.13
	70	0.48
	60	0.17
	50	0.051
	40	0.17
0.857	80	12.7
	70	6.4
	60	2.5
	50	0.88
	40	0.38
	1 N KOH	
0.057	80	1.0
	70	0.43
	60	0.13
	50	0.05
	40	0.015
0.107	80	3.7
	70	1.5
	60	0.56
	50	0.19
	40	0.06

TABLE XXI

CURRENT-TEMPERATURE VALUES FOR THE ANODIC OXIDATION OF ACETYLENE ON Pt-Au ALLOY IN 1 N H_2SO_4 (P_A=1 atm)

Potential v (SHE)	Temperature °C	Current ma
	40Pt-60Au	
0.75	80	2.56
	70	1.12
	60	0.38
	50	0.13
	40	0.045
0.80	80	8.21
	70	3.92
	60	1.55
	50	0.59
	40	0.19
	20Pt-80Au	
0.75	80	1.36
	70	0.63
	60	0.26
	50	0.105
	40	0.038
0.80	80	2.80
	70	1.31
	60	0.58
	50	0.24
	40	0.01

TABLE XXII

CURRENT-TEMPERATURE VALUES FOR THE ANODIC OXIDATION OF ACETYLENE ON 40Pt-60Au ALLOY IN 1 N KOH (P_A=1 atm)

Potential v (SHE)	Temperature °C	Current ma
	Above Transition Region	
0.207	80	6.64
	70	3.78
	60	2.12
	50	1.21
	40	0.68
0.257	80	16.6
	70	10.2
	60	6.4
	50	3.88
	40	2.11
	Below Transition Region	
-0.03	80	0.46
	70	0.21
	60	0.088
	50	0.037
	40	0.014
0.02	80	1.74
	70	0.79
	60	0.32
	50	0.12
	40	0.049

TABLE XXIII

CURRENT-TEMPERATURE VALUES FOR THE ANODIC OXIDATION OF ACETYLENE ON 20Pt-80Au ALLOY IN 1 N KOH (P_A=1 atm)

Potential v (SHE)	Temperature °C	Current ma
	Above Transition Region	
0.31	80	17.4
	70	10.8
	60	6.6
	50	4.2
	40	2.18
0.36	80	54.5
	70	32.2
	60	19.6
	50	11.6
	40	6.5
	Below Transition Region	
0.01	80	1.52
	70	0.63
	60	0.26
	50	0.10
	40	0.036
0.06	80	4.7
	70	1.90
	60	0.83
	50	0.33
	40	0.13

TABLE XXIV

CURRENT-PRESSURE VALUES FOR THE ANODIC OXIDATION OF ACETYLENE ON 80Pt-20Au ALLOY IN 1 N H_2SO_4 AT 80°C

Potential v (SHE)	C_2H_2 Partial Pressure atm	Current ma
0.697	1.0	0.48
	0.5	0.55
	0.3	0.65
	0.1	0.90
	0.05	1.22
	0.01	1.63
0.747	1.0	2.42
	0.5	2.86
	0.1	3.78
	0.05	4.45
	0.01	5.0
0.797	1.0	7.55
	0.3	9.0
	0.1	9.8
	0.05	10.5
	0.01	11.2

TABLE XXV

CURRENT-PRESSURE VALUES FOR THE ANODIC OXIDATION OF ACETYLENE ON 80Pt-20Au ALLOY IN 1 N KOH AT 80°C

Potential v (SHE)	C_2H_2 Partial Pressure atm	Current ma
-0.043	1.0	0.091
	0.5	0.122
	0.3	0.151
	0.1	0.875
	0.03	3.05
	0.01	5.60
0.007	1.0	0.45
	0.5	0.62
	0.3	0.74
	0.1	1.18
	0.03	1.74
	0.01	2.05
0.057	1.0	2.26
	0.5	2.64
	0.3	3.02
	0.1	3.62
	0.03	3.02
	0.01	2.26

TABLE XXVI

CURRENT-PRESSURE VALUES FOR THE ANODIC OXIDATION OF ACETYLENE ON 60Pt-40Au ALLOY IN 1 N H_2SO_4 at 80°C

Potential v (SHE)	C_2H_2 Partial Pressure atm	Current ma
0.647	1.0	0.18
	0.5	0.19
	0.3	0.196
	0.1	0.22
	0.03	0.23
	0.01	0.25
0.697	1.0	0.41
	0.5	0.47
	0.3	0.48
	0.1	0.54
	0.03	0.63
	0.01	0.67
0.747	1.0	1.09
	0.5	1.39
	0.3	1.6
	0.1	1.96
	0.03	2.56
	0.01	2.94

TABLE XXVII

CURRENT-PRESSURE VALUES FOR THE ANODIC OXIDATION OF ACETYLENE ON 60Pt-40Au ALLOY IN 1 N KOH AT 80°C

Potential v (SHE)	C_2H_2 Partial Pressure atm	Current ma
-0.043	1.0	0.098
	0.3	0.135
	0.1	0.195
	0.05	0.24
	0.03	0.30
	0.01	0.37
0.007	1.0	0.41
	0.5	0.48
	0.3	0.55
	0.1	0.80
	0.05	1.08
	0.03	1.36
	0.01	1.51
0.057	1.0	2.5
	0.5	2.8
	0.3	3.1
	0.1	3.4
	0.03	2.7
	0.01	2.1

TABLE XXVIII

CURRENT-PRESSURE VALUES FOR THE ANODIC OXIDATION OF ACETYLENE ON 40Pt-60Au ALLOY IN 1 N H_2SO_4 AT 80°C

Potential v (SHE)	C_2H_2 Partial Pressure atm	Current ma
0.697	1.0	0.63
	0.5	0.68
	0.3	0.71
	0.1	0.82
	0.05	0.94
	0.01	1.06
0.747	1.0	1.75
	0.5	2.05
	0.3	2.4
	0.1	3.0
	0.05	3.8
	0.01	4.4
0.797	1.0	6.35
	0.5	7.1
	0.3	7.6
	0.1	7.8
	0.05	8.6
	0.01	8.5

TABLE XXIX

CURRENT-PRESSURE VALUES FOR THE ANODIC OXIDATION OF ACETYLENE ON 40Pt-60Au ALLOY IN 1 N KOH AT 80°C

Potential v (SHE)	C_2H_2 Partial Pressure atm	Current ma
-0.043	1.0	0.076
	0.5	0.087
	0.3	0.097
	0.1	0.121
	0.03	0.151
	0.01	0.135
0.007	1.0	0.28
	0.5	0.35
	0.3	0.40
	0.1	0.47
	0.03	0.54
	0.01	0.50
0.257	1.0	3.4
	0.5	2.5
	0.3	1.9
	0.1	1.18
	0.03	0.7
	0.01	0.45

TABLE XXX

CURRENT-PRESSURE VALUES FOR THE ANODIC OXIDATION OF ACETYLENE ON 20Pt-80Au ALLOY IN 1 N H_2SO_4 AT 80°C

Potential v (SHE)	C_2H_2 Partial Pressure atm	Current ma
0.697	1.0	0.62
	0.5	0.67
	0.3	0.70
	0.1	0.76
	0.03	0.79
	0.01	0.76
0.747	1.0	1.44
	0.5	1.51
	0.3	1.52
	0.1	1.52
	0.03	1.44
	0.01	1.36
0.797	1.0	4.0
	0.7	4.15
	0.5	4.3
	0.3	4.2
	0.1	3.6
	0.03	2.7
	0.01	2.56

TABLE XXXI

CURRENT-PRESSURE VALUES FOR THE ANODIC OXIDATION OF ACETYLENE ON 20Pt-80Au ALLOY IN 1 N KOH AT 80°C

Potential v (SHE)	C_2H_2 Partial Pressure atm	Current ma
0.007	1.0	0.167
	0.5	0.157
	0.3	0.151
	0.1	0.12
	0.05	0.092
	0.01	0.064
0.057	1.0	0.415
	0.5	0.362
	0.3	0.31
	0.1	0.21
	0.05	0.128
	0.01	0.078
0.257	1.0	4.5
	0.5	2.86
	0.3	2.1
	0.1	1.36
	0.05	0.95
	0.01	0.82
0.287	1.0	7.5
	0.5	5.3
	0.3	3.8
	0.1	2.2
	0.05	1.51
	0.01	1.36

TABLE XXXII

CURRENT-PRESSURE VALUES FOR THE ANODIC OXIDATION OF ACETYLENE ON SMOOTH Pt* AT 80°C

Potential v (SHE)	Partial Pressure atm	Current ma
	1 N H_2SO_4	
0.697	1.0	0.35
	0.7	0.38
	0.3	0.47
	0.1	0.6
	0.03	0.71
	0.01	1.0
0.747	1.0	1.85
	0.7	2.05
	0.3	2.44
	0.1	3.5
	0.03	4.5
	0.01	4.9
	1 N KOH	
0.007	1.0	0.31
	0.5	0.42
	0.3	0.48
	0.1	0.75
	0.03	1.34
	0.01	1.70
0.057	1.0	1.43
	0.5	2.3
	0.1	3.3
	0.03	4.9
	0.01	3.3

*Electrode Area = 13.6 cm^2

VITA

Wu, Christopher Kuo-chieh was born April 3, 1936, in Canton, China. In 1950 he migrated to Taipei, Taiwan, where he attended Taiwan Provincial Ching-kung High School. In 1958, he entered National Taiwan University, receiving a Bachelor of Science degree in Chemical Engineering in June of 1962.

In January, 1964, he came to the University of Missouri at Rolla for advanced studies and received the Master of Science in Chemical Engineering in January of 1966.

In January, 1966 he continued work toward the degree of Doctor of Philosophy in Chemical Engineering.

He was a graduate assistant in Chemical Engineering from September 1964 to June 1965. He also received a research assistantship from June 1965 to June 1966 supported by the Office of Naval Research, a Monsanto Research Fellowship from June 1966 to 1967, and a Space Sciences Materials Research Fellowship from 1967 to 1968.